Check for updates

NIST Special Publication 260
NIST.SP.260-229r1

Certification of Standard Reference Material® 1568c Rice Flour



Laura J. Wood
Charles A. Barber
Colleen E. Bryan Sallee
Monique E. Johnson
Shaun Kotoski
Stephen E. Long
Tomohiro Narukawa
Rick L. Paul
Nicholas Sharp
John R. Sieber
Maria I. Vega Martinez
James H. Yen
Lee L. Yu

This publication is available free of charge from:
https://doi.org/10.6028/NIST.SP.260-229r1

NIST NATIONAL INSTITUTE OF STANDARDS AND TECHNOLOGY
U.S. DEPARTMENT OF COMMERCE

NIST Special Publication 260
NIST.SP.260-229r1

Certification of Standard Reference Material® 1568c Rice Flour

Laura J. Wood*, Charles A. Barber†, Colleen E. Bryan Sallee, Monique E. Johnson, Shaun Kotoski†, Stephen E. Long*, Rick L. Paul, Nicholas Sharp, John R. Sieber*, Maria I. Vega Martinez, Lee L. Yu
Chemical Sciences Division
Material Measurement Laboratory

James H. Yen
Statistical Engineering Division
Information Technology Laboratory

Tomohiro Narukawa
Reference Material Evaluation Group
Research Institute for Material and Chemical Measurement
National Metrology Institute of Japan

* Retired NIST Author
† Former NIST employee; all work for this publication was done while at NIST

This publication is available free of charge from:
https://doi.org/10.6028/NIST.SP.260-229r1

January 2026



U.S. Department of Commerce
Howard Lutnick, Secretary

National Institute of Standards and Technology
Craig Burkhardt, Acting Under Secretary of Commerce for Standards and Technology and Acting NIST Director

NIST.SP.260-229r1
January 2026

Certain equipment, instruments, software, or materials, commercial or non-commercial, are identified in this paper in order to specify the experimental procedure adequately. Such identification does not imply recommendation or endorsement of any product or service by NIST, nor does it imply that the materials or equipment identified are necessarily the best available for the purpose.

NIST Technical Series Policies
Copyright, Use, and Licensing Statements
NIST Technical Series Publication Identifier Syntax

Publication History
Approved by the NIST Editorial Review Board on 2025-12-18
Supersedes NIST.SP.260-229 (July 2022) https://doi.org/10.6028/NIST.SP.260-229

How to Cite this NIST Technical Series Publication
Wood LJ, Barber CA, Bryan Sallee CE, Johnson ME, Kotoski S, Long SE, Narukawa T, Paul RL, Sharp N, Sieber JR, Vega Martinez MI, Yen JH, Yu LL. (2026) Certification of Standard Reference Material® 1568c Rice Flour. (National Institute of Standards and Technology, Gaithersburg, MD), NIST Special Publication (SP) NIST SP 260-229r1. https://doi.org/10.6028/NIST.SP.260-229r1

Author ORCID iDs

Barber CA:	0000-0002-4968-7486
Bryan Sallee CE:	0000-0002-2334-3925
Johnson ME:	0000-0001-5096-2003
Long SE:	0000-0001-5764-0744
Narukawa T:	0000-0002-6339-7506
Paul RL:	0000-0002-6366-1901
Sharp N:	0000-0002-3926-1246
Sieber JR:	0000-0003-1748-3718
Vega Martinez MI:	0000-0002-3094-7866
Wood LJ:	0000-0002-4294-7636
Yen JH:	0000-0001-5242-7629
Yu LL:	0000-0002-8043-6853

Contact Information
Please address technical questions you may have about this SRM to srms@nist.gov where they will be assigned to the appropriate Technical Project Leader responsible for support of this material. For sales and customer service inquiries, please contact srminfo@nist.gov

Abstract

The National Institute of Standards and Technology (NIST) SRM 1568c Rice Flour has value assignments for over 30 analytes, including arsenic species. This material is intended to be used for the evaluation of methods for the determination of elements and arsenic species in this and similar matrices. The material was purchased from commercial vendors. Measurement results were obtained from NIST, National Metrology Institute of Japan (NMIJ), and interlaboratory comparison exercises. This document describes the material, sample preparations, results, and data analysis.

Keywords

Arsenic Species; Elements; Moisture; Standard Reference Material® (SRM®); Rice Flour.

Table of Contents

1. Introduction 1
2. Material 4
2.1. Acquisition & Packaging 4
2.2. Irradiation 4
2.3. Storage 4
3. Element-Related Analytes 5
4. Experimental Procedures 6
4.1. NIST Methods and Procedures 6
4.1.1. Desiccator Drying 6
4.1.2. Forced Air Drying 6
4.1.3. ICP-OES Analysis 7
4.1.4. ID-CV-ICP-MS Analysis 10
4.1.5. ICP-MS Analysis 14
4.1.6. INAA Analysis 16
4.1.6.1. Irradiation Procedure 17
4.1.6.2. Gamma-Ray Spectrometry 18
4.1.6.3. Spectrum and Data Evaluation 18
4.1.7. TNPGAA Analysis 21
4.1.7.1. Analytical Method 23
4.1.7.2. Irradiations 23
4.1.7.3. Data Evaluation 24
4.1.8. WDXRF Analysis 26
4.1.9. LC-ICP-MS 31
4.2. NMIJ Method for Arsenic Species 34
4.2.1. Instrumentation 34
4.2.2. Materials 34
4.2.3. Extraction procedure for arsenic species 35
4.2.4. Calculations 36
4.3. Interlaboratory Studies 37
4.3.1. HAMQAP Exercise 5 37
4.3.2. HAMQAP Exercise 6 37
5. Measurement Results 38
5.1. Moisture 38
5.1.1. NIST Moisture Results 38

5.1.2. Moisture Value Assignment and Dry-Mass Conversions 39
5.1.3. NMIJ Moisture Results 39
5.2. Elements 40
5.2.1. Aluminum Results 41
5.2.2. Arsenic Results 42
5.2.3. Bromine Results 44
5.2.4. Cadmium Results 45
5.2.5. Calcium Results 47
5.2.6. Chlorine Results 49
5.2.7. Copper Results 50
5.2.8. Iron Results 52
5.2.9. Lead Results 54
5.2.10. Magnesium Results 56
5.2.11. Manganese Results 58
5.2.12. Mercury Results 60
5.2.13. Molybdenum Results 62
5.2.14. Phosphorus Results 64
5.2.15. Potassium Results 66
5.2.16. Rubidium Results 68
5.2.17. Selenium Results 69
5.2.18. Sodium Results 71
5.2.19. Strontium Results 73
5.2.20. Sulfur Results 75
5.2.21. Zinc Results 77
5.2.22. Silicon Results 79
5.3. Arsenic Species 80
5.3.1. Organic Arsenical Results 80
5.3.2. Inorganic Arsenical Results 82
5.4. Proximates 84
5.4.1. Fat Results 84
5.4.2. Protein Results 85
5.4.3. Carbohydrates Results 85
5.4.4. Solids Results 86
5.4.5. Ash Results 86
5.4.6. Calories Results 87

6. Statistical Approaches for Value Assignment **88**
7. Certificate of Analysis **89**
References **90**
Appendix A. List of Acronyms **93**
Appendix B. Change Log **94**

List of Tables

Table 1. Methods Used for Elemental Determinations. **5**
Table 2. Microwave Settings for Digestion of SRM 1568c Samples for ICP-OES Analysis. **8**
Table 3. Standards and Approximate Mass Fractions for ICP OES Analyses. **8**
Table 4. ICP-OES Parameters Used to Measure Element Mass Fractions. **9**
Table 5. Uncertainty Budget for ICP-OES Analysis. **10**
Table 6. Microwave Settings for Digestion of SRM 1568c Samples for ID-CV-ICP-MS Analysis. **10**
Table 7. Uncertainty Budget for ID-CV-ICP-MS Analysis. **13**
Table 8. Standards and Approximate Mass Fractions for ICP-MS Analyses. **15**
Table 9. ICP-MS Parameters Used to Measure Elements. **15**
Table 10. Uncertainty Budget for ICP-MS Analysis. **16**
Table 11. SRM solutions and final standard mass fractions for INAA analysis. **17**
Table 12. Nuclides measured, gamma-ray peak energies, and interferences. **18**
Table 13. Uncertainty Budget for INAA Analysis. **21**
Table 14. H sensitivities for urea standards. **22**
Table 15. Sensitivities for S/H ratio standards. **22**
Table 16. Uncertainty Budget for TNPGAA Analysis. **26**
Table 17. Absorption Corrections for WDXRF Measurements. **28**
Table 18. Elements Excluded from Use as Calibration Materials Used for XRF Measurements. **28**
Table 19. Uncertainty Budget for WDXRF Analysis. **30**
Table 20. LC Parameters for Separating Arsenic Species in Rice Samples. **32**
Table 21. Uncertainty Budget for LC-ICP-MS Analysis. **33**
Table 22. NIST Results for Moisture, %. **38**
Table 23. Summary NMIJ Moisture Determinations. **40**
Table 24. Summary of Results for Aluminum (Al), mg/kg. **41**
Table 25. Summary of NIST Results for Arsenic (As), mg/kg. **42**
Table 26. Summary of HAMQAP Exercise 6 Results for Arsenic (As), mg/kg. **43**
Table 27. Summary of Results for Bromine (Br), mg/kg. **44**

Table 28. Summary of Results for Cadmium (Cd), mg/kg. 45
Table 29. Summary of Results for Calcium (Ca), mg/kg. 47
Table 30. Summary of HAMQAP Exercise 5 Results for Calcium (Ca), mg/kg. 48
Table 31. Summary of Results for Chlorine (Cl), mg/kg. 49
Table 32. Summary of Results for Copper (Cu), mg/kg. 50
Table 33. Summary of NIST Results for Iron (Fe), mg/kg. 52
Table 34. Summary of HAMQAP Exercise 5 Results for Iron (Fe), mg/kg. 53
Table 35. Summary of Results for Lead (Pb), mg/kg. 54
Table 36. Summary of Results for Magnesium (Mg), mg/kg. 56
Table 37. Summary of Results for Manganese (Mn), mg/kg. 58
Table 38. Summary of Results for Mercury (Hg), mg/kg. 60
Table 39. Summary of Results for Molybdenum (Mo), mg/kg. 62
Table 40. Summary of Results for Phosphorus (P), mg/kg. 64
Table 41. Summary of NIST Results for Potassium (K), mg/kg. 66
Table 42. Summary of HAMQAP Results for Potassium (K), mg/kg. 67
Table 43. Summary of Results for Rubidium (Rb), mg/kg. 68
Table 44. Summary of Results for Selenium (Se), mg/kg. 69
Table 45. Summary of Results for Sodium (Na), mg/kg. 71
Table 46. Summary of Results for Strontium (Sr), mg/kg. 73
Table 47. Summary of Results for Sulfur (S), mg/kg. 75
Table 48. Summary of Results for Zinc (Zn), mg/kg. 77
Table 49. Summary of Results for Silicon (Si), mg/kg. 79
Table 50. Summary of NIST Results for Organic Arsenicals: MMA and DMA; mg/kg. 80
Table 51. Summary of NIST Results for Organic Arsenic Acids: MMA and DMA; mg/kg. 81
Table 52. Summary of NIST Results for Inorganic Arsenic Species: AsIII, AsV, and iAs; mg/kg. 82
Table 53. Summary of NIST Results for Total Inorganic Arsenic (iAs); mg/kg. 83
Table 54. Summary of Results for Total Fat, %. 84
Table 55. Summary of Results for Protein, %. 85
Table 56. Summary of Results for Carbohydrates, %. 85
Table 57. Summary of HAMQAP 6 Results for Solids, %. 86
Table 58. Summary of Results for Ash, %. 86
Table 59. Summary of Results for Calories, kcal/100 g. 87

List of Figures

Fig. 1. NIST adaptation of the AOAC INTERNATIONAL food composition triangle. 2
Fig. 2. Sales History of Rice Flour SRMs. 2
Fig. 3. Location of Customers for the Rice Flour SRMs. 3
Fig. 4. Typical Chromatogram of a SRM 1568c Sample Spiked with TMAO. 32
Fig. 5. Exemplar Chromatograms of the Mixed Standard Solution and SRM 1568c Extracts. 35
Fig. 6. Calibration Curves for iAs, MMA, and DMA. 36
Fig. 7. Mass Loss (% Moisture) of SRM 1568c as a Function of Method. 39
Fig. 8. NMIJ's Mass Loss (% Moisture) of SRM 1568c. 40
Fig. 9. Aluminum (Al) Mass Fraction as a Function of Bottle Number. 41
Fig. 10. Arsenic (As) Mass Fraction as a Function of Bottle Number. 42
Fig. 11. Comparison of Arsenic (As) Mass Fraction Values by Method. 43
Fig. 12. Bromine (Br) Mass Fraction as a Function of Bottle Number. 44
Fig. 13. Cadmium (Cd) Mass Fraction as a Function of Bottle Number. 46
Fig. 14. Comparison of Cadmium (Cd) Mass Fraction Values by Method. 46
Fig. 15. Calcium (Ca) Mass Fraction as a Function of Bottle Number. 47
Fig. 16. Comparison of Calcium (Ca) Mass Fraction Values by Method. 48
Fig. 17. Chlorine (Cl) Mass Fraction as a Function of Bottle Number. 49
Fig. 18. Copper (Cu) Mass Fraction as a Function of Bottle Number. 50
Fig. 19. Comparison of Copper (Cu) Mass Fraction Values by Method. 51
Fig. 20. Iron (Fe) Mass Fraction as a Function of Bottle Number. 52
Fig. 21. Comparison of Iron (Fe) Mass Fraction Values by Method. 53
Fig. 22. Lead (Pb) Mass Fraction as a Function of Bottle Number. 55
Fig. 23. Comparison of Lead (Pb) Mass Fraction Values by Method. 55
Fig. 24. Magnesium (Mg) Mass Fraction as a Function of Bottle Number. 56
Fig. 25. Comparison of Magnesium (Mg) Mass Fraction Values by Method. 57
Fig. 26. Manganese (Mn) Mass Fraction as a Function of Bottle Number. 58
Fig. 27. Comparison of Manganese (Mn) Mass Fraction Values by Method. 59
Fig. 28. Mercury (Hg) Mass Fraction as a Function of Bottle Number. 60
Fig. 29. Comparison of Mercury (Hg) Mass Fraction Values by Method. 61
Fig. 30. Molybdenum (Mo) Mass Fraction as a Function of Bottle Number. 62
Fig. 31. Comparison of Molybdenum (Mo) Mass Fraction Values by Method. 63
Fig. 32. Phosphorous (P) Mass Fraction as a Function of Bottle Number. 64
Fig. 33. Comparison of Phosphorus (P) Mass Fraction Values by Method. 65
Fig. 34. Potassium (K) Mass Fraction as a Function of Bottle Number. 66

Fig. 35. Comparison of Potassium (K) Mass Fraction Values by Method. 67
Fig. 36. Rubidium (Rb) Mass Fraction as a Function of Bottle Number. 68
Fig. 37. Selenium (Se) Mass Fraction as a Function of Bottle Number. 69
Fig. 38. Comparison of Selenium (Se) Mass Fraction Values by Method. 70
Fig. 39. Sodium (Na) Mass Fraction as a Function of Bottle Number. 71
Fig. 40. Comparison of Sodium (Na) Mass Fraction Values by Method. 72
Fig. 41. Strontium (Sr) Mass Fraction as a Function of Bottle Number. 73
Fig. 42. Comparison of Strontium (Sr) Mass Fraction Values by Method. 74
Fig. 43. Sulfur (S) Mass Fraction as a Function of Bottle Number. 75
Fig. 44. Comparison of Sulfur (S) Mass Fraction Values by Method. 76
Fig. 45. Zinc (Zn) Mass Fraction as a Function of Bottle Number. 77
Fig. 46. Comparison of Zinc (Zn) Mass Fraction Values by Method. 78
Fig. 47. Silicon (Si) Mass Fraction as a Function of Bottle Number. 79
Fig. 48. NIST's Organic Arsenic Acids Mass Fractions as Functions of Bottle Number. 80
Fig. 49. NMIJ's Organic Arsenical Mass Fractions as Functions of Sample Index. 81
Fig. 50. Comparison of MMA and DMA Mass Fraction Values by Method. 81
Fig. 51. Inorganic Arsenic Species Mass Fractions as Functions of Bottle Number. 82
Fig. 52. NMIJ's Total Inorganic Arsenic (iAs) Mass Fractions as a Function of Sample Index. 83
Fig. 53. Comparison of Total Inorganic Arsenic (iAs) Mass Fraction Values by Method. 83

1. Introduction

The elemental mass fraction and composition of rice is reflective of the environment in which it is grown, yielding information both about the agricultural area of origin and the dietary exposure to environmental contaminants. Rice flour is the basis of numerous food products including cereals, crackers, and biscuits for infants whose developing central nervous systems are particularly vulnerable to the presence of environmental toxins such as lead, cadmium, mercury, and arsenic. Because toxicity depends on the form (species) of the toxin, it becomes necessary not only to determine total element content, but also to differentiate and quantitate the various inorganic and organic forms of these metals. The U.S. Food and Drug Administration (FDA) monitors levels of arsenic and arsenic species in certain foods, dietary supplements, and cosmetics [1].

The National Institute of Standards and Technology (NIST)'s first rice flour Standard Reference Material® (SRM®), SRM 1568 Rice Flour [2], became available in 1978. This SRM delivered values for 17 elements, including arsenic, cadmium, and mercury. SRM 1568 was replaced by SRM 1568a [3] in 1988, delivering values for 26 elements including lead. SRM 1568a was replaced by SRM 1568b [4] in 2013, delivering values for 20 elements and three arsenic species. SRM 1568b was replaced by SRM 1568c Rice Flour [5] in 2022. SRM 1568c originally delivered certified values for 16 elements and non-certified values for an additional five elements, three arsenic species, and six proximates. Results provided by the National Metrology Institute of Japan (NMIJ) in 2025 enables certifying the values for the arsenic species.

The Standard Reference Material® (SRM®) 1568 Rice Flour series of certified reference materials are in sector 5 of the AOAC INTERNATIONAL food composition triangle [6, 7] (Fig. 1). The information provided in this diagram is used by measurement laboratories in support of nutrition labeling. Laboratories needing a rice flour or similar material for the demonstration of method validity and accuracy when analyzing food products to generate data for nutrition labels can use the currently available edition of SRM 1568. The SRM can also be used to test methodologies for food safety.

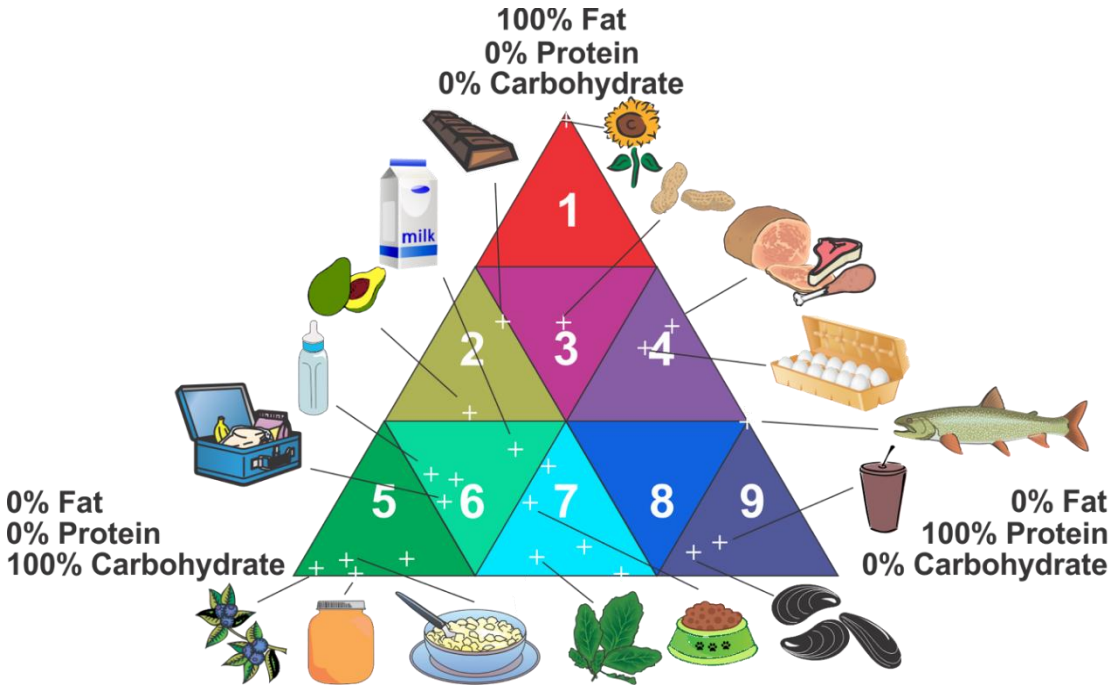


Fig. 1. NIST adaptation of the AOAC INTERNATIONAL food composition triangle.
The white "+" depict the location of available food-matrix reference materials.

The sales history of the SRM 1568 series from the first available sales record in 1990 to the version date of this document is displayed in Fig. 2. The proportion of sales to various countries or geographical regions over the past 35 years is displayed in Fig. 3.

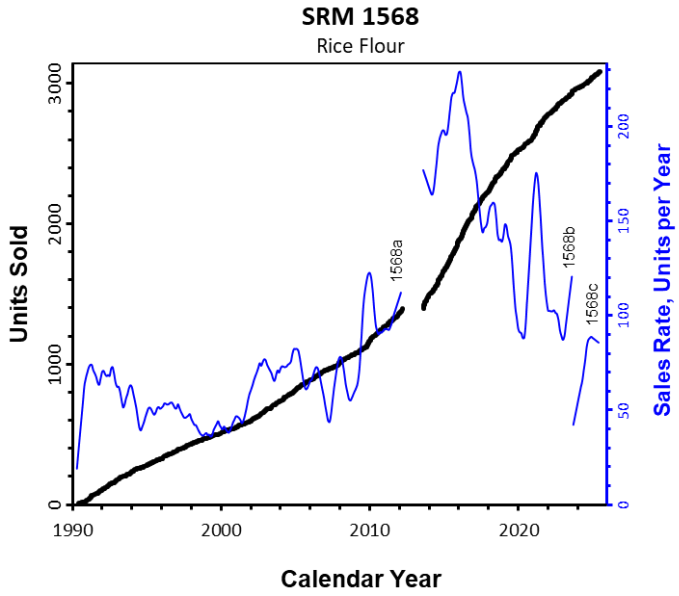


Fig. 2. Sales History of Rice Flour SRMs.
The thick black line depicts the cumulative distribution of sales as a function of the order date, plotted using the "Units Sold" axis at the left of the graph. The thin blue line depicts the sales rate (the first derivative of the cumulative distribution), plotted using the "Sales Rate, Units per Year" axis to the right of the graph.

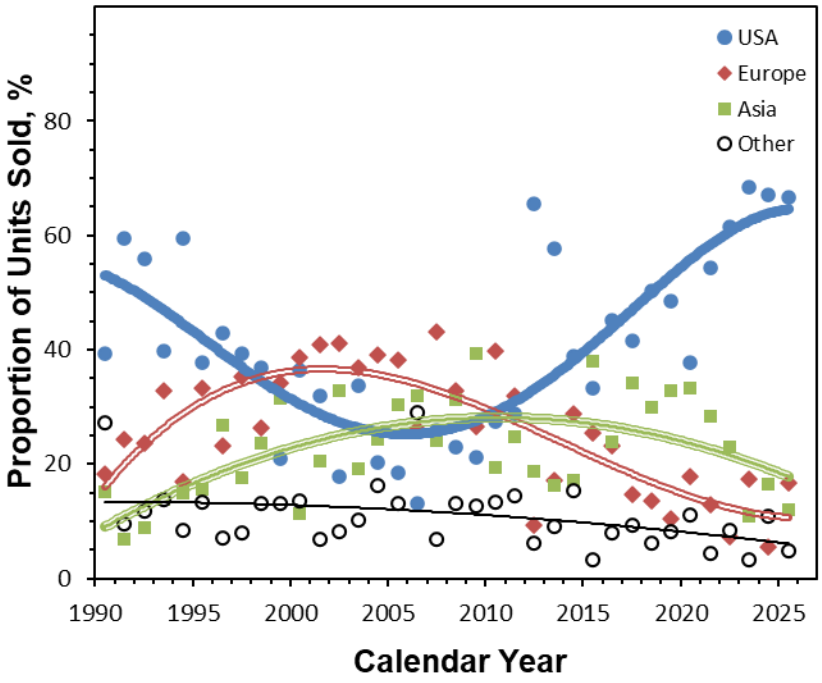


Fig. 3. Location of Customers for the Rice Flour SRMs.

The solid circles and the thick trendline display the proportion of sales to customers within the USA. Solid diamonds and the double-line display the proportion of units sold to customers in Europe. Solid squares and the triple-line display the proportion sold to customers in Asia. The open circles and thin single-line display the proportion of units sold to customers elsewhere.

2. Material

2.1. Acquisition & Packaging

The material used to produce SRM 1568c Rice Flour was procured from three commercial vendors of brown rice flour. Eighty-eight kilograms of brown rice flour were blended and bottled at NIST (Gaithersburg, MD). All 88 kg of rice flour were double blended for 30 min using a ceramic-lined cone blender. Fifty grams of material were placed into pre-washed amber bottles under an environmental hood with a dust collector using a polytetrafluoroethylene (PTFE)-lined hopper and trough. A total of 1723 bottles were filled.

2.2. Irradiation

The bottled units of SRM 1568c were irradiated by Neutron Products, Inc. (Dickerson, MD) in the six cardboard containers sent from NIST. The target for the absorbed dose was 6 kGy to 10 kGy. The actual absorbed doses measured by Neutron Products were 6.0 kGy to 8.6 kGy.

2.3. Storage

The bottles of SRM 1568c have been stored at room temperature (18 °C to 22 °C) at NIST since their production.

3. Element-Related Analytes

A summary of the element-related analytes (total element, inorganic arsenic species, organic arsenic acids) analyzed for value assignment in SRM 1568c is listed in Table 1. The table also lists the methods used by participants in NIST's Health Assessment Measurements Quality Assurance Program (HAMQAP) interlaboratory studies (see Section 4.3).

Table 1. Methods Used for Elemental Determinations.

Name	Symbol	NIST Methods	NMIJ Methods	HAMQAP Methods [a]
Aluminum	Al	ICP-MS		
Arsenic	As	ICP-MS, INAA		ICP-OES, ICP-MS
Inorganic Arsenic	iAs	LC-ICP-MS	HPLC-ICP-MS	
Arsenic Acid	As III	LC-ICP-MS		
Arsenous Acid	As V	LC-ICP-MS		
Dimethylarsinic Acid	DMA	LC-ICP-MS	HPLC-ICP-MS	
Monomethylarsonic Acid	MMA	LC-ICP-MS	HPLC-ICP-MS	
Bromine	Br	INAA		
Cadmium	Cd	ICP-MS		AAS, ICP-MS, ICP-OES, ID ICP-MS
Calcium	Ca	ICP-OES, WDXRF		ICP-MS, ICP-OES, ID ICP-MS
Chlorine	Cl	WDXRF		
Copper	Cu	ICP-OES, WDXRF		
Iron	Fe	ICP-OES, WDXRF		ICP-MS, ICP-OES, ID ICP-MS
Lead	Pb	ICP-MS		ICP-MS, ICP-OES, ID ICP-MS
Magnesium	Mg	ICP-OES, WDXRF		
Manganese	Mn	ICP-OES, WDXRF		
Mercury	Hg	ID-CV-ICP-MS		
Molybdenum	Mo	ICP-MS, INAA		
Phosphorus	P	ICP-OES, WDXRF		
Potassium	K	ICP-OES, WDXRF		ICP-MS, ICP-OES, ID ICP-MS
Rubidium	Rb	ICP-MS		
Selenium	Se	ICP-MS, INAA		
Strontium	Sr	ICP-MS, ICP-OES		
Sodium	Na	ICP-OES		ICP-MS, ICP-OES
Sulfur	S	TNPGAA, WDXRF		
Zinc	Zn	ICP-OES, WDXRF		

[a] Not all participants in the HAMQAP studies reported the method they used.

Acronyms:

AAS	Atomic Absorption Spectroscopy
HPLC-ICP-MS	High-Performance Liquid Chromatography Inductively Coupled Plasma Mass Spectrometry
ICP-MS	Inductively Coupled Plasma Mass Spectrometry
ICP-OES	Inductively Coupled Plasma Optical Emission Spectrometry
ID ICP-MS	Isotope Dilution Inductively Coupled Plasma Mass Spectrometry
ID-CV-ICP-MS	Isotope Dilution Cold Vapor Inductively Coupled Plasma Mass Spectrometry
INAA	Instrumental Neutron Activation Analysis
LC-ICP-MS	Liquid Chromatography Inductively Coupled Plasma Mass Spectrometry
TNPGAA	Thermal Neutron Prompt Gamma-Ray Activation Analysis
WDXRF	Wavelength Dispersive X-ray Fluorescence Spectrometry

4. Experimental Procedures

4.1. NIST Methods and Procedures

4.1.1. Desiccator Drying

Single aliquots from each of 12 freshly opened bottles were placed in pre-weighed, glass weighing vessels (m_b) to an approximate depth of 1 cm. The bottles were rotated to mix the contents prior to sampling. The vessels were again weighed (m_w) and placed in a desiccator over magnesium perchlorate ($Mg(ClO_4)_2$). The samples were removed from the desiccator on day 5, weighed, returned to the desiccator, and the results (m_d) recorded. The weighing process was repeated on day 7, day 14, day 22, day 28, day 35, and day 42. All weighings were performed using the same balance, serviced and calibrated annually by Mettler Toledo, LLC. Prior to each use, balance calibration was verified by using standard masses ranging from 0.5 g to 20 g that are traceable to the International System of Units (SI) through the standard mass set maintained by the Inorganic Chemical Metrology Group.

The moisture was calculated, assuming that all changes in mass were due to loss of moisture alone, using the following equations:

$$\text{Moisture content} = 100 * \frac{m_w - m_d}{m_w - m_b} \quad (1)$$

$$U_{95}(\text{Moisture content}) = 2.2 * \sqrt{u_a^2 + u_{b1}^2 + u_{b2}^2 + u_{b3}^2} \quad (2)$$

where: u_a = standard deviation for the sample weighings (where n=12 refers to the individual number of samples taken from the bottles),

u_{bi} = standard uncertainties of each weighing, each estimated to be ± 0.01/√3 mg. For each u_{bi} this value is converted to moisture content by division of the mean sample mass value.

U_{95} = the expanded uncertainty, expressed at an approximate confidence level of 95 % by choosing the expansion factor 2.2, calculated based on degrees of freedom.

4.1.2. Forced Air Drying

Single aliquots from each of 12 freshly opened bottles were placed in pre-weighed, glass weighing vessels (m_b) to an approximate depth of 1 cm. The bottles were rotated to mix the contents prior to sampling. The vessels were again weighed (m_w) and placed in a forced-air drying oven set at 90 °C with caps removed. After 4 h, the samples were removed, capped, and allowed to cool to room temperature in a desiccator. Cooled samples were removed from the desiccator, weighed, and the results (m_d) recorded. All weighings were performed using the same balance, serviced and calibrated annually by Mettler Toledo, LLC. Prior to each use, balance calibration was verified by using standard masses ranging from 0.5 g to 20 g that are traceable to the SI through the standard mass set maintained by the Inorganic Chemical Metrology Group.

The moisture was calculated, assuming that all changes in mass were due to loss of moisture alone, using the following equations:

$$\text{Moisture content} = 100 * \frac{m_w - m_d}{m_w - m_b} \quad (3)$$

$$U_{95}(\text{Moisture content}) = 2.2 * \sqrt{u_a^2 + u_{b1}^2 + u_{b2}^2 + u_{b3}^2} \quad (4)$$

where: u_a = standard deviation for the sample weighings (where n=12 refers to the individual number of samples taken from the bottles).

u_{bi} = standard uncertainties of each weighing, each estimated to be ± 0.01/√3 mg. For each u_{bi} this value is converted to moisture content by division of the mean sample mass value.

U_{95} = the expanded uncertainty, expressed at an approximate confidence level of 95 % by choosing the expansion factor 2.2, calculated based on degrees of freedom.

4.1.3. ICP-OES Analysis

Mass fractions of Ca, Cu, Fe, K, Mg, Mn, Na, P, Sr, and Zn in SRM 1568c Rice Flour were determined at NIST using ICP-OES. Two 0.5 g aliquots were taken from each of 10 bottles of SRM 1568c Rice Flour and were placed into PTFE microwave vessels. Two 0.5 g aliquots were taken from each of two bottles of SRM 1568b Rice Flour and prepared along with the samples for quality assurance. For the determination of Fe, four aliquots were taken from one bottle of SRM 1568b for quality assurance and for the determination of Na, four aliquots were taken from one bottle of 1567b Wheat Flour for quality assurance. All samples were analyzed in as-received condition. Twelve procedural reagent blanks were also prepared along with the samples. Concentrated nitric acid (HNO_3, 10 mL) was added to each vessel, and indium (0.25 mL of a 100 mg/kg In solution) and scandium (0.5 mL of a 100 mg/kg Sc solution) were added as internal standards to improve the precision of the instrumental measurements to all samples except those to be analyzed for Na. The In solution was prepared in-house from Indium Corporation of America Lot # JK 1171 to a final concentration of 1.5 % (volume fraction) HNO_3. The Sc solution was prepared from SRM 3148a Scandium (Sc) Standard Solution Lot No. 100701 to a final concentration of 1.5 % (volume fraction) HNO_3. For Na measurements, strontium (0.25 mL of a 0.1 µg/kg Sr solution) was added as an internal standard. The Sr solution was prepared from SRM 3153a Strontium (Sr) Standard Solution Lot # 990906) to a final concentration of 1.5 % (volume fraction) HNO_3. All weighings were performed using a Mettler AT261 Delta Range analytical balance serviced and calibrated annually by Mettler Toledo, LLC. Prior to each use, calibration is verified by using standard masses ranging from 0.5 g to 20 g that are traceable to the SI through the standard mass set maintained by the Inorganic Chemical Metrology Group.

All prepared samples, controls, and blanks were digested using a CEM MARS microwave sample preparation system according to the microwave procedure in Table 2. After microwave digestion, solutions were transferred to PTFE beakers and heated on a hot plate with a surface temperature of approximately 180 °C until the volume was reduced to near dryness. Samples were then diluted using 1.5 % (volume fraction) HNO_3 and transferred to polyethylene bottles.

All samples were prepared using Optima grade HNO_3 from Fisher Scientific. Samples and acids were diluted using 18 MΩ·cm water. All dilute acid concentrations are expressed in volume fractions with respect to the concentrated acid.

Table 2. Microwave Settings for Digestion of SRM 1568c Samples for ICP-OES Analysis.

Step	Power (W)	Power Setting (%)	Ramp Time (min)	Temperature (°C)	Hold Time (min)
1	1600	85	20	170	20
2	1600	100	20	195	20

Analyte mass fractions were calculated by the method of standard additions to compensate for any matrix effects. Sample solutions contained the approximate analyte mass factions list in Table 3. From each sample solution, two aliquots were taken, and a matrix matched spike was added to one. The mass fraction in the sample solution, mass fractions added (spike) to the second aliquot, and the total mass fraction expected in the spiked solution are listed in Table 3. Analyte mass fractions for Fe were calculated by the method of external standard calibration.

Table 3. Standards and Approximate Mass Fractions for ICP OES Analyses.

Analyte		SRM		Mass Fraction in Sample Solution (mg/kg)	Mass Fraction Added (Spike) (mg/kg)	Total Mass Fraction in Spiked Aliquot (mg/kg)
Element	Symbol	Number	Lot			
Calcium	Ca	3109a	130213	0.07	0.14	0.21
Copper	Cu	3114	120618	0.03	0.09	0.12
Iron	Fe	3126a	140812	0.4	0.0	0.4
Potassium	K	3141a	140813	0.4	0.7	1.1
Magnesium	Mg	3131a	140110	0.3	0.4	0.7
Manganese	Mn	3132	050429	0.3	0.7	1.0
Sodium	Na	3152a	120715	0.4	0.45	0.85
Phosphorus	P	3139a	060717	0.4	0.9	1.3
Strontium	Sr	3153a	990906	0.007	0.006	0.13
Zinc	Zn	3168a	120629	0.3	0.8	1.1

A Perkin-Elmer Optima 8300 Dual View ICP-OES was used for analysis. The mass fractions of the analytes in the sample, control, and blank solutions were measured according to the parameters in Table 4.

Table 4. ICP-OES Parameters Used to Measure Element Mass Fractions.

Analyte		Wavelength		Integration Time	Read Time	Number
Element	Symbol	(nm)	Plasma View	(s)	(s)	of Runs
Calcium	Ca	317.933	Axial	0.10	1	2
Copper	Cu	224.700	Axial	0.10	1	2
Iron	Fe	259.939	Axial	0.10	1	2
Potassium	K	766.550	Radial	0.10	1	2
Magnesium	Mg	285.213	Axial	0.10	1	2
Manganese	Mn	257.610	Axial	0.10	1	2
Sodium	Na	589.478	Radial	0.10	1	2
Phosphorus	P	214.914	Axial	0.20	1	2
Zinc	Zn	213.857	Axial	0.10	1	2
Indium	In	230.606	Axial	0.10/0.20	1	2
Scandium	Sc	361.383	Axial/Radial	0.10	1	2
Strontium	Sr	421.552	Axial/Radial	0.10	1	2
Yttrium	Y	324.227	Axial	0.10	1	2

Four instrumental measurements were averaged for each sample aliquot and each spiked aliquot. All results were corrected for the mean blank values from their corresponding runs by subtracting the mean total micrograms found in the blanks from the total micrograms found in each individual sample. After exporting raw data to Microsoft Excel, final mass fractions were calculated using the method of standard additions.

Table 5 describes the uncertainty budget for determination of Ca, Cu, Fe, K, Mg, Mn, Na, P, Sr, and Zn by ICP-OES. The table provides the names and symbols for recognized uncertainty components, the basis for determining the contributions to the total uncertainty, whether the contributions are determined by current experiment (Type A) or from other sources (Type B), and the number of associated degrees of freedom (DF). Type B components typically are associated with large numbers of degrees of freedom, where “large” can be any value greater than 60, the number of DF for a Student’s *t* 95 % confidence expansion factor of 2.0.

Table 5. Uncertainty Budget for ICP-OES Analysis.

Component	Basis	Type	DF
Sample Replication, s_{sample}	The uncertainty due to sample preparation and measurement is estimated by calculating the standard deviation of the mean. (n = 4 or 6,19 or 21; SRM 1568b and SRM 1568c respectively)	A	3,5 (1568b) 18,20 (1568c)
Blank Replication, s_{blank}	The uncertainty due to blank preparation and measurement is estimated by calculating the standard deviation of the mean. (n = 10)	A	9
Moisture Correction, $s_{moisture}$	The uncertainty due to the moisture correction is estimated by calculating the standard deviation of the mean then converting percent moisture to mass. (n = 10)	A	9
Primary Standard, u_s	The uncertainty associated with the primary standards is calculated to be the expanded uncertainty divided by the expansion factor, k, obtained from the Certificate of Analysis for each SRM used as the standard addition spike.	B	> 60
Weighing of Standards, u_{b1}	The uncertainty for each weighing of the standard is ± 0.01 mg based on the certificate of calibration for the balance. This uncertainty is normalized by division by √3.	B	> 60
Weighing of Samples, u_{b2}	The uncertainty for each weighing of the sample is ± 0.01 mg based on the certificate of calibration for the balance. This uncertainty is normalized by division by √3.	B	> 60

4.1.4. ID-CV-ICP-MS Analysis

The mass fraction of Hg in SRM 1568c Rice Flour was determined at NIST using ID-CV-ICP-MS. Single 0.5 g aliquots were taken from each of 6 bottles of SRM 1568c Rice Flour and four 0.5 aliquots from a single bottle of SRM 1568b, used for quality assurance, were placed into quartz microwave vessels. Each sample was spiked with an accurately weighed aliquot of ^{201}Hg followed by the addition of 6 g high purity HNO_3 (Fisher Scientific, Suwanee, GA). Four procedural blanks, containing a small aliquot of ^{201}Hg spike only, were carried through the entire sample processing and measurement scheme. All weighings were performed using a Sartorius MSE524S analytical balance serviced and calibrated annually by Pipette Repair Service, Inc. Prior to each use, calibration was verified by using standard masses ranging from 0.5 g to 20 g that are traceable to the SI through the standard mass set maintained by the Inorganic Chemical Metrology Group.

Microwave digestion was carried out in an Anton Paar (Ashland, VA) Multiwave 3000 microwave using the program described in Table 6.

Table 6. Microwave Settings for Digestion of SRM 1568c Samples for ID-CV-ICP-MS Analysis.

Step	Power (W)	Ramp Time (min)	Hold Time (min)
1	600	10	5
2	1400	5	20

Microwave settings for digestion in Table 6 include a 30 min cool down. After cooling to room temperature, the contents were transferred to 50 mL polypropylene centrifuge tubes and diluted to approximately 0.15 ng/g ^{201}Hg, which was suitable for measurement by cold-vapor ICP-MS. Approximately 0.5 g of high purity hydrochloric acid (HCl) (Fisher Scientific, Suwanee, GA) was added to each sample for additional Hg stabilization. Analytical measurements were completed within one day of dilution to reduce the risk of external contamination and Hg losses from the solutions during storage.

Mercury measurements were made using cold-vapor Hg generation coupled with ICP-MS isotope ratio measurements. The Hg vapor was generated using tin (II) chloride reductant (10 % mass fraction in 7 % volume fraction HCl) and separated from the liquid phase using a commercial (CETAC) glass reaction/separator cell. The vapor was transferred to Thermo Electron X Series II ICP-MS (Bremen, Germany) with 1/16 inch (1.6 mm) internal diameter Viton tubing, using an argon carrier gas flow rate of approximately 100 mL/min. This gas stream was mixed with the plasma injector gas stream using a plastic T piece. The ICP-MS was operated in a dry plasma mode, which necessitated slight re-tuning of the ion lenses relative to an aqueous aerosol sample introduction system. All samples were transferred to the instrument in manual sequence, and the timing of the sample uptake was adjusted to allow sufficient time to measure the instrument background prior to measurement of the sample. The ^{201}Hg and ^{202}Hg isotopes were monitored for a duration of 60 s in a pulse counting Time-Resolved-Analysis (TRA) mode to recover the individual ion count rates. The isotope-time profiles were downloaded to a Microsoft Excel spreadsheet for calculation of background corrected ^{201}Hg/^{202}Hg ratios using Isotope Dilution Assistant (IDA) v0.9 [8,9]. The instrument detector dead-time was 33 ns.

The working ^{201}Hg isotopic spike solution was prepared by accurate gravimetric dilution of a master stock solution, which was calibrated by reverse isotope dilution using a high-purity primary standard (SRM 3133 Mercury (Hg) Standard Solution, Lot # 160921). Two separate stock solutions were prepared by serial dilution. Two spike calibration mixtures were prepared from each of these solutions, generating four spike mixtures, and these were measured using cold-vapor ICP-MS, under the same conditions as the samples (double IDMS).

Moisture content was determined from a single sub-sample for each bottle of candidate SRM 1568c and four replicate subsamples from a single bottle of SRM 1568b. Approximately 1 g of each sample was weighed into a glass weighing bottle, dried for 2 h at 90 °C in an ED 23-UL oven (Binder, Inc., Bohemia, NY), stored in a glass desiccator over DRIERITE desiccant (W. A. Hammond DRIERITE Co. LTD, Xenia, OH) until cooled to room temperature, and weighed again for moisture mass loss.

The following functional relationship was used to calculate each of the individual replicate ID ICP-MS mass fraction results:

$$c_{\mathrm{S}} = \left(\frac{M_{\mathrm{S}}K(A_{\mathrm{S}} - B_{\mathrm{S}}FR)}{(BFR - A)} - S_{\mathrm{B}}\right) * \frac{D_{\mathrm{C}}}{W} \quad (5)$$

where C_S = wet mass fraction of mercury in the sample (µg/g),
M_S = absolute mass of ^{201}Hg spike added (µg),
K = natural to spike (^{202}Hg/^{201}Hg) atomic weight ratio,
A_S = fractional abundance of the reference isotope (^{202}Hg) in the spike,
B_S = fractional abundance of the spike isotope (^{201}Hg) in the spike,
F = discrimination correction factor for measured ratio R,
R = detector dead-time corrected ^{202}Hg/^{201}Hg ratio,
B = natural fractional abundance of the spike isotope (^{201}Hg),
A = natural fractional abundance of the reference isotope (^{202}Hg),
S_B = absolute mean measured blank (µg),
D_c = wet-dry mass correction factor,
W = mass of sample aliquot taken (g).

The overall mean of the four procedural blank measurements (S_B) was not used to correct the sample measurement data since the ^{202}Hg counts in the blanks were extremely low and were not greater than the instrument background signal.

Table 7 describes the uncertainty budget for the determination of Hg by ID-CV-ICP-MS. The table provides the names and symbols for recognized uncertainty components, the basis for determining the contributions to the total uncertainty, whether the contributions are determined by the current experiment (Type A) or from other sources (Type B), and the number of associated degrees of freedom (DF). Type B components typically are associated with large numbers of degrees of freedom, where “large” can be any value greater than 60, the number of DF for a Student’s *t* 95 % confidence expansion factor of 2.0.

Table 7. Uncertainty Budget for ID-CV-ICP-MS Analysis.

Uncertainty	Basis	Type	DF
Sample Replication, R_1	Standard uncertainty of sample measurements based on four or five replicate measurements incorporating sample heterogeneity and sample digestion, with degrees of freedom n - 1	A	2 or 5
Calibration of isotopic spike, R_2	Standard uncertainty of the spike calibration measurements (reverse IDMS) using four independently prepared calibration mixes	A	3
Moisture Correction, D_c	Standard deviation of moisture correction factor repeatability as a percentage of the mean Hg mass fraction	A	3 or 5
Natural / spike atomic weight ratio, *K*	Uncertainty of the factor K, the IUPAC atomic weight for mercury, divided by the atomic weight of the spike determined by isotopic measurements	B	> 60
Abundance of ^{202}Hg in the spike, A_s	Uncertainty of the spike isotopic composition, and relative impact on the measurement of Hg in SRM 1568b and SRM 1568c by double IDMS	B	> 60
Abundance of ^{201}Hg in the spike, B_s	Uncertainty of the spike isotopic composition, and relative impact on the measurement of Hg in SRM 1568b and SRM 1568c by double IDMS	B	> 60
^{201}Hg/^{202}Hg ratio measurement, *R*	Uncertainty of the dead-time corrected ICP-MS isotope ratio measurements based on the pooled standard deviation of approximately 500 ratio measurement points and subtraction of the instrument blank counts on each isotope	**B**	> 60
Mass discrimination correction, *F*	Uncertainty of the correction factor (T/E) for the instrument mass bias / mass discrimination and the impact on the measured mass fraction of Hg in SRM 1568b and SRM 1568c using a double IDMS approach	B	> 60
Abundance of ^{201}Hg in the sample, *B*	Uncertainty of the sample isotopic composition, and relative impact on the measurement of Hg in SRM 1568b and SRM 1568c by double IDMS	B	> 60
Abundance of ^{202}Hg in the sample, *A*	Uncertainty of the sample isotopic composition, and relative impact on the measurement of Hg in SRM 1568b and SRM 1568c by double IDMS	B	> 60
Mass measurement of sample aliquot, *W*	Relative standard uncertainty due to weighing on a four- place balance, calculated using observed standard deviation and assuming a rectangular distribution	B	> 60
Mass of ^{201}Hg added, M_s	Relative standard uncertainty of the primary calibrant SRM 3133, the stated COA expanded uncertainty divided by coverage factor k = 2.183	B	> 60

4.1.5. ICP-MS Analysis

Mass fractions of Al, As, Cd, Mo, Pb, Rb, Se, and Sr in SRM 1568c Rice Flour were determined at NIST using ICP-MS. Two 0.5 g aliquots were taken from each of 10 bottles of SRM 1568c Rice Flour and were placed into PTFE microwave vessels. Four 0.5 g aliquots were taken from one bottle of SRM 1568b Rice Flour and prepared along with the samples for quality assurance. Ten procedural reagent blanks were also prepared along with the samples. To each vessel, 10 mL of concentrated HNO_3 was added along with 0.5 mL of an internal standard solution containing 200 ng/g Bi, 200 ng/g Sb, and 200 ng/g Y to improve the precision of the instrumental measurements. The internal standard solution was prepared from SRM 3106 Bismuth (Bi) Standard Solution Lot # 180815, SRM 3102a Antimony (Sb) Standard Solution Lot # 149011, and SRM 3167a Yttrium (Y) Standard Solution Lot # 120314 with a final acid concentration of 1.5 % HNO_3 (volume fraction). All weighings were performed using a Mettler AT261 Delta Range analytical balance serviced and calibrated annually by Mettler Toledo, LLC. Prior to each use, calibration was verified by using standard masses ranging from 0.5 g to 20 g that are traceable to the SI through the standard mass set maintained by the Inorganic Chemical Metrology Group.

All prepared samples, controls, and blanks were digested using a CEM MARS microwave sample preparation system according to the microwave procedure in Table 2. After microwave digestion, solutions were transferred to PTFE beakers and were heated on a hot plate with a surface temperature of approximately 180 °C until the volume was reduced to near dryness. Samples were then diluted using 1.5 % (volume fraction) HNO_3 and transferred to polyethylene bottles.

All samples were prepared using Optima grade HNO_3 from Fisher Scientific. Samples and acids were diluted using 18 MΩ·cm water. All dilute acid concentrations are expressed in volume fractions with respect to the concentrated acid.

All samples were analyzed in as-received condition. The results for SRM 1568b were corrected for moisture content determined by drying at 90 °C for 2 h, a procedure described in the COA for SRM 1568b. The results for SRM 1568c were corrected for moisture content according to the procedure listed above in Section 3.1.1.2. The moisture content was determined at the time samples were taken, and values were reported on a dry-mass basis.

Analyte mass fractions were calculated by the method of standard additions to compensate for any matrix effects. From each sample dilution, two aliquots were taken; a matrix matched spike was added to one. The sample mass fraction dilutions, mass fractions of the matrix matched spike solution added to the second aliquot, and the total mass fraction expected in the spiked solution are listed in Table 8.

Table 8. Standards and Approximate Mass Fractions for ICP-MS Analyses.

Analyte		SRM		Mass Fraction in Sample Solution (mg/kg)	Mass Fraction Added (Spike) (mg/kg)	Total Mass Fraction in Spiked Aliquot (mg/kg)
Element	Symbol	Number	Lot			
Aluminum	Al	3101a	140903	0.07	0.14	0.21
Arsenic	As	3103a	100818	0.03	0.09	0.12
Cadmium	Cd	3108	130116	0.4	0.0	0.4
Molybdenum	Mo	3134	130418	0.4	0.7	1.1
Lead	Pb	3128	301026	0.3	0.4	0.7
Rubidium	Rb	3145a	150622	0.3	0.7	1.0
Selenium	Se	3149	100901	0.4	0.45	0.85
Strontium	Sr	3153a	990906	0.4	0.9	1.3

An Agilent 7500cs ICP-MS, equipped with a Peltier-cooled, inert sample introduction system, was used for analysis. The mass fractions of analytes in the solutions were measured according to the parameters in Table 9 using H_2 as a collision gas to minimize polyatomic interferences. Ten instrumental measurements were taken and averaged for each sample aliquot and each spiked aliquot. All results were corrected for the mean blank values from their corresponding runs by subtracting the mean total micrograms found in the blanks from the total micrograms found in each individual sample.

Table 9. ICP-MS Parameters Used to Measure Elements.

Analyte		Mass	Integration Time	Read Time	Number
Element	Symbol	(amu)	(s)	(s)	of Runs
Aluminum	Al	27	0.1	3	3
Arsenic	As	75	0.1	3	2
Cadmium	Cd	114	0.1	3	2
Molybdenum	Mo	98	0.1	3	2
Lead	Pb	206	0.1	3	2
Rubidium	Rb	85	0.1	3	2
Selenium	Se	78	0.1	3	2
Strontium	Sr	86	0.1	3	2
Scandium	Sc	45	0.1	3	2
Bismuth	Bi	209	0.1	3	2
Strontium	Sr	121	0.1	3	2
Yttrium	Y	89	0.1	3	2

Table 10 describes the uncertainty budget for determination of Al, As, Cd, Pb, Mo, Rb, Se, and Sr by ICP-MS. The table provides the names and symbols for recognized uncertainty components, the basis for determining the contributions to the total uncertainty, whether the contributions are determined by the current experiment (Type A) or from other sources (Type B), and the number of associated degrees of freedom (DF). Type B components typically are associated with large numbers of degrees of freedom, where “large” can be any value greater than 60, the number of DF for a Student’s *t* 95 % confidence expansion factor of 2.0.

Table 10. Uncertainty Budget for ICP-MS Analysis.

Uncertainty	Basis	Type	DF
Sample Replication, s_{sample}	The uncertainty due to sample preparation and measurement is estimated by calculating the standard deviation of the mean. (n = 4, 19, 20; SRM 1568b and SRM 1568c respectively)	A	3, 18, 19
Blank Replication, s_{blank}	The uncertainty due to blank preparation and measurement is estimated by calculating the standard deviation of the mean. (n = 10, 8 for Al)	A	9, 7
Moisture Correction, $s_{moisture}$	The uncertainty due to the moisture correction is estimated by calculating the standard deviation of the mean, then converting percent moisture to mass. (n = 10)	A	9
Primary Standard, u_s	The uncertainty associated with the primary standards is calculated to be the expanded uncertainty divided by the expansion factor, k, obtained from the COA for each SRM used as the standard addition spike.	B	> 60
Weighing of Standards, u_{b1}	The uncertainty for each weighing of the standard is ± 0.01 mg based on the certificate of calibration for the balance. This uncertainty is normalized by division by √3.	B	> 60
Weighing of Samples, u_{b2}	The uncertainty for each weighing of the sample is ± 0.01 mg based on the certificate of calibration for the balance. This uncertainty is normalized by division by √3.	B	> 60

4.1.6. INAA Analysis

Mass fractions of As, Br, Mo, and Se in SRM 1568c Rice Flour were determined at NIST using INAA. A total of 10 bottles of candidate SRM 1568c were sampled for analysis by INAA. Bottles were inverted and rotated to mix the material before sampling. Two aliquots of the rice flour powder were removed from each bottle, each weighing nominally 300 mg to 335 mg, exact masses known, and placed into polyethylene irradiation vials obtained from Posthumus Plastics (Beverwijk, Netherlands), which are cylinders approximately 8 mm wide and 9 mm long. Vials were weighed to ± 0.01 mg on an analytical balance before and after addition of the powder. All weighings were performed using a Mettler Toledo XP205DR analytical balance with calibration verified using Troemner calibrated masses. Each vial was sealed with a snap-cap after sample addition. Six aliquots weighing nominally 250 mg to 275 mg, exact masses known, from a single bottle of SRM 1568b Rice Flour were also analyzed as described previously for quality assurance.

Standard solutions were prepared by gravimetrically diluting and mixing selected single element SRM 3100 series solutions with either dilute nitric acid (< 5 % volume fraction) for As, Cd, Mo, and Se, and ultrapure water for Br, as shown in Table 11. Cadmium and selenium were also included in the intermediate solution; however, the Cd level was below the limit of detection in the samples and is not reported here. Measurement of 75Se (t1/2 = 120 d) requires a longer decay time for samples to allow for decay of shorter-lived nuclides that can create high Compton background in the Se peak energy region (264 keV), therefore Se will be included in an upcoming report of analysis after additional counts have been performed. For preparation of standards for irradiation, 18 vials were filled to maximum capacity with

approximately 0.15 g of cellulose (SPEX 2642 cellulose binder with particle size at or below 20 μm) to create identical sample geometries to rice flour samples and controls. Approximately 0.15 g of a mixed solution containing As and Mo were pipetted into 9 vials and approximately 0.15 g of Br solution was pipetted into the other 9 vials. Vials were weighed before and after addition of cellulose to determine cellulose mass, and again after deposition of solution to determine solution mass. Vials were placed in a fume hood to air-dry overnight before being sealed with a snap-cap. Previous results have shown that the deposited solution is distributed sufficiently uniformly that geometry effects are not observable when the vials are measured at-contact with HPGe detector heads. To determine whether blank corrections were necessary for As, Br, or Mo in the cellulose, four vials containing approximately 0.15 g cellulose each were also prepared and sealed with no solution added.

Table 11. SRM solutions and final standard mass fractions for INAA analysis.

Element	SRM Number	Lot Number	Mass Fraction in Solution (mg/kg)	Uncertainty (mg/kg)
Arsenic (As)	3103a	100818	13.43	0.01
Bromine (Br)	3184	151130	15.79	0.02
Molybdenum (Mo)	3134	130418	13.60	0.02
Selenium (Se)	3149	100901	12.974	0.033

4.1.6.1. Irradiation Procedure

Two polyethylene irradiation capsule rabbits were prepared for analysis of candidate SRM 1568c. Each rabbit contained 24 vials, a mixture of standards, controls, samples, and cellulose blanks, placed perpendicular to the neutron field in three columns of eight. Additionally, each rabbit contained 27 polyethylene-sealed iron foils (mass of approximately 0.007 g, 6 mm diameter, and 0.1 mm thick) that were placed before and after each vial to measure and correct for neutron flux gradients during irradiation and between each rabbit shot. Due to concerns that Br might be present in the vials as well as the cellulose (necessitating a blank correction for the samples as well as standards), a third rabbit was later prepared containing four Br standards, three empty vials, and one vial with cellulose. This rabbit was irradiated in an identical manner to the other two.

The rabbits were irradiated at the NIST Center for Neutron Research (NCNR) RT-2 irradiation facility [10]. RT-2 has a thermal neutron flux of approximately 3×10^{13} $cm^{-2}s^{-1}$ and a dimensionless thermal/epithermal ratio of approximately 350. Each rabbit was irradiated for 16 h, but because of a known neutron flux gradient from one end of the rabbit to the other [11], the rabbit was flipped midway through the irradiation, resulting in 8 h irradiation in each orientation.

4.1.6.2. Gamma-Ray Spectrometry

The rabbits were stored in a lead cave for approximately 2 d before being unpacked and prepared for counting. Samples, controls, standards, and flux monitors were counted using the sample changer attached to the “Alena” detector (Model: GEM-45P4-76-PL) from ORTEC and a LYNX-MCA digital signal processor from Mirion Technologies (formerly Canberra). The detector was configured to have a shaping time of 12 µs and a gamma-energy range of 13 keV to 3000 keV and was energy-calibrated using an Eu-152 source. Pileup rejection circuitry was used to minimize the need for potential pileup corrections, and because the dead-time between the samples, standards, and controls was nominally identical, no pileup correction was performed. A subsequent pileup calibration study indicated that any pileup effects were insignificant.

Arsenic, Mo, and Br were determined by counting after 3 d of decay for 2.5 h for the samples, standards, controls, and blanks at 10 cm. The samples, standards, and controls were stored in a radioactivity hood for 7 to 8 months after irradiation to allow decay of short-lived and intermediate nuclides prior to counting for Se determination. Selenium was determined by counting after 7 months to 8 months of decay for 20 h for SRM 1568c samples, 10 h for SRM 1568b controls, and 8 h for blanks at 5 cm. Due to an oversight, only 19 of the original 20 irradiated vials of SRM 1568c were measured for Se.

4.1.6.3. Spectrum and Data Evaluation

Gamma-ray spectra were evaluated using the Nuclear Data/Canberra VAX/VMS neutron-activation analysis software package. Peak identifications and peak area calculations for each spectrum were done with the program ND-PEAK V16.9. Peak area calculations were checked with an interactive peak-fitting utility that is part of the Nuclear Data/Canberra SPECTROSCOPY ASSISTANT PROGRAM V2.5. Additional peak integrations were performed using the SUM4 algorithm [12]. All gamma-ray count rates for samples and standards were corrected for radioactive decay between the end of irradiation and the start of count, for radioactive decay during data acquisition, neutron flux gradients, and neutron flux differences between each rabbit irradiation, and spectral interferences where applicable. The bromine count rate for both standards and samples was also for Br in the cellulose and vials (see below). Table 12 lists the nuclides analyzed, their corresponding half-lives, and the energies of the gamma rays used in the analysis.

Table 12. Nuclides measured, gamma-ray peak energies, and interferences.

Analyte		Half-Life	Gamma Energy	Count,	Detector,	Number of
Element	Nuclide	(d)	(KeV)	Decay	Geometry	Standards
Arsenic	^{76}As	1.097	559.08	2.5 h, 3 d	Alena, 10 cm	9
Bromine	^{82}Br	1.4708	554.3	2.5 h, 3 d	Alena, 10 cm	9
Molybdenum	^{99}Mo	2.7477	140.47	2.5 h, 3 d	Alena, 10 cm	9
Selenium	^{75}Se	119.78	264.66	20 h, 7 m – 8 m	Alena, 5 cm	9

The program AUTONAA was used to perform the quantitative evaluation by first calculating massic count rates for each element based on the irradiated standards. Massic count-rate

values and statistical uncertainties for multiple standards were combined and propagated to yield one value and associated uncertainty for each of one or more gamma-ray lines in each element being assayed. Count rates of the elements in the samples were compared to those of the standards for the calculation of elemental mass fractions. The resulting elemental mass fraction values were exported to a spreadsheet for the final statistical evaluation.

While there may be some uncertainty sources defined in the equation that are not applied to this analysis since their contributions were significantly (> 1000 times) less than other sources of uncertainty, the following is the general-use equation for propagating uncertainties for concentration determination using INAA:

$$w_{x(unk)} = \frac{w_{x(std)}+M_{std}}{M_{unk}}\left(\frac{A_{0(unk)}}{A_{0(std)}}\right)R_{\theta}R_{\varphi}R_{\sigma}R_{\varepsilon}\left(1-\frac{blank}{m_{x(unk)}}\right)/DF \quad (6)$$

where: $w_{x(unk)}$ = mass fraction of element x in the unknown sample (mg/kg).

$w_{x(std)}$ = mass fraction of element x in the comparator standard (mg/kg).

M_{std} = total mass of the comparator standard (mg).

M_{unk} = total mass of the unknown sample (mg).

$A_{0(unk)}$ = decay corrected count rate of the unknown sample (Counts per second). This uncertainty is accounted for in the sample measurement replication.

$A_{0(std)}$ = decay and blank corrected count rate of the comparator standard (Counts per second). This uncertainty is accounted for in the standard measurement replication.

R_{θ} = ratio of isotopic abundances for the unknown and standard (dimensionless). This ratio is typically not mentioned because the isotopic abundances for most elements are identical, and thus the uncertainty contribution is significantly less than other sources.

R_{ϕ} = ratio of neutron fluences (dimensionless). This uncertainty includes contributions from neutron self-shielding and irradiation geometries.

R_{σ} = ratio of effective cross sections between comparator and sample (usually 1) (dimensionless). This ratio is usually never an issue unless neutron shielding in a sample causes the neutron energy spectrum to change between the samples and comparators; which would be a rare event.

R_{ε} = ratio of counting efficiencies between the standard and sample (dimensionless). This uncertainty is accounted for in counting geometry and photon attenuation.

$\frac{blank}{m_{x(unk)}}$ = mass of element x in the blank divided by the mass of x in the unknown; creates a relative correction factor for the contribution of the blank on the total mass fraction (mg/mg). This uncertainty is typically not reported unless a blank correction is performed. Typically, blanks only become an issue when the samples and standards are packaged differently, and elements that are known to exist in blank materials are being reported.

DF = the drying factor of the rice flour sample or control as determined from moisture determination on replicate portions of the material. See below.

The use of the vials and cellulose matrix for the standards resulted in no necessary geometry corrections. Neutron self-shielding corrections were negligible due to the similarity in matrix between the rice flour and cellulose.

Flux monitor corrections were calculated by measuring the activity of each flux monitor in each rabbit. The flux monitors were then treated as standards in the VMS program and standard constants, or essentially counts per second (cps) per mg, values were calculated. The difference in standard constant between bracketing foils was calculated and then applied to the standards, samples, and controls to account for axial flux dependence in RT-2. Additionally, the average iron flux value for each rabbit was compared to the other two rabbits to determine if there were any changes in the neutron fluence each rabbit experienced. Typical in-rabbit flux corrections ranged from ± 2 % while rabbit-to-rabbit variation was less than 0.1 %.

No blank corrections were necessary for As, Se, and Mo. However, Br was found to be present in both the cellulose and empty vials. Corrections were made to the standards data by using Br standards data to determine the mass of Br in the blank cellulose, adjusting the calculated Br content of the standards to reflect the additional Br from the cellulose, followed by recalculation of Br in the cellulose using the adjusted standards data. Successive iterations were performed until the calculated Br content of the standards remained constant to at least 3 significant figures in successive iterations. Because the cellulose contained a significant fraction of Br, the blank correction resulted in about a 36 % correction in the calculated Br content of the standards. Subsequent analysis of the three empty vials yielded an average of 2.6 ng ± 0.3 ng with the uncertainty equal to 1 standard deviation (1s) of Br per vial. This resulted in a correction of 0.8 % to the mass fractions determined for SRM 1568c.

Elemental mass fractions were measured relative to dry mass for both the SRM and control. Moisture determination was performed by drying 1 g portions of SRM 1568c (one portion from each of 10 bottles) and SRM 1568b (five portions from one bottle) in an oven at 90° C for 4 h, as described on the COA for SRM 1568b. Drying factors determined from the two materials were 0.8973 ± 0.0004 (1s) for SRM 1568c and 0.9125 ± 0.0003 (1s) for SRM 1568b. Because pellets prepared from SRM 1568c were found to lose mass a week or two after preparation and because the original drying determination was a few weeks before sample preparation for INAA, a second drying determination was performed using 1 g aliquots about two weeks after pellet preparation. The new drying factor was found to be 0.8988 ± 0.0008 (1s), indicating that the material in the bottles had lost about 0.016 % of moisture content over the (2 to 3) month period. Interpolating between the two dates of moisture determination, and assuming a constant H loss, the drying factor for SRM 1568c determined for the date of sample preparation and weighing was 0.8978.

Table 13 describes the uncertainty budget for determination of As, Br, Mo, and Se by INAA. The table provides the names and symbols for recognized uncertainty components, the basis for determining the contributions to the total uncertainty, whether the contributions are determined by the current experiment (Type A) or from other sources (Type B), and the number of associated degrees of freedom (DF). Type B components typically are associated with large numbers of degrees of freedom, where “large” can be any value greater than 60, the number of DF for a Student’s *t* 95 % confidence expansion factor of 2.0.

Table 13. Uncertainty Budget for INAA Analysis.

Uncertainty	Basis	Type	DF
Sample Measurement Replication	s/√n, where s is standard deviation of the sample data, and n is the number of samples analyzed. (n=19 for Se, n=20 for As, Br, and Mo)	A	18, 19
Standard Measurement Replication	s/√n, where s is standard deviation of the standard data, and n is the number of standards analyzed.	A	8
Dry Mass Determination	Standard deviation of the mean of values from drying of multiple samples.	B	4
Neutron Flux Correction	Estimated from counting statistics of the Fe 1098 keV and 1291 keV peaks.	B	> 60
Standard Mass (Purity)	Calculated as the uncertainty in the elemental mass fraction in NIST standard solutions (listed on the certificate) divided by 2, assuming the certificate uncertainty is an expanded uncertainty with coverage factor of 2.	B	> 60
Peak Integration	Estimated from results of peak integration by 2 different methods using the normal distribution method.	B	> 60
Blank Correction (Br only)	Uncertainty in the corrected Br standard mass fraction, calculated as the relative uncertainty on Br mass fraction determined in the four cellulose blanks (s/√4 = 0.6 %) times the correction as a fraction of the uncorrected value (0.355) = 0.355 * 0.6 % = 0.21 % (n=4 cellulose, n=3 vials)	B	3, 2

4.1.7. TNPGAA Analysis

The mass fraction of S in SRM 1568c Rice Flour was determined at NIST using TNPGAA. A total of 6 bottles were inverted and rotated to mix the material before sampling for analysis of sulfur by PGAA. Sulfur was measured by first determining the H mass fraction by TNPGAA, followed by determination of the S/H mass fraction ratio by CNPGAA (see below). For H determination, two aliquots nominally weighing 750 mg were removed from each bottle and pressed into 12.7 mm diameter pellets using a stainless-steel die and hydraulic press at 10 000 pounds' force (44 000 Newtons) for 3 s to 5 s. For S/H determination, one pellet weighing between 1500 mg and 1800 mg was removed from each bottle and pelletized in an identical manner. Each pellet was then weighed to ± 0.01 mg using an analytical balance and sealed into a bag of fluorinated ethylene propylene (FEP) film. All weighings were performed using a Mettler Toledo XP205DR analytical balance, with calibration verified using Troemner calibrated masses. One bottle of SRM 1568b Rice Flour was analyzed for quality assurance. Five nominal 750 mg portions and five portions weighing between 1600 mg and 1900 mg were pelletized as described above and used for determination of H and S/H respectively. Weighing of pellets and packaging in FEP were performed as described above.

Standards for measurement of H by TNPGAA were prepared by pressing five nominal 750 mg portions of SRM 912b Urea in the manner described previously. Urea was used as a H standard because its hydrogen density when pelletized (determined as cps H as a function of pellet thickness) was in better agreement to that of the pelletized rice flour samples than other H containing compounds (e.g., mannitol, benzoic acid, tris hydroxymethyl aminomethane). Pellets

were weighed and packaged in FEP as previously described. Pellet masses and H sensitivities were determined by TNPGAA and are given in Table 14.

Table 14. H sensitivities for urea standards.

Standard	Pellet mass (mg)	Measured H sensitivity (cps H / mg H)
A	720.14	2.411
B	722.88	2.400
C	761.81	2.418
D	753.11	2.404
E	773.09	2.391
	Mean	2.405
	SD	0.010
	% SD	0.425

Standards for the NIST PGAA measurements were created from a mixture of NIST SRMs and from high purity reagents. The standard for measurement of S/H ratios were pressed pellets of mixtures of L-cystine (SRM 143d Cystine), graphite (Spectrographic Services, 200 mesh), and urea (SRM 912a Urea), and sodium sulfate (Alpha Puratronic, 99.9955 % metals basis), graphite, and urea. These pellets were previously prepared for measurement of sulfur in SRM 2684c Bituminous Coal [13] and in SRM 2718a Green Petroleum Coke [14] by TNPGAA. Mixtures were prepared by weighing components into a plastic vial and shaking the vial in a Spex Mixer Mill for approximately 20 min. Samples weighing from 750 mg to 1000 mg were pelletized, weighed, and sealed into FEP bags as described above. Pellet compositions and sensitivity ratios measured by CNPGAA are given in Table 15.

Table 15. Sensitivities for S/H ratio standards.

Standard	Composition	Measured H/S sensitivity (cps H /mg H) / (cps S/mg S)
UGNa3_2	Urea, graphite, Na_2SO_4 7.045 % S, 2.452 % H	16.33
UGNa3_3	Urea, graphite, Na_2SO_4 7.045 % S, 2.452 % H	16.43
UGC2a	Urea, cystine, graphite 5.115 % S, 3.994 % H	16.27
UGC3a	Urea, cystine, graphite 5.264 % S, 3.398 % H	16.40
UGC3C	Urea, cystine, graphite 5.264 % S, 3.398 % H	16.45
UGC5a	Urea, cystine, graphite 5.373 % S, 3.691 % H	16.30
UGC5E	Urea, cystine, graphite 5.373 % S, 3.691 % H	16.58
	Mean	16.39
	SD	0.11
	% SD	0.657

Elemental mass fractions were measured relative to dry mass for both SRM 1568c and the control, SRM 1568b. Moisture determination was performed by drying 1 g portions of SRM 1568c (one portion from each of 10 bottles) and SRM 1568b (five portions from one bottle) in an oven at 90 °C for 4 h, as described on the COA for SRM 1568b. Drying factors determined from the two materials were 0.8973 ± 0.0004 (1s) for SRM 1568c and 0.9125 ± 0.0003 (1s) for SRM 1568b. Because pellets prepared from SRM 1568c were found to lose mass a week or two after preparation and because the original drying determination was performed approximately two months before preparation of pellets for PGAA, a second drying determination was performed using 1 g aliquots about two weeks after pellet preparation. The new drying factor was found to be 0.8988 ± 0.0008 (1s) indicating that the material in the bottles had lost about 0.016 % of moisture content over the 2 month to 3 month period. Interpolating between the two dates of moisture determination, and assuming a constant H loss, the drying factor for SRM 1568c determined for the date of sample preparation and weighing was 0.8985.

4.1.7.1. Analytical Method

Although the NIST TNPGAA instrument at vertical tube (VT) 5 has ample sensitivity to measure H in rice flour with less than 1 % counting statistics with a few minutes of irradiation, achieving 1 % counting statistics for sulfur at the level present in the rice flour would take irradiation times of greater than one week per sample. By contrast, elemental sensitivities measured using the neutron guide “D” (NGD) cold neutron PGAA instrument are 15 times to 20 times greater than thermal, hence elemental mass fractions can be measured in a fraction of the time necessary for TNPGAA. However, elemental sensitivities are difficult to calibrate in hydrogenous targets for CNPGAA due to energy change of cold neutrons in a room temperature target [15], while accurate sensitivity calibration is much more easily achieved in TNPGAA since no neutron energy change occurs [16,17]. Using a combination of CNPGAA and TNPGAA allows us to combine the improved sensitivity of CNPGAA with the accurate calibration of TNPGAA. The method takes advantage of the fact that element sensitivity ratios are not affected by differences in neutron scattering power and sample geometry [18] and utilizes measurement of H mass fractions by TNPGAA combined with measurement of the ratio of S/H mass fraction by CNPGAA [19].

4.1.7.2. Irradiations

Measurement of H was performed using the TNPGAA instrument at VT5 at the NCNR. Six samples, controls, and urea standards in FEP bags were irradiated in an aluminum sample chamber in air, suspended by PTFE strings in an aluminum sample frame, for 10 minutes each. This irradiation was sufficient to yield counting statistics of 0.4 % for the H peak at 2223 keV. A 139 mg titanium foil was irradiated at regular intervals to monitor any variation in the neutron fluence rate and sample positioning within the beam over the course of the investigation. Prompt gamma rays were measured using a high purity germanium detector (designated as “TNPGAA”, Canberra (Mirion) Model GC4018) with 40 % efficiency (relative to NaI). The signal

was processed using a digital signal processor (Canberra (Mirion) Lynx) and gamma-ray spectra up to 11 MeV were collected on a computer workstation using Canberra (Mirion) software.

Measurement of H/S ratio was performed using the CNPGAA instrument at NGD at the NCNR [20]. Samples, controls, and mixed H/S standards in FEP bags were irradiated in an aluminum sample chamber in air, suspended by PTFE strings in an aluminum sample frame. Samples and controls were irradiated for approximately 24 h to achieve counting statistics of 1.2 % or better for the sulfur peak at 841 keV. Mixed standards for H/S determination were irradiated for 10 min to 20 min to achieve counting statistics of 0.5 % or better for H and S peaks. To correct for spectral interferences by K and Cl at the sulfur energy, pellets of K_2CO_3 and NH_4Cl mixed with graphite were irradiated overnight. Prompt gamma rays were measured using a high purity germanium detector (designated as “Homer”, Canberra (Mirion) Model GR3519, Serial Number 6470) with 40 % efficiency (relative to NaI). The signal was processed using a digital signal processor (Canberra (Mirion) Lynx) and gamma-ray spectra up to 11 MeV were collected on a computer workstation using Canberra (Mirion) software.

4.1.7.3. Data Evaluation

All spectra for both TNPGAA and CNPGAA were analyzed using Canberra (Mirion) software. H peaks (2223 keV) for TNPGAA and H and S peaks (841 keV) for CNPGAA were analyzed using the standard Canberra (Mirion) peak search and the interactive peak search, as well as PeakEasy software and the SUM4 code [12]. No pileup corrections were necessary since pileup rejection circuitry was used. Corrections for neutron self-absorption and Gamma-ray self-shielding were minimal for TNPGAA irradiations due to the similarity between sample and urea standard matrices, and unnecessary for CNPGAA since element ratios were measured. For determination of Cl and K spectral interferences by CNPGAA, Cl and K peaks at 787 keV and 770 keV, respectively, were also integrated. For K, the interference factor was calculated from the ratio of the sulfur interference peak at 843 keV to the K reference peak at 770 keV measured in the K_2CO_3 spectrum, and the magnitude (cps) of the K interference for each sample determined by multiplying this ratio by the count rate of K at 770 keV in the sample spectrum. A similar procedure was used for correction of Cl interference using data from the NH_4Cl/graphite pellet and the reference peak at 787 keV. Correction for Cl interference resulted in an approximately 0.25 % correction in the S count rate for both samples and controls. The K interference resulted in an approximately 7.5 % correction in S count rate for SRM 1568b controls, while the correction for SRM 1568c samples was significantly greater (approximately 16 %) due to a greater K count rate.

Because S was measured relative to H, careful monitoring of the mass of the pressed pellets was necessary since a change in moisture content over the course of the investigation would result in a change in H content. Sample and control pellets for both CNPGAA and TNPGAA were reweighed both before and after irradiation. Pellets of SRM 1568c lost mass since initial preparation, presumably due to loss of moisture upon exposure to air. Relative mass loss was between 0.7 % and 2 % for all pellets. Corrections for loss of H were made assuming all mass was lost as H_2O and using a fraction of 0.1119 for H in H_2O, resulting in relative corrections of about 0.2 % for H determined by TNPGAA and 0.4 % for determination of S. For SRM 1568b, a

slight gain (a few tenths of a percent relative) in mass since pellet preparation was noted, presumably due to absorption of moisture, resulting in a correction of less than 0.2 % for both measured H and S.

Hydrogen for use as a comparator was calculated using the average H sensitivity (S_H) from five urea standard pellets and determined as cps H/(mass of pellet * 0.0671), where 0.0671 is the mass fraction of H in urea. Since no significant variation in H sensitivity was observed with urea pellet mass (which ranged from about 720 mg to 770 mg) and since all rice flour pellets for TNPGAA were within this mass range, the H sensitivity was assumed to be constant over this mass range. The H count rate for each sample or control was corrected for differences in neutron flux between samples and standards as determined from Ti flux monitor irradiation, and for moisture change from exposure to air as described above. H mass fraction, w_H in each rice flour pellet was then determined, relative to pellet dry mass, as:

$$w_H = 100[[(C_H/S_H)(\phi_{corr})] - H_{change}]/(m_{sa}\, DF) \quad (7)$$

where: C_H = count rate of H in the sample or control by TNPGAA,
S_H = average sensitivity of H (cps H/mg H) determined from standards,
ϕ_{corr} = correction for differences in neutron flux between samples and standards,
m_{sa} = wet (as received) mass of the sample,
H_{change} = loss or gain of H in the pellet since preparation, and
DF = drying factor for that material.

The sulfur mass fraction, w_S, was then calculated using the hydrogen mass fraction determined by TNPGAA and S and H count rates and sensitivity ratio determined by CNPGAA, using:

$$w_S = w_H[(C'_S - INT_{K+Cl})/C'_H][S'_H/S'_S]H_{changecorr} \quad (8)$$

where: C'_S = count rates (cps) for S for each sample or control as determined by CNPGAA,
C'_H = count rates (cps) for H for each sample or control as determined by CNPGAA,
INT_{K+Cl} = total interference correction for K and Cl in cps, determined as above,
S'_H/S'_S = average sensitivity ratio for H/S, (cps H/mg H)/(cps S/mg S), as determined from the 7 mixed standards by CNPGAA, and
$H_{changecorr}$ = correction for H loss or gain in the CNPGAA pellet since sample preparation.

In Equation 5, H was determined in this investigation as a comparator element for determination of S. Although total H in the samples was determined from this equation relative to dry mass by determination of H in a wet sample and applying a drying factor, this value does not reflect the true H mass fraction of a dry sample. To obtain the true dry sample hydrogen content, the hydrogen mass fraction calculated from Equation 5 must be further corrected to account for hydrogen lost as H_2O upon drying. The “dry” hydrogen mass fraction, w_{HDry}, in %, is calculated using:

$$w_{HDry} = 100[[(C_H - INT_{K+Cl}/S_H)(\phi_{corr})] - m_{sa}\, mf\, 0.1119]/(m_{sa}\, DF)H_{changecorr} \quad (9)$$

where: m_{sa} = wet mass of the sample in mg,
mf = moisture mass fraction determined by oven drying, and
0.1119 = mass fraction of H in water.

Table 16 describes the uncertainty budget for determination of S by TNPGAA. The table provides the names and symbols for recognized uncertainty components, the basis for determining the contributions to the total uncertainty, whether the contributions are determined by the current experiment (Type A) or from other sources (Type B), and the number of associated degrees of freedom (DF). Type B components typically are associated with large numbers of degrees of freedom, where "large" can be any value greater than 60, the number of DF for a Student's *t* 95 % confidence expansion factor of 2.0.

Table 16. Uncertainty Budget for TNPGAA Analysis.

Uncertainty	Basis	Type	DF
Sample Measurement Replication	$s/\sqrt{n}$, where s is standard deviation of the sample data, and *n* is the number of samples analyzed.	A	11
Urea Standard Measurement Replication	$s/\sqrt{n}$, where s is standard deviation of the standard data, and *n* is the number of standards analyzed.	A	4
Dry Mass Determination	Standard deviation of the mean of values from drying of multiple samples.	A	4
Neutron fluence rate variation/Sample positioning	Estimated from the standard deviation of repeated measurements of a titanium foil, n=25.	A	24
Standard Mass (Purity)	Estimated from manufacturers' specification of material purity or (for NIST standard solutions) uncertainty in spectrometric standard mass fraction (given on the certificate)/2, assuming the certificate uncertainty is an expanded uncertainty with coverage factor of 2.	B	> 60
Peak Integration	Estimated from results of peak integration by 2 different methods using the normal distribution method.	B	> 60
Matrix Match Uncertainty	An added uncertainty of 0.2 % was added to account for the fact that the urea was not an exact matrix match for the rice flour samples. Hence the effects of neutron scattering for the urea could differ slightly from that observed by the samples resulting in a slightly higher or lower H sensitivity.	B	> 60
Loss or gain of H as moisture during the investigation	Estimated as 25 % of the moisture loss or gain.	B	> 60

4.1.8. WDXRF Analysis

Mass fractions of Na, Mg, Al, Si, P, S, Cl, K, Ca, Mn, Fe, Cu, Zn, Br, and Rb in SRM 1568c Rice Flour were determined at NIST using WDXRF. Two 4.5 g aliquots were taken from each of six bottles of SRM 1568c Rice Flour and four 4.5 g aliquots were taken from one bottle of SRM 1568b Rice Flour and prepared along with the samples for quality assurance. Aliquots were weighed into glass containers and stored under vacuum in a desiccator over $Mg(ClO_4)_2$ for at least 21 d. Briquettes were pressed from approximately 4 g of each dried powder sample using a steel pressing die containing an aluminum cap. A polished steel die pellet was inserted, along with the ram cylinder, and the die was pressed at 20 tons (18143.7 kg) for 24 s. Briquettes were immediately placed into liquid sample cells fitted with 6 µm polypropylene film, which prevents loose powder from dropping into the spectrometer, and the sample cells were placed into a second desiccator. When all briquettes had been prepared, the desiccator was evacuated, and the briquettes were stored under vacuum for two weeks prior to analysis.

Blanks of cellulose were prepared from Alfa Aesar Microcrystalline Cellulose A17730, lot 10200883 and Whatman Cellulose Powder CF11. The cellulose powders were pressed into briquettes without drying.

A Malvern Panalytical Model ZETIUM Ultimate wavelength dispersive X-ray fluorescence spectrometer was used to perform measurements of the K-$L_{2,3}$ characteristic X-ray lines of all elements. Background measurement and subtraction were made for each of the following elements: Na, Mg, Al, Si, Cl, Ca, Mn, Fe, Cu, and Zn. All measurements were performed in a helium environment with the generator operated at 4.0 kW of X-ray power. Sample holders with 32 mm inner diameter support rings were used to carry all briquettes in liquid cells into the spectrometer and to hold them in the measurement position. The mask between the sample and the collimator was set to view a 29 mm circular area of the sample, and the spinner was used. Counting times were chosen to obtain relative counting statistical errors ranging from 0.1 % to 1.0 % depending on the X-ray count rate for each element and the number of measurements of background.

Calibration curves were calculated in the software provided with the X-ray spectrometer (SuperQ). The general calibration algorithm is:

$$C_i = D_i + L_k R_k + E_i R_i \frac{R_i}{R_{Rh}} \left(1 + \sum_j \frac{\alpha_{ij}}{R_j}\right) \quad (10)$$

where: C = mass fraction,
D = intercept,
E = inverse sensitivity,
L = slope,
R_i = net or gross count rate,
R_{Rh} = gross Compton scatter count rate,
i = analyte element index,
j = interfering element, and
k = presenting a spectral overlap.

The R_{Rh} term is for the Rh tube used as an internal reference for Mn, Fe, Cu, Zn, and Rb. For Si, the single calibrant and the Whatman cellulose blank defined the calibration line. For Rb, the single calibrant and both cellulose blanks defined the calibration line.

The term containing the α factor for X-ray absorption was used for elements for which an internal reference approach did not correct for all interelement effects (i.e., Mg, P, S, Cl, K, Ca, Mn, Fe, and Zn). The absorption factors were calculated empirically based on the measured count rates of the interfering elements. Absorption corrections were made as described in Table 17.

Table 17. Absorption Corrections for WDXRF Measurements.

Element	Self-Absorption Correction	Other Absorption Corrections
Mg	No	S, Cl, K, Ca, Fe
P	Yes	Mg, S, Cl, K, Ca, Fe
S	No	Cl, K, Ca
Cl	Yes	S, K, Ca
K	Yes	P, S, Cl, Fe
Ca	Yes	P, S, K
Mn	No	P, S, K, Ca, Fe
Fe	No	K, Ca
Zn	No	K, Ca, Fe

For all other combinations of elements, the product of the mass fraction of interfering element and any calculated correction factor was too low to have a significant effect.

A line overlap correction was used for the overlap of Zn L-series lines on Na. Line overlaps for S and Ca on Mg had no effect on calculated model parameters, indicating there are no effects of higher order S and Ca peaks on Mg.

Calibration standards were chosen from among the available powdered food and vegetable matter SRMs as described in Table 18 and were prepared in the same way as the samples of candidate SRM 1568c and SRM 1568b. For some analytes, selected certified and reference values were observed to be obvious outliers and were excluded from use as listed below in Table 18:

Table 18. Elements Excluded from Use as Calibration Materials Used for XRF Measurements.

	Na	Mg	Al	Si	P	S	Cl	K	Ca	Fe	Cu	Zn
SRM 1515	X					X						
SRM 1547	X							X				
SRM 1549		X	X									
SRM 1566b		X			X			X				
SRM 1571		X				X						
SRM 1572			X									
SRM 1573a	X									X	X	X
SRM 1575		X	X									
SRM 1575a		X										
SRM 1577b			X									
SRM 3232	X		X					X	X	X		
SRM 3233										X		
SRM 3234	X											
SRM 3252		X			X		X	X				
SRM 3281		X			X							
SRM 3287		X										
SRM 3290		X			X							X

Both cellulose blanks were found to be contaminated with Cl and K and thus were not included in the Cl and K calibrations. The Alfa Aesar cellulose was found to be contaminated with Si and was not used in the Si calibration. Bromine was measured, but no calibrants were available to enable quantification.

Except for Si and Rb, statistical weighting was applied to emphasize lower mass fraction calibration points in the regression calculations because XRF data is heteroscedastic. The weighting, called "square-root" weighting in the SuperQ software, was done during regression in the calculation of goodness of fit, *K*, calculated using:

$$K = \sqrt{\frac{1}{m-k}\sum\frac{(C_{chem}-C_{calc})^2}{(C_{chem}-C_0)}} \quad (11)$$

where: m = the number of calibration standards,
k = the number of calculated parameters in Equation 8,
C_{chem} = the assigned value for the calibration standard,
C_{calc} = the value for the calibration standard calculated from the fit to Equation 8, and
C_0 = a constant called the weighting factor.

The weighting factor is set manually. The lower is the value of C_0; the greater is the weight on the lowest mass fraction points. With only one calibrant each for Si and Rb, the mass fraction range was narrow making weighting unnecessary.

Table 19 describes the uncertainty budget for determination of Na, Mg, Al, Si, P, S, Cl, K, Ca, Mn, Fe, Cu, Zn, Br, and Rb using WDXRF. The table provides the names and symbols for recognized uncertainty components, the basis for determining the contributions to the total uncertainty, whether the contributions are determined by current experiment (Type A) or from other sources (Type B), and the number of associated degrees of freedom (DF). Type B components typically are associated with large numbers of degrees of freedom, where "large" can be any value greater than 60, the number of DF for a Student's *t* 95 % confidence expansion factor of 2.0.

Table 19. Uncertainty Budget for WDXRF Analysis.

Uncertainty	Basis	Type	DF
Variability of Sample Preparation and Measurement, *s*	Standard deviation of the calculated mass fractions for *n* specimens.	A	n-1
Uncertainty of Calibrant Measurement and Empirical Model Fit, u_f	Estimated from the fit of Eq. 8 to the calibration data. This estimator accounts for repeatability of briquette preparation and measurement and for biases among the calibration standards. The estimate is calculated from the *K* factor (see Eq. 9), using the equation below, where C_{calc} is now the calculated result for each sample of candidate SRM 1568c. $U_f = K\sqrt{(C_{calc} - C_0)}$ Each analyte has a different number of calibrants, *m*, and calculated correction coefficients, *k*. For Si with one calibrant, this value was set equal to the combined standard uncertainty of the certificate value for the calibrant SRM. For Rb, this value was set equal to the mean difference between zero and the calculated values for the cellulose blanks = 0.4 mg/kg.	A	(m – k)
Combined standard uncertainty, u_c	$U_c = \sqrt{\frac{s^2}{n} + \frac{u_f^2}{(m-k)}}$		
$U_{k=2}$	Expanded uncertainty estimate with expansion factor, *k*, set equal to 2, *i.e.*, $U_{k=2} = 2u_c$.		

4.1.9. LC-ICP-MS

Arsenic species including monomethylarsonic acid (MMA), dimethylarsinic acid (DMA), and inorganic arsenic (iAs), defined as the sum of arsenic from arsenous acid (AsIII) and arsenic acid (AsV), were determined in SRM 1568c Rice Flour at NIST using LC-ICP-MS. Duplicate 1 g samples from each of six bottles of candidate SRM 1568c and one bottle of SRM 1568b, used as a control, were weighed into 50 mL polyethylene tubes.

A Mettler model AT261 Delta Range analytical balance was used for weighing during the preparation of samples and standards. The balance is serviced and calibrated annually by Mettler Toledo, LLC. Prior to use, calibration of the balance was verified using standard masses ranging from 0.5 g to 50 g that are traceable to the SI through the standard mass set maintained by the Inorganic Chemical Metrology Group. A 10 mL solution containing 0.2 mol/L HNO_3 and 6 % H_2O_2 in water was added to each tube. Four procedural blanks were prepared similarly. The samples and the blanks were loosely capped and transferred to a Fisher Scientific Isotemp oven (model 737F), preheated to 90 °C. The samples and blanks were removed from the oven after 3 h. After the temperature was equilibrated with the room temperature at 21 °C, the samples were centrifuged at 419 rad/s (4000 rpm) in a Jouan model C312 centrifuge for 30 min. The supernatant of each sample was manually filtered through a 0.45 µm syringe filter and transferred to a 50 mL polystyrene tube. An unspiked sample was prepared by weighing 2 g of the filtrate into a 4 mL polypropylene tube containing 0.1 g of 1 mg/kg trimethylarsine oxide (TMAO) serving as the internal standard. A spiked sample was prepared by weighing 0.5 g of the unspiked sample and 0.1 g of spiking standard into a 0.75 mL polypropylene autosampler vial for calibration by the method of standard addition. The spiking standard contained 0.01 mg/kg AsIII and 0.1 mg/kg each of MMA, DMA, and AsV. The spiking standard was prepared from SRM 3030 Monomethylarsonic Acid Standard Solution, SRM 3031 Dimethylarsinic Acid Standard Solution, SRM 3036 Arsenic Acid (AsV) Standard Solution, and SRM 3037 Arsenous Acid (AsIII) Standard Solution. A separate measurement of AsIII and AsV was made of the unspiked samples using a six-point external calibration curve. Independently, 1 g samples from each bottle of candidate SRM 1568c and SRM 1568b were transferred into weighing vessels and dried in the oven preheated to 90 °C for 2 h. The difference between the masses before and after drying was used to determine the moisture content of the sample.

All samples were prepared using Optima grade HNO_3, Fisher brand ACS Reagent grade H_2O_2, and Puratronic grade ammonium carbonate purchased from Fisher Scientific. TMAO was obtained from Waco Chemical. Locally prepared sub-boiling distilled water was used as a solvent in the preparation of samples, standards, and dilute acids. The concentration of dilute acid is expressed as the volume fraction of the acid relative to the solution.

A Perkin-Elmer LC system coupled to a Perkin-Elmer model Elan DRC II ICP-MS was used for analysis. The LC system consisted of a Peltier-cooled Series 200 autosampler and a Series 200 quaternary pump. Separation of As species was performed using a PRP-X100 anion exchange column from Hamilton and arsenic from each species was determined at 75 amu by ICP-MS in normal mode. Table 20 lists the parameters for the LC method. Set up and optimization of the ICP-MS were performed daily.

Table 20. LC Parameters for Separating Arsenic Species in Rice Samples.

Parameter	Value
Guard Column	PEEK X-100 Guard Column
Analytical Column	PRP X-100 (4.1 mm x 250 mm, 10 µm)
Mobile Phase (1.0 mL/min)	20 mmol/L ammonium carbonate in water, pH 10

The dilute HNO_3 and H_2O_2 in the extraction solution are strong oxidizers that can oxidize AsIII to AsV. Yet, AsIII was found in the extract of rice flour samples as shown in Fig. 4.

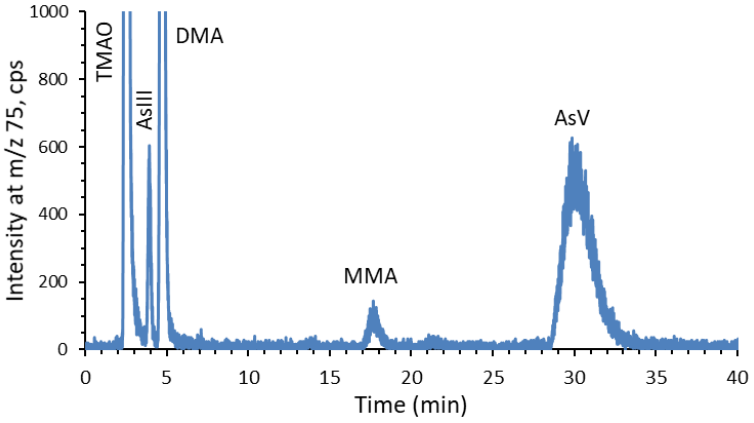


Fig. 4. Typical Chromatogram of a SRM 1568c Sample Spiked with TMAO.

Therefore, the standard addition approach cannot be used for the calibration of iAs measurement because some of the AsIII in the spike can be oxidized to AsV. An external calibration curve approach was used for the calibration of AsIII and AsV measurements. The *p*-values of one-way analysis of variance (ANOVA) of the duplicate samples of MMA, DMA, and iAs are 0.043, 0.443, and 0.533, respectively. The *p*-value of MMA is less than the 0.05 criterion. The *p* values for other As species are greater than 0.05 and, hence, these species have no detectable inhomogeneity. For this report, all As species are considered homogeneous in the data analysis by treating the duplicates of each bottle as independent samples.

The mass fractions of MMA and DMA were calculated according to the method of standard addition:

$$x = \frac{usp}{sp - usp} \frac{w_{sp}}{w_{sa}} c \frac{dil}{1 - F} \tag{12}$$

where: x = mass fraction of the analyte in the sample,
sp = internal-standard-corrected count rate of the spiked measurement sample,
usp = internal-standard-corrected count rate of the unspiked measurement sample,
w_{sa} = mass of the sample,
w_{sp} = mass of the spike solution,
c = mass fraction of the analyte in the spike solution,
dil = dilution factor of the sample, and
F = mass fraction of moisture in the sample.

The mass fractions of AsIII and AsV were calculated using external calibration:

$$y = \frac{s-b}{r} * \frac{dil}{1-F} \quad (13)$$

where: y = mass fraction of the analyte in the sample,
s = intensity of the sample,
b = intercept and the slope of the calibration curve, and
r = slope of the calibration curve.

The uncertainty of the measurement is calculated using the following:

$$U = k_v \sqrt{u_{\text{reps}}^2 + u_{\text{repb}}^2 + u_{\text{curve}}^2 + u_{b1}^2 + u_{b2}^2 + u_{b3}^2} \quad (14)$$

where: k_v = Student's t coverage factor for a 95 % confidence level with the v degrees of freedom,
u_{reps} = standard uncertainty of replicate LC-ICP-MS measurements of 12 SRM 1568c samples,
u_{repb} = standard uncertainty of replicate LC-ICP-MS measurements of 2 blanks,
u_{curve} = standard uncertainty of the slope of the calibration curve multiplied by the sample mean, and
u_{bi} = uncertainty in the three weighings.

Table 21 describes the uncertainty budget for determination of arsenic species by LC-ICP-MS. The table provides the names and symbols for recognized uncertainty components, the basis for determining the contributions to the total uncertainty, whether the contributions are determined by current experiment (Type A) or from other sources (Type B), and the number of associated degrees of freedom (DF). Type B components typically are associated with large numbers of degrees of freedom, where "large" can be any value greater than 60, the number of DF for a Student's t 95 % confidence expansion factor of 2.0.

Table 21. Uncertainty Budget for LC-ICP-MS Analysis.

Source	Basis	Type	DF
Sample replication (u_{reps})	Standard uncertainty of replicate LC-ICP-MS measurements of 12 candidate SRM 1568c samples	A	11
Blank replication (u_{reps})	Standard uncertainty of replicate LC-ICP-MS measurements of 2 blanks	A	1
Curve fitting (u_{curve})	Standard uncertainty of the slope of the calibration curve multiplied by the sample mean	A	4
Calibrant (B_1)	Taken from the Certificate of Analysis of SRMs 3030-3037. Converted from expanded uncertainty to standard uncertainty by dividing by 2.	B	> 60
Density (B_2)	Estimated 0.001 g/mL uncertainty in density measurement, assuming uniform distribution, normalized by dividing by √3.	B	> 60
Weighing (B_3)	Estimated 0.082 mg weighing uncertainty due to the calibration of the balance used for weighing the mass of the samples [6], assuming uniform distribution, normalized by dividing by √3.	B	> 60

4.2. NMIJ Method for Arsenic Species

SRM 1568c was originally released with the arsenic species as non-certified mass fraction values since they were determined using just one method. Through written communications and inquiries at conferences, customers of this SRM requested that its arsenic species mass fraction values be elevated to certified values. Results from an independent high-performance liquid chromotography inductively coupled plasma-mass spectrometry (HPLC-ICP-MS) method for arsenic species were provided through collaboration with the expertise in arsenic speciation analysis at the National Metrology Institute of Japan (NMIJ) [21,22,23,24].

4.2.1. Instrumentation

An ICP-MS 7500c (Agilent, Tokyo, Japan) equipped with a Micromist nebulizer (100 µL type) and a Scott spray chamber (2 ℃) was used. The operating parameters for the ICP-MS were: incident rf power 1600 W, outer Ar gas flow rate 15 L/min, intermediate Ar gas flow rate 0.9 L/min, carrier Ar gas flow rate 0.78 L/min, and make-up Ar gas flow rate 0.38 mL/min. The ICP-MS was operated using He as the collision cell gas (3 mL/min) to reduce some polyatomic molecular interferences. An HPLC was used for separation of arsenic species.

Arsenic species were separated by HPLC and directly introduced into the ICP-MS. A CAPCELLPAK C18 MG column (250 mm × ID 4.6 mm, Osaka Soda, Osaka, Japan) was used with the mobile phase containing 10 mmol/L sodium 1-butanesulfonate, 4 mmol/L malonic acid, 4 mmol/L tetramethylammonium hydroxide, and 0.05 % methanol (pH 3.0) at a flow rate of 0.75 mL/min. The exit of the HPLC column was connected to the nebulizer of the ICP-MS with PEEK tubing. The sample injection volume was 50 µL.

A heating dry block system (Digi PREP, SCP Science Inc., Canada) was used for heat-assisted extraction.

4.2.2. Materials

Six bottles of NIST SRM 1568c Rice Flour were analyzed.

NIST SRM 1568b was used as a control material. The certified value of inorganic arsenic (iAs, As(III) + As(V)) is (0.092 ± 0.040) mg/kg, that of dimethylarsinic acid (DMA) is (0.180 ± 0.012) mg/kg, and that of monomethylarsonic acid (MMA) is (0.011 ± 0.0035) mg/kg.

NIST SRM 3030 Monomethylarsonic Acid Standard Solution (17.64 ± 0.15) mg/kg [25], NIST SRM 3031 Dimethylarsinic Acid Standard Solution (20.47 ± 0.18) mg/kg [26], NIST SRM 3036 Arsenic Acid (AsV) Standard Solution (0.9706 ± 0.0044) mg/g [27], and NIST SRM 3037 Arsenous Acid (AsIII) Standard Solution (1.0442 ± 0.0020) mg/g [28] were used to prepare the calibration standard solution.

NMIJ CRM 7901-a Arsenobetaine Solution (24.40 ± 0.67) mg/kg [29] was used as the source for the arsenobetaine (AsB) used as the internal standard solution.

The acids used were of ultrapur® grade (Kanto Chemical Co., Inc., Tokyo, Japan), and the organic solvent used was of HPLC grade (Kanto). Sodium 1-butanesulfonate (Tokyo Chemical

Industry Co., Ltd., Tokyo, Japan), malonic acid (Fuji Film Wako Pure Chemical Industries, Ltd., Osaka, Japan), and tetramethylammonium hydroxide (Tama Chemicals Co., Ltd., Kanagawa, Japan) were obtained as indicated. Ultrapure water was generated with a Milli Q-Labo filter (Nippon Millipore Ltd, Tokyo, Japan) and was used throughout.

4.2.3. Extraction procedure for arsenic species

Arsenic species in the rice flour samples were extracted by a heat-assisted technique using acid solvent. A portion of rice flour sample (≈ 0.5 g) was accurately weighed into a 10 mL glass tube and 2 g of 0.15 mol/L HNO_3 + 0.30 mol/L H_2O_2 was added as the extracting solvent. The tube was capped and placed in a dry heating block system at 100 ℃ for 2 h. After cooling to room temperature, 1 g of the internal standard solution (AsB, ≈ 50 ng/g as As) and 7 g of water were added (total liquid phase: 10 g). The tube was centrifuged at 419 rad/s (4000 rpm) for 10 min, and then the liquid phase was then passed through a 0.45 µm syringe-type polyvinylidene difluoride membrane filter. The filtrate was analyzed by HPLC-ICP-MS. In the HPLC-ICP-MS measurement, injection volume was 50 µL. For As measurement, m/z 75 was monitored, and the measurement time was 10 min.

Chromatograms of the mixed standard solution and the SRM 1568c extracts are displayed in Fig. 5. Using just acid extraction, the peaks of As(III) and MMA are close to each other. Since the amount of MMA is very small compared to As(III), H_2O_2 was added to the extraction solvent to oxidize As(III) to As(V) during the extraction process. This greatly simplified the MMA analysis. The iAs in SRMs 1568b and 1568c was measured as As(V).

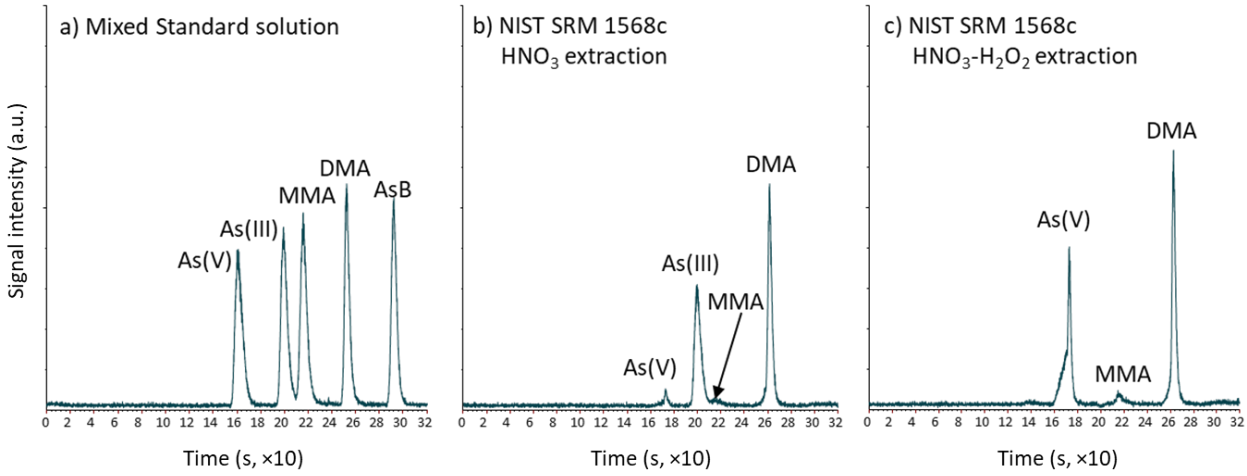


Fig. 5. Exemplar Chromatograms of the Mixed Standard Solution and SRM 1568c Extracts.

Panel a) Mixed standard solution; the concentration of each species ≈ 10 ng/g as As.
Panel b) SRM 1568c following extraction with 0.15 mol/L HNO_3.
Panel c) SRM 1568c following extraction with 0.15 mol/L HNO_3 + 0.30 mol/L H_2O_2.

Three calibrants were gravimetrically prepared from the mixed standard solution. One calibrant was prepared from just the internal standard. Each calibrant was determined in triplicate. The resulting linear calibration functions for iAs, MMA, and DMA are shown in Fig. 6.

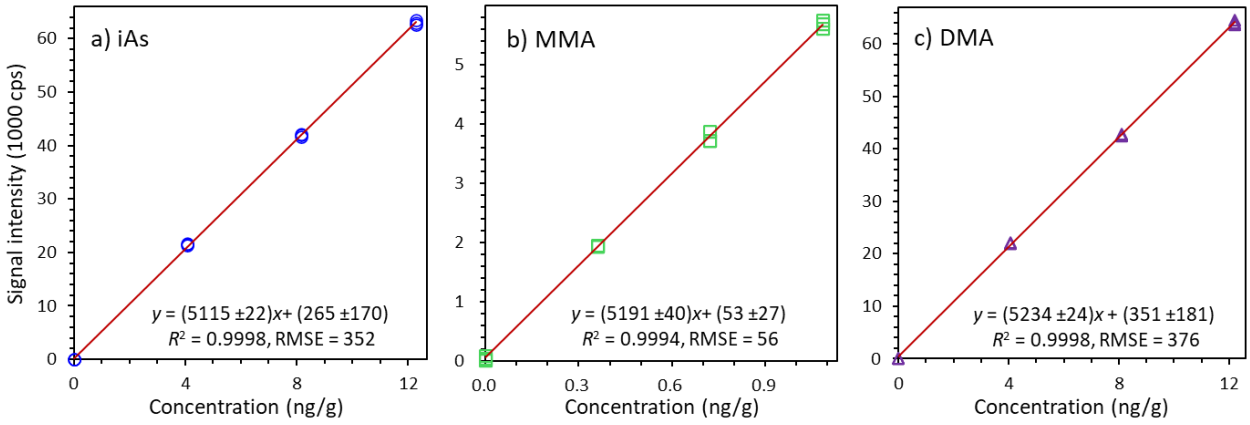


Fig. 6. Calibration Curves for iAs, MMA, and DMA.

Panel a) iAs; Panel b) MMA; Panel c) DMA.

4.2.4. Calculations

The iAs, MMA, and DMA mass fractions were calculated using external calibration with internal standard adjustment:

$$w_{\text{anal}} = \left(\frac{A_{\text{anal}} \times \left(\frac{A_{\text{IS,ref}} \times w_{\text{IS,sam}}}{w_{\text{IS,ref}} \times A_{\text{IS,sam}}} \right) - b}{a} - w_{\text{blank}} \right) \times \frac{m_{\text{sol}}}{m_{\text{sam}}} \times \frac{1}{1 - w_{\text{water}}} \times \frac{1}{1000} \qquad (15)$$

where: w_{anal} = mass fraction of the analyte in the sample in mg/kg,
A_{anal} = peak area of the analyte,
$A_{\text{IS,refl}}$ = peak area of the IS in the reference,
$A_{\text{IS,sam}}$ = peak area of the IS in the sample,
$w_{\text{IS,ref}}$ = mass fraction of IS in the reference in ng/g,
$w_{\text{IS,sam}}$ = mass fraction of IS in the sample in ng/g,
a = slope of the calibration curve,
b = intercept of the calibration curve,
w_{blank} = mass fraction of analyte in the blank in mg/kg,
m_{sam} = mass of the sample in g,
m_{sol} = mass of the diluted solution in g,
w_{H2O} = mass fraction of moisture in the sample in g/g.

The calibration parameters are estimated using the IS-adjusted peak areas.

Only the uncertainties related to the standard solution and the measurement results are included. The uncertainty of the standard solution was adopted from the NIST certificate.

The 95 % level of confidence expanded uncertainty of the mass fraction estimates is calculated using the following:

$$U = k \sqrt{\begin{array}{c} u^2(m_{\text{sam}}) + u^2(m_{\text{sol}}) + u^2(w_{\text{blank}}) + u^2(F) + u^2(\text{Cal}) \\ + u^2(a) + u^2(b) + u^2(A_{\text{sam}}) \end{array}} \qquad (16)$$

where: k = Student's t coverage factor for a 95 % confidence level,
$u(m_{sam})$ = standard uncertainty in mass of the sample,
$u(m_{sol})$ = standard uncertainty in mass of the diluted solution,
$u(w_{blank})$ = standard uncertainty in mass of mass fraction in the blank,
$u(F)$ = standard uncertainty in dry mass correction factor: $F = 1/(1-w_{water})$,
$u(\text{cal})$ = standard uncertainty in the standard solution.
$u(a)$ = asymptotic standard error of slope,
$u(b)$ = asymptotic standard error of intercept,
$u(A_{sam})$ = standard uncertainty of sample peak area replicates (repeatability),

4.3. Interlaboratory Studies

Laboratories participating in NIST's HAMQAP Exercise 5 and HAMQAP Exercise 6 reported values for Ca, Fe, K, Na, As, Cd, Pb, Hg, and proximates in SRM 1568c. The quantitative results from these exercises are reported here in full. The reported results from each participating organization have been assigned an arbitrary numeric code, and specific method information reported by each laboratory is provided below in the appropriate subsection of Section 5 Measurement Results.

4.3.1. HAMQAP Exercise 5

For Exercise 5 [30], NIST distributed candidate SRM 1568c Rice Flour to 29 laboratories for the determination of Ca, K, and Na and to 30 laboratories for the determination of Fe. Participants were asked to use in-house analytical methods to determine Ca, Fe, K, and Na in three samples (0.5 g or greater) taken from one bottle of the rice flour material. Results were to be reported in mg/kg.

4.3.2. HAMQAP Exercise 6

For Exercise 6 [31], NIST distributed candidate SRM 1568c Rice Flour to 41 laboratories for the determination of As and Cd, 43 laboratories for the determination of Pb, and 40 laboratories for the determination of Hg. Participants were asked to use in-house analytical methods to determine As, Cd, Pb, and Hg in three samples (0.5 g or greater) taken from one bottle of the rice flour material. Results were to be reported in mg/kg on an as-received basis.

NIST also distributed SRM 1568c Rice Flour for the determination of proximates, in which 18 laboratories received samples for the determination of fat, 20 laboratories received samples for the determination of protein, 17 laboratories received samples for the determination of carbohydrates and solids, 21 laboratories received samples for the measurement of ash, and 14 laboratories received samples for the determination of calories. Participants were asked to use in-house analytical methods to determine proximates in three samples taken from one bottle of the rice flour material. Participants were to use a sample size appropriate for their in-house method of analysis and to report results in g/100 g except for calories, which were to be reported in kcal/100g.

5. Measurement Results

5.1. Moisture

5.1.1. NIST Moisture Results

A combination of NIST results for 28 d in a desiccator over magnesium perchlorate and 4 h at 90 °C in a forced-air drying oven were used for conversion of HAMQAP results from as-received to a dry-mass basis. Moisture results from two NIST methods are tabulated in Table 22, including summary statistics where *N* = number of values and SD = standard deviation of values.

Table 22. NIST Results for Moisture, %.

	Desiccator[a]							FAIR[b]	Combined[c]	
Bottle #	5 Day	7 Day	14 Day	22 Day	28 Day	35 Day	42 Day		Mean	SD
39	7.30	7.94	9.00	9.48	9.68	9.90	10.01	10.45	10.07	0.540
183	7.54	8.10	9.07	9.53	9.70	9.90	10.01	9.27	9.49	0.305
326	7.29	7.92	8.96	9.46	9.65	9.85	9.97	10.15	9.90	0.350
470	6.94	7.62	8.74	9.29	9.51	9.74	9.87	9.60	9.56	0.064
613	6.95	7.61	8.71	9.25	9.47	9.70	9.83	9.72	9.59	0.173
757	7.05	7.70	8.79	9.33	9.54	9.76	9.88	9.54	9.54	0.005
901	6.87	7.59	8.77	9.30	9.53	9.75	9.89	9.41	9.47	0.083
1044	7.16	7.81	8.90	9.40	9.59	9.80	9.91	9.64	9.62	0.037
1188	7.04	7.71	8.84	9.34	9.55	9.75	9.88	9.70	9.62	0.107
1331	7.03	7.68	8.84	9.33	9.53	9.74	9.86	9.60	9.57	0.046
1475	6.97	7.63	8.77	9.30	9.52	9.73	9.86	9.54	9.53	0.016
1618	7.14	7.79	8.89	9.39	9.61	9.80	9.92	9.56	9.59	0.035
N:	12	12	12	12	12	12	12	12	12	
Mean:	7.11	7.76	8.86	9.37	9.57	9.79	9.91	9.68	9.62	
SD:	0.19	0.16	0.11	0.09	0.07	0.07	0.06	0.32	0.18	

[a] Desiccator drying over magnesium perchlorate
[b] Forced air drying for 4 h @ 90° C
[c] Combination of results from 28-d desiccator drying and forced air drying replicates

Moisture results from the two NIST methods are visualized in Fig. 7, displaying results from multiple days of desiccator drying and 4 h forced-air drying at 90 °C.

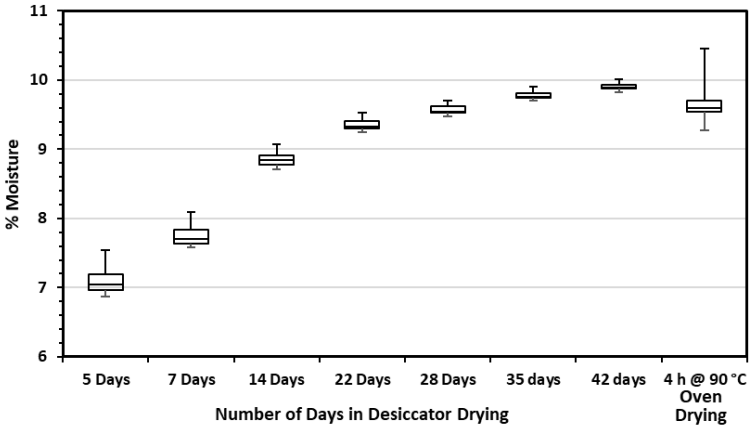


Fig. 7. Mass Loss (% Moisture) of SRM 1568c as a Function of Method.

The box plots show the interquartile ranges that the medium line divides the upper and lower quartiles. The whiskers indicate the minimum and maximum percent moisture values.

5.1.2. Moisture Value Assignment and Dry-Mass Conversions

The assigned value for moisture content was determined using two NIST techniques. The average of the two method means was used to estimate a dry-mass proportion of (0.9037 ± 0.0011), which was used to convert HAMQAP data from an as-received to a dry-mass basis. The uncertainty shown on this value is an expanded uncertainty. A relative uncertainty component for the conversion factor (0.1 %) obtained from the moisture measurements is incorporated in the uncertainties of the estimated analyte values, reported on a dry-mass basis. The uncertainty shown on this value is an approximate 95 % level of confidence expanded uncertainty, U_{95}.

The moisture correction of the HAMQAP results was achieved by multiplying the as-received measurements by a conversion factor equal to the inverse of the dry-mass proportion. The HAMQAP results for ash and solids are not moisture-corrected due to the nature of the analytes.

5.1.3. NMIJ Moisture Results

Between December 2024 and January 2025, six bottles of SRM 1568c and one bottle of SRM 1568b were sent to the National Metrology Institute of Japan (NMIJ) for arsenic speciation analysis. The moisture content of these materials was determined to enable metrologically traceable conversion of wet mass results to dry mass.

Moisture content was determined by measuring the mass loss after drying duplicate ≈1 g portions of the rice flour materials from each bottle at 90 °C in an oven. SRM 1568b was heated for 2 h, SRM 1568c was heated for 4 h. The results of these measurements are listed in Table 23. The results for SRM 1568c are displayed in Fig. 8.

Table 23. Summary NMIJ Moisture Determinations.

	Moisture Content (%)			
Bottle ID	A	B	Mean	SD
1568b	9.01	8.95	8.98	0.04
1568c-1	10.27	10.25	10.26	0.02
1568c-2	10.27	10.34	10.30	0.04
1568c-3	10.21	10.15	10.18	0.04
1568c-4	10.20	10.24	10.22	0.03
1568c-5	10.31	10.21	10.26	0.07
1568c-6	10.32	10.26	10.29	0.05
		N:	6	
		Mean, Pooled SD:	10.25	0.05
		SD:	0.05	

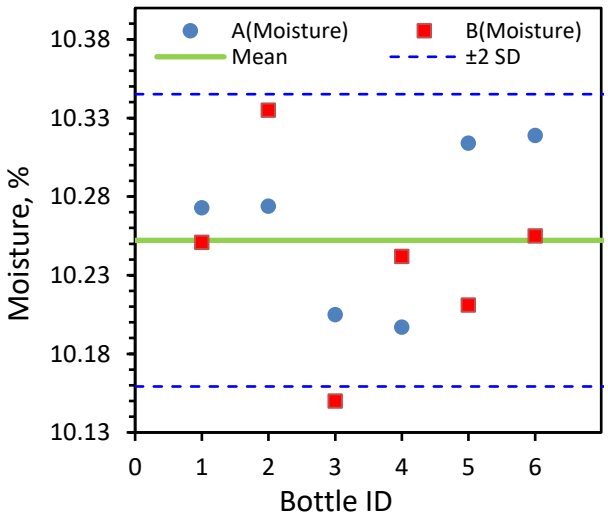


Fig. 8. NMIJ's Mass Loss (% Moisture) of SRM 1568c.

5.2. Elements

All NIST total element results were determined on a dry-mass basis. In all cases, the quality assurance measurement results were concordant with the certified values delivered by the control material, SRM 1568b Rice Flour. No bottling-order trend was apparent for any element.

Results from the HAMQAP participants were provided on an as-received basis. Prior to combination with NIST results, HAMQAP results were converted to a dry-mass basis, assuming a moisture content of 9.62 % (see Section 5.1.2).

In addition to the measurement results, the summary table or tables for each analyte also list the number of accepted results (*N*), the arithmetic mean of the accepted results (Mean), the standard deviation of the accepted results (SD), and the square root of the sum of the squares of the measurement SDs (Pooled SD).

5.2.1. Aluminum Results

The NIST ICP-MS results for aluminum (Al) on a dry-mass basis are summarized in Table 24. Columns A and B are used in the table below to distinguish between the first and second aliquot taken from each bottle. These results are displayed as a function of the sample bottle number in Fig. 9. The uncertainty budget for determination of Al using this method is presented in Section 4.1.5.

Table 24. Summary of Results for Aluminum (Al), mg/kg.

	NIST ICP-MS			
Bottle #	A	B	Mean	SD
15	2.82	2.06	2.44	0.54
187	2.53	2.66	2.59	0.09
360	2.64	2.47	2.55	0.12
532	2.36		2.36	
704	1.60	1.85	1.73	0.18
877	2.75	1.93	2.34	0.58
1049	4.30	2.10	3.20	1.56
1221	2.03	4.42	3.22	1.70
1393	1.72	3.88	2.80	1.53
1651	4.48	6.69	5.58	1.56
		N:	10	
		Mean, Pooled SD:	2.88	1.09
		SD:	1.04	

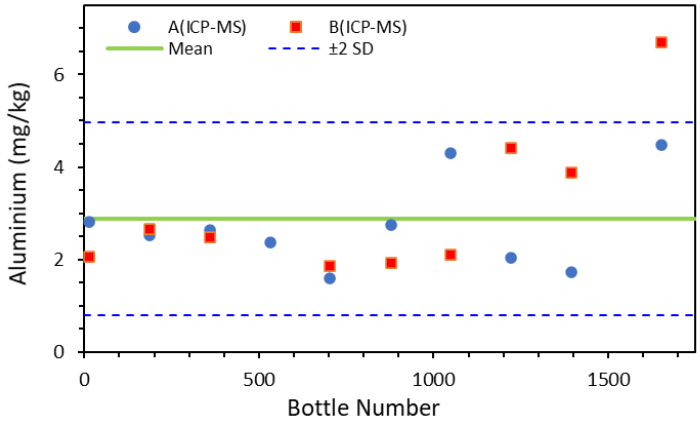


Fig. 9. Aluminum (Al) Mass Fraction as a Function of Bottle Number.

5.2.2. Arsenic Results

The NIST ICP-MS and INAA results for arsenic (As) on a dry-mass basis are summarized in Table 25. Columns A and B are used in the table below to distinguish between the first and second aliquot taken from each bottle. These results are displayed as a function of the sample bottle number in Fig. 10. The uncertainty budgets for determination of As using these methods are presented in Sections 4.1.5 and 4.1.6.

Table 25. Summary of NIST Results for Arsenic (As), mg/kg.

NIST ICP-MS

Bottle #	A	B	Mean	SD
2	0.360	0.378	0.369	0.013
15	0.234	0.346	0.290	0.079
187	0.298	0.431	0.365	0.094
356	0.359	0.375	0.367	0.011
360	0.394	0.442	0.418	0.033
532	0.377	0.398	0.388	0.015
704	0.391	0.209	0.300	0.129
877	0.391	0.309	0.350	0.058
1049	0.454	0.410	0.432	0.031
1221	0.329	0.213	0.271	0.082
1393	0.343	0.351	0.347	0.006
1651		0.409	0.409	
		N:	12	
		Mean, Pooled SD:	0.359	0.064
		SD:	0.051	

NIST INAA

Bottle #	A	B	Mean	SD
20	0.371	0.360	0.366	0.008
154	0.358	0.369	0.364	0.008
441	0.358	0.358	0.358	0.000
728	0.362	0.358	0.360	0.003
872	0.344	0.361	0.353	0.012
882	0.372	0.353	0.363	0.013
1159	0.354	0.364	0.359	0.007
1302	0.356	0.349	0.353	0.005
1456	0.358	0.352	0.355	0.004
1589	0.347	0.365	0.356	0.013
		N:	10	
		Mean, Pooled SD:	0.359	0.008
		SD:	0.005	

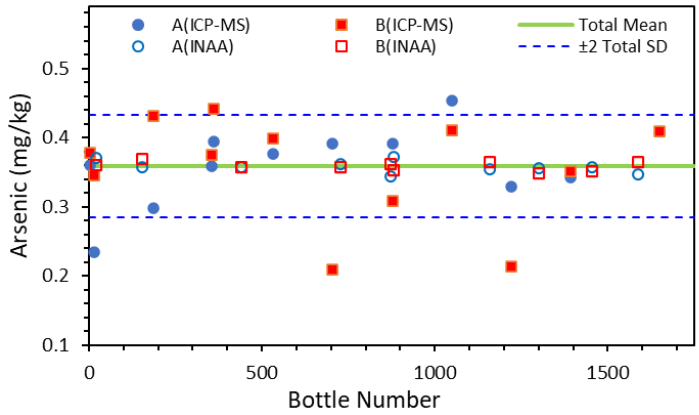


Fig. 10. Arsenic (As) Mass Fraction as a Function of Bottle Number.

The as-received results for As from HAMQAP Exercise 6 are summarized in Table 26. Columns A, B, and C are used in the table below to distinguish between the different aliquots taken by each participating laboratory from a single bottle.

Table 26. Summary of HAMQAP Exercise 6 Results for Arsenic (As), mg/kg.

HAMQAP Exercise 6 [a]

Lab	A	B	C	Mean	SD	Method
1	0.36	0.36	0.37	0.360	0.005	ICP-MS
2	0.32	0.32	0.32	0.322	0.001	ICP-MS
11	0.34	0.34	0.33	0.335	0.009	ICP-MS
15	0.36	0.38	0.37	0.372	0.010	ICP-MS
17	0.31	0.31	0.32	0.316	0.007	ICP-MS
19	0.37	0.37	0.40	0.380	0.017	ICP-MS
20	0.36	0.35	0.34	0.350	0.010	ICP-MS
21	0.37	0.38	0.39	0.380	0.010	ICP-OES
27	0.31	0.30	0.30	0.302	0.008	ICP-MS
30	0.37	0.38	0.38	0.375	0.005	ICP-MS
33	0.33	0.32	0.34	0.328	0.008	ICP-MS
34	0.29	0.29	0.29	0.286	0.001	ICP-MS
39	0.37	0.36	0.38	0.367	0.009	ICP-MS
46	0.34	0.31	0.32	0.323	0.015	ICP-MS
63	0.32	0.34	0.33	0.331	0.007	ICP-OES
66	0.31	0.31	0.30	0.306	0.002	ICP-MS
69	0.34	0.35	0.36	0.350	0.010	ICP-MS
70	0.36	0.35	0.34	0.353	0.010	ICP-MS
73	0.40	0.38	0.39	0.389	0.008	ICP-MS
			N:	19		
			Mean, Pooled SD:	0.343	0.008	
			SD:	0.029		

[a] Five results excluded based on being outside the dataset's consensus tolerance limits and seven results for incorrect or no analytical method reported.

The summary results for the three datasets are compared in Fig. 11, with the HAMQAP results corrected to a dry-mass basis assuming a moisture content of 9.62 %.

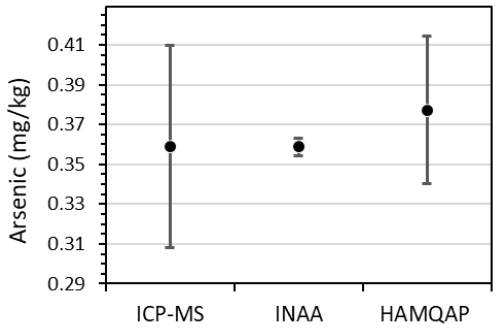


Fig. 11. Comparison of Arsenic (As) Mass Fraction Values by Method.

Each dot represents a mean arsenic mass fraction estimate for SRM 1568c by method. The error bars represent measurement repeatability standard deviations.

5.2.3. Bromine Results

The NIST INAA results for bromine (Br) on a dry-mass basis are summarized in Table 27. Columns A and B are used in the table below to distinguish between the first and second aliquot taken from each bottle. The results are displayed in Fig. 12 as a function of the sample bottle number. The uncertainty budget for determination of Br using this method is presented in Section 4.1.6.

Table 27. Summary of Results for Bromine (Br), mg/kg.

	NIST INAA			
Bottle #	A	B	Mean	SD
20	0.997	0.957	0.977	0.028
154	0.95	0.969	0.960	0.013
441	0.967	0.956	0.962	0.008
728	0.977	0.977	0.977	0.000
872	0.935	0.978	0.957	0.030
882	0.999	0.977	0.988	0.016
1159	0.966	1.009	0.988	0.030
1302	0.964	0.958	0.961	0.004
1456	0.965	0.933	0.949	0.023
1589	0.946	0.979	0.963	0.023
		N:	10	
		Mean, Pooled SD:	0.968	0.020
		SD:	0.013	

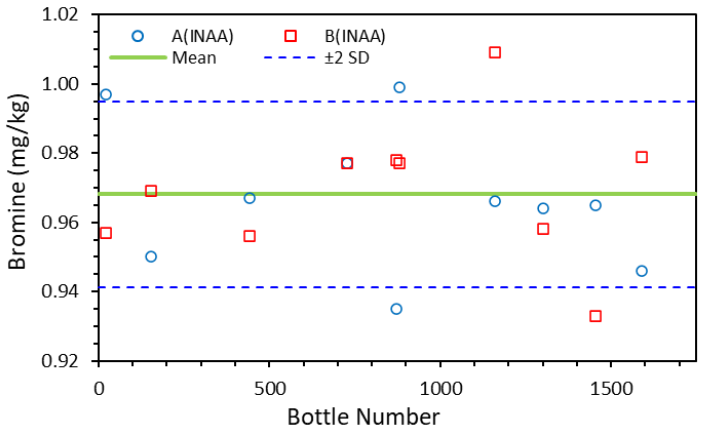


Fig. 12. Bromine (Br) Mass Fraction as a Function of Bottle Number.

5.2.4. Cadmium Results

The NIST ICP-MS and HAMQAP Exercise 5 results for cadmium (Cd) are summarized in Table 28. Columns A, B, and C are used in the table below to distinguish between the different aliquots taken from each bottle or by each participating laboratory from a single bottle. The NIST results are reported on a dry-mass basis; the HAMQAP results are reported on an as-received basis. The NIST results are displayed as a function of the sample bottle number in Fig. 13. The uncertainty budget for the determination of Cd by the NIST ICP-MS method is presented in Section 4.1.5.

Table 28. Summary of Results for Cadmium (Cd), mg/kg.

NIST ICP-MS

Bottle #	A	B	Mean	SD
15	0.0111	0.0097	0.0104	0.0010
187	0.0103	0.0089	0.0096	0.0009
360	0.0103	0.0085	0.0094	0.0013
532	0.0093	0.0103	0.0098	0.0007
704	0.0096	0.0092	0.0094	0.0003
877	0.0096	0.0091	0.0094	0.0003
1049	0.0097	0.0101	0.0099	0.0003
1221	0.0102	0.0111	0.0107	0.0007
1393	0.0092	0.0094	0.0093	0.0002
1651	0.0095		0.0095	
		N:	10	
		Mean, Pooled SD:	0.0097	0.0007
		SD:	0.0005	

HAMQAP Exercise 5 [a]

Lab	A	B	C	Mean	SD	Method
1	0.008	0.009	0.010	0.009	0.001	ICP-MS
2	0.011	0.012	0.011	0.011	0.001	ICP-MS
5	0.009	0.008	0.009	0.009	0.000	ICP-MS
11	0.007	0.009	0.007	0.008	0.001	ICP-MS
15	0.009	0.009	0.009	0.009	0.000	ICP-MS
20	0.009	0.010	0.009	0.009	0.001	ICP-MS
21	0.010	0.010	0.010	0.010	0.000	ICP-OES
27	0.008	0.007	0.008	0.008	0.000	ICP-MS
30	0.009	0.009	0.009	0.009	0.000	ICP-MS
33	0.010	0.010	0.009	0.010	0.000	AAS
42	0.008	0.008	0.009	0.008	0.000	ID ICP-MS
52	0.012	0.010	0.013	0.012	0.002	ICP-OES
56	0.011			0.011		ICP-MS
59	0.009	0.009	0.009	0.009	0.000	ID ICP-MS
69	0.010	0.010	0.010	0.010	0.000	ICP-MS
74	0.008			0.008		ID ICP-MS
			N:	16		
			Mean, Pooled SD:	0.009	0.001	
			SD:	0.001		

[a] Twelve results excluded based on being below the participant's detection limit or outside the dataset's consensus tolerance limits and one result for no analytical method reported.

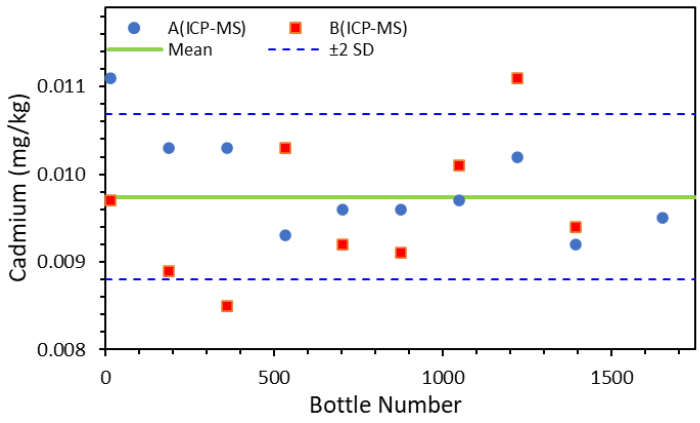


Fig. 13. Cadmium (Cd) Mass Fraction as a Function of Bottle Number.

The summary results for the two datasets are compared in Fig. 14, with the HAMQAP results corrected to a dry-mass basis assuming a moisture content of 9.62 %.

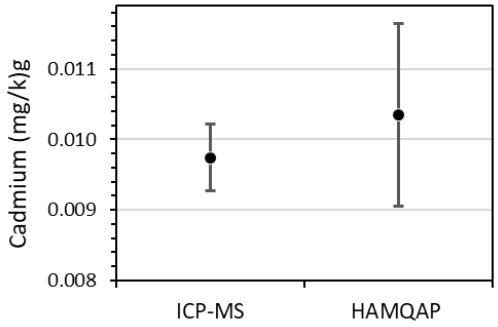


Fig. 14. Comparison of Cadmium (Cd) Mass Fraction Values by Method.

Each dot represents a mean cadmium mass fraction estimate for SRM 1568c by method. The error bars represent measurement repeatability standard deviations.

5.2.5. Calcium Results

The NIST ICP-OES and WDXRF results for calcium (Ca) on a dry-mass basis are summarized in Table 29. Columns A and B are used in the table below to distinguish between the first and second aliquot taken from each bottle. The results are displayed in Fig. 15 as a function of the sample bottle number. The uncertainty budgets for these methods are presented in Sections 4.1.3 and 4.1.8.

Table 29. Summary of Results for Calcium (Ca), mg/kg.

NIST ICP-OES

Bottle #	A	B	Mean	SD
13	95.7	97.6	96.6	1.4
13-1	112.0		112.0	
185	108.2	74.2	91.2	24.0
358	138.0	123.6	130.8	10.2
530	111.3	93.6	102.5	12.5
702	89.1	96.0	92.6	4.9
875	105.7	102.1	103.9	2.5
1048	90.4	122.6	106.5	22.8
1219	212.2	104.3	158.2	76.3
1392	88.1	108.6	98.4	14.5
1564	88.5	101.0	94.7	8.8
		N:	11	
		Mean, Pooled SD:	108	27
		SD:	20	

NIST WDXRF

Bottle #	A	B	Mean	SD
57	101.5	86.5	94.0	10.7
344	87.6	87.5	87.5	0.0
631	88.4	85.2	86.8	2.3
919	90.7	86.6	88.7	2.9
1206	91.4		91.4	
1493	87.4	91.3	89.4	2.8
		N:	6	
		Mean, Pooled SD:	89.6	4.8
		SD:	2.7	

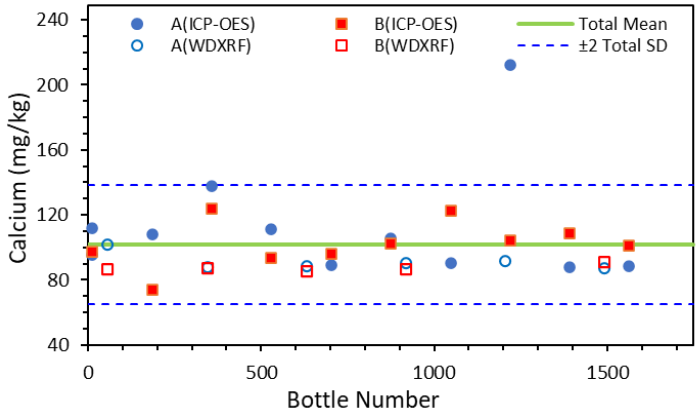


Fig. 15. Calcium (Ca) Mass Fraction as a Function of Bottle Number.

The as-received results for Ca from HAMQAP Exercise 5 are summarized in Table 30. Columns A, B, and C are used in the table below to distinguish between the different aliquots taken by each participating laboratory from a single bottle.

Table 30. Summary of HAMQAP Exercise 5 Results for Calcium (Ca), mg/kg.

HAMQAP Exercise 5 [a]

Lab	A	B	C	Mean	SD	Method
1	115.0	111.0	110.0	112.0	2.6	ID ICP-MS
2	132.4	129.7	111.8	124.6	11.2	ICP-OES
3	84.7	78.2	81.5	81.5	3.3	ICP-MS
5	114.0	116.0	92.0	107.3	13.3	ICP-OES
7	93.5	93.8	94.5	94.0	0.5	ICP-OES
15	91.9	92.9	112.0	98.9	11.3	ICP-OES
16	114.6	121.9	101.8	112.8	10.2	ICP-OES
25	82.9	90.1	86.4	86.5	3.6	ICP-OES
29	89.8	93.9	91.4	91.7	2.1	ICP-OES
30	90.3	103.0	112.0	101.8	10.9	ICP-OES
33	100.0	96.3	100.9	99.0	2.4	ICP-MS
34	93.1	97.7	94.3	95.0	2.4	ICP-MS
35	99.7	106.0	104.0	103.2	3.2	ICP-OES
41	98.5	118.2	119.3	112.0	11.7	ICP-MS
45	120.2	134.9	143.6	132.9	11.8	ICP-OES
47	99.2	80.1	87.2	88.8	9.7	ICP-OES
51	88.1	87.5	89.0	88.2	0.8	ICP-MS
			N:	17		
			Mean, Pooled SD:	102	6	
			SD:	14		

[a] One result excluded based on being outside the dataset's consensus tolerance limits and one result for no analytical method reported.

The summary results for the three datasets are compared in Fig. 16, with the HAMQAP results corrected to a dry-mass basis assuming a moisture content of 9.62 %.

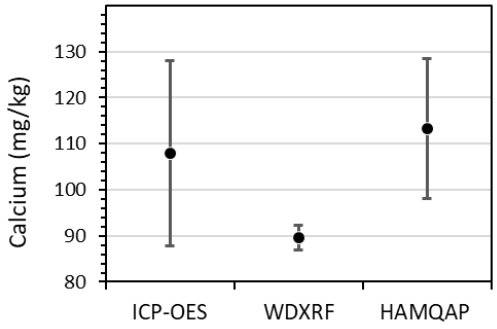


Fig. 16. Comparison of Calcium (Ca) Mass Fraction Values by Method.

Each dot represents a mean calcium mass fraction estimate for SRM 1568c by method. The error bars represent measurement repeatability standard deviations.

5.2.6. Chlorine Results

The NIST WDXRF results for chlorine (Cl) on a dry-mass basis are summarized in Table 31. Columns A and B are used in the table below to distinguish between the first and second aliquot taken from each bottle. The results are displayed in Fig. 17 as a function of the sample bottle number. The uncertainty budget for determination of Cl using this method is presented in Section 4.1.8.

Table 31. Summary of Results for Chlorine (Cl), mg/kg.

	NIST WDXRF			
Box	A	B	Mean	SD
57	290.7	288.1	289.4	1.8
344	278.1	290.7	284.4	8.9
631	290.8	299.9	295.4	6.4
919	292.3	309.1	300.7	11.9
1206	302.1		302.1	
1493	284.7	286.3	285.5	1.1
		N:	6	
		Mean, Pooled SD:	293.0	7.3
		SD:	7.6	

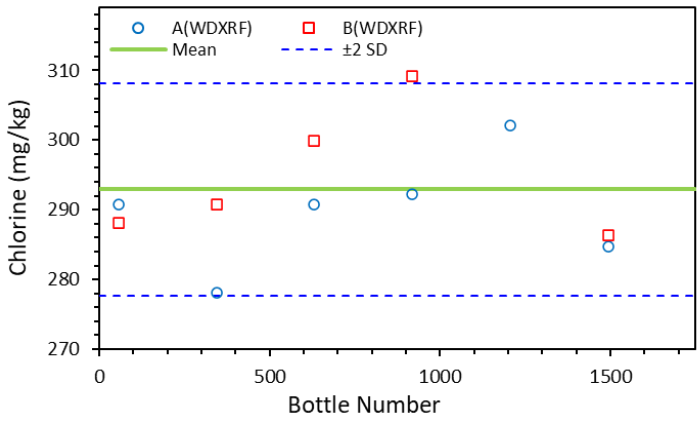


Fig. 17. Chlorine (Cl) Mass Fraction as a Function of Bottle Number.

5.2.7. Copper Results

The NIST ICP-OES and WDXRF results for copper (Cu) on a dry-mass basis are summarized in Table 32. Columns A and B are used in the table below to distinguish between the first and second aliquot taken from each bottle. The NIST Cu results are displayed as a function of the sample bottle number in Fig. 18. The two methods' summary results are compared in Fig. 19. The uncertainty budgets for determination of Cu using these methods are presented in Sections 4.1.3 and 4.1.8.

Table 32. Summary of Results for Copper (Cu), mg/kg.

NIST ICP-OES

Bottle #	A	B	Mean	SD
13	3.90	3.25	3.58	0.46
13-1	2.84		2.84	
185	2.55	3.79	3.17	0.88
358	2.70	3.20	2.95	0.35
530	2.38	2.91	2.64	0.37
702	2.74	2.83	2.79	0.06
875	2.88	2.96	2.92	0.06
1048	4.54	2.50	3.52	1.44
1219	3.34	2.09	2.72	0.89
1392	2.69	2.35	2.52	0.24
1564	2.83	2.98	2.91	0.10
		N:	11	
		Mean, Pooled SD:	2.96	0.65
		SD:	0.34	

NIST WDXRF

Bottle #	A	B	Mean	SD
57	3.27	2.79	3.03	0.34
344	3.60	3.02	3.31	0.42
631	2.61	2.74	2.67	0.09
919	3.11	2.93	3.02	0.12
1206	3.49	3.53	3.51	0.03
1493	3.12	3.56	3.34	0.31
		N:	6	
		Mean, Pooled SD:	3.15	0.26
		SD:	0.30	

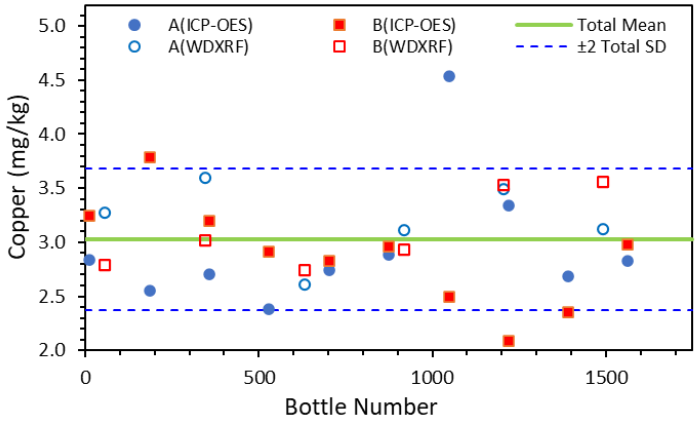


Fig. 18. Copper (Cu) Mass Fraction as a Function of Bottle Number.

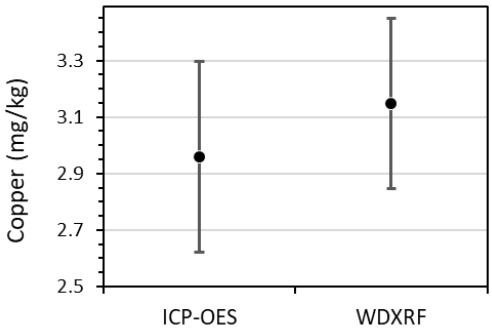


Fig. 19. Comparison of Copper (Cu) Mass Fraction Values by Method.

Each dot represents a mean copper mass fraction estimate for SRM 1568c by method. The error bars represent measurement repeatability standard deviations.

5.2.8. Iron Results

The NIST ICP-OES and WDXRF results for iron (Fe) on a dry-mass basis are summarized in Table 33. Columns A and B are used in the table below to distinguish between the first and second aliquot taken from each bottle. The results are displayed in Fig. 20 as a function of the sample bottle number. The uncertainty budgets for determination of Fe using these methods are presented in Sections 4.1.3 and 4.1.8.

Table 33. Summary of NIST Results for Iron (Fe), mg/kg.

NIST ICP-OES

Bottle #	A	B	Mean	SD
15	13.37		13.37	
187	11.85	8.55	10.20	2.33
360	12.94	12.64	12.79	0.21
532	8.93	14.77	11.85	4.13
704	11.74	11.49	11.62	0.17
877	11.90	12.63	12.27	0.52
1049	11.25	11.43	11.34	0.12
1221	11.87	14.41	13.14	1.80
1393	11.46	12.81	12.14	0.95
1651	11.23	13.98	12.60	1.94
		N:	10	
		Mean, Pooled SD:	12.13	1.85
		SD:	0.94	

NIST WDXRF

Bottle #	A	B	Mean	SD
57	14.33	13.71	14.02	0.44
344	12.90	13.44	13.17	0.38
631	13.52	13.94	13.73	0.30
919	15.31	13.52	14.42	1.26
1206	14.58		14.58	
1493	13.59	14.13	13.86	0.38
		N:	6	
		Mean, Pooled SD:	13.96	0.60
		SD:	0.51	

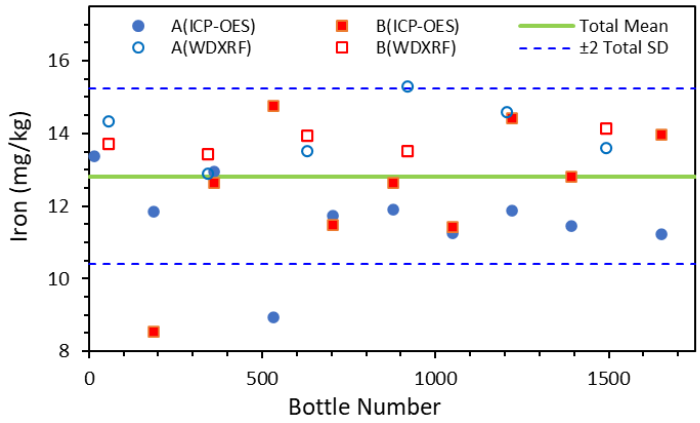


Fig. 20. Iron (Fe) Mass Fraction as a Function of Bottle Number.

The as-received results for Fe from HAMQAP Exercise 5 are summarized in Table 34. Columns A, B, and C are used in the table below to distinguish between the different aliquots taken by each participating laboratory from a single bottle.

Table 34. Summary of HAMQAP Exercise 5 Results for Iron (Fe), mg/kg.

			HAMQAP Exercise 5 [a]			
Lab	A	B	C	Mean	SD	Method
1	15.1	14.3	13.8	14.4	0.7	ID ICP-MS
2	20.7	19.2	19.8	19.9	0.8	ICP-OES
3	11.0	11.0	11.0	11.0	0.0	ICP-MS
5	8.0	7.0	6.0	7.0	1.0	ICP-OES
7	11.7	11.7	11.9	11.8	0.1	ICP-OES
16	11.0	9.8	9.0	9.9	1.0	ICP-OES
25	11.7	11.0	11.1	11.3	0.4	ICP-OES
29	19.7	17.5	17.9	18.4	1.2	ICP-OES
30	16.7	17.3	17.1	17.0	0.3	ID ICP-MS
33	14.7	12.4	12.1	13.1	1.4	ICP-MS
34	11.8	12.1	10.5	11.5	0.9	ICP-MS
35	11.8	12.0	11.9	11.9	0.1	ICP-OES
41	13.2	15.9	17.9	15.7	2.4	ICP-MS
47	12.1	9.3	10.4	10.6	1.4	ICP-OES
51	12.2	11.9	11.8	12.0	0.2	ICP-MS
			N:	15		
			Median, Pooled SD:	13.0	0.8	
			SD:	3.6		

[a] Two results excluded based on being outside the dataset's consensus tolerance limits and one result for incomplete analytical method reported.

The summary results for the three datasets are compared in Fig. 21, with the HAMQAP results corrected to a dry-mass basis assuming a moisture content of 9.62 %.

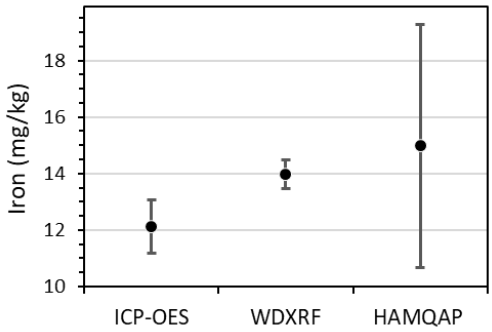


Fig. 21. Comparison of Iron (Fe) Mass Fraction Values by Method.

Each dot represents a mean iron mass fraction estimate for SRM 1568c by method. The error bars represent measurement repeatability standard deviations.

5.2.9. Lead Results

The NIST ICP-MS and HAMQAP Exercise 6 results for lead (Pb) are summarized in Table 35. Columns A, B, and C are used in the table below to distinguish between the different aliquots taken from each bottle or by each participating laboratory from a single bottle. The NIST results are reported on a dry-mass basis; the HAMQAP results are reported on an as-received basis. The NIST results are displayed in Fig. 22 as a function of the sample bottle number. The summary results for the two datasets are compared in Fig. 23, with the HAMQAP results corrected to a dry-mass basis assuming a moisture content of 9.62 %. The uncertainty budget for determination of Pb using the NIST ICP-MS method is presented in Section 4.1.5.

Table 35. Summary of Results for Lead (Pb), mg/kg.

NIST ICP-MS

Bottle #	A	B	Mean	SD
15	0.027	0.013	0.0202	0.0098
187	0.025	0.012	0.0186	0.0096
360	0.020	0.020	0.0201	0.0002
532	0.014	0.047	0.0305	0.0234
704	0.011	0.019	0.0146	0.0058
877	0.012	0.012	0.0120	0.0001
1049	0.037	0.017	0.0266	0.0140
1221	0.011	0.018	0.0145	0.0048
1393	0.009	0.015	0.0121	0.0041
1651	0.014		0.0137	
		N:	10	
		Mean, Pooled SD:	0.0183	0.0011
		SD:	0.0063	

HAMQAP Exercise 6 [a]

Lab	A	B	C	Mean	SD	Method
1	0.012	0.012	0.012	0.012	0.000	ICP-MS
2	0.013	0.012	0.013	0.013	0.001	ICP-MS
5	0.024	0.018	0.019	0.02	0.003	ICP-MS
11	0.015	0.014	0.009	0.013	0.003	ICP-MS
15	0.016	0.014	0.014	0.015	0.001	ICP-MS
17	0.025	0.021	0.026	0.024	0.003	ICP-OES
22	0.025	0.027	0.025	0.026	0.001	ICP-MS
27	0.033	0.025	0.022	0.027	0.006	ICP-MS
31	0.024	0.024	0.028	0.025	0.002	ID ICP-MS
33	0.014	0.014	0.015	0.014	0.000	ICP-MS
39	0.016	0.013	0.015	0.015	0.002	ICP-MS
41	0.015	0.012	0.013	0.013	0.002	ICP-MS
42	0.012	0.011	0.011	0.011	0.000	ID ICP-MS
52	0.008	0.008	0.008	0.008	0.000	ICP-OES
56	0.019			0.019		ICP-MS
59	0.01	0.01	0.01	0.01	0.000	ID ICP-MS
66	0.013	0.013	0.013	0.013	0.000	ICP-MS
69	0.01	0.01	0.01	0.01	0.000	ICP-MS
74	0.0135			0.0135		ID ICP-MS
			N:	19		
			Mean, Pooled SD:	0.016	0.002	
				0.006		

[a] Twelve results excluded based on being below the participant's detection limit or outside the dataset's consensus tolerance limits and one result for no analytical method reported.

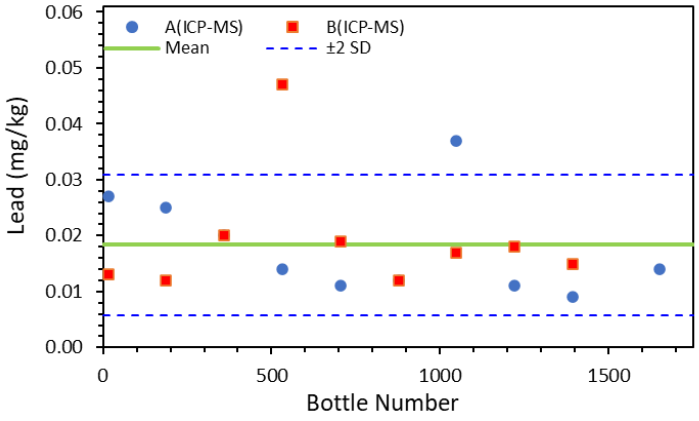


Fig. 22. Lead (Pb) Mass Fraction as a Function of Bottle Number.

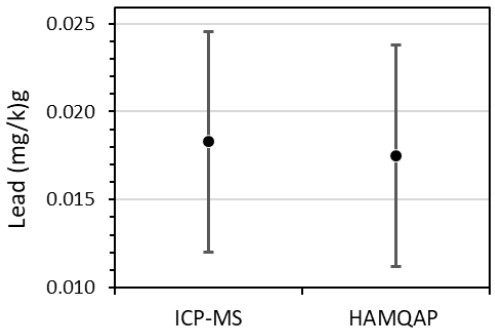


Fig. 23. Comparison of Lead (Pb) Mass Fraction Values by Method.

Each dot represents a mean lead mass fraction estimate for SRM 1568c by method. The error bars represent measurement repeatability standard deviations.

5.2.10. Magnesium Results

The NIST ICP-OES and WDXRF results for magnesium (Mg) on a dry-mass basis are summarized in Table 36. Columns A and B are used in the table below to distinguish between the first and second aliquot taken from each bottle. The results are displayed in Fig. 24 as a function of the sample bottle number. The summary results for these datasets are compared in Fig. 25. The uncertainty budgets for determination of Mg using these methods are presented in Sections 4.1.3 and 4.1.8.

Table 36. Summary of Results for Magnesium (Mg), mg/kg.

NIST ICP-OES

Bottle #	A	B	Mean	SD
13	1362	1341	1352	15
13-1	1440		1440	
185	1287	1360	1324	52
358	1370	1356	1363	9
530	1367	1357	1362	7
702	1377	1342	1360	25
875	1354	1355	1355	1
1048	1309	1345	1327	25
1219	1442	1330	1386	79
1392	1361	1331	1346	21
1564	1365	1353	1359	8
		N:	11	
		Mean, Pooled SD:	1361	33
		SD:	31	

NIST WDXRF

Bottle #	A	B	Mean	SD
57	1596	1624	1610	20
344	1520	1594	1557	52
631	1534	1535	1535	1
919	1574	1601	1588	19
1206	1530	1588	1559	41
1493	1559	1557	1558	1
		N:	6	
		Mean, Pooled SD:	1568	29
		SD:	27	

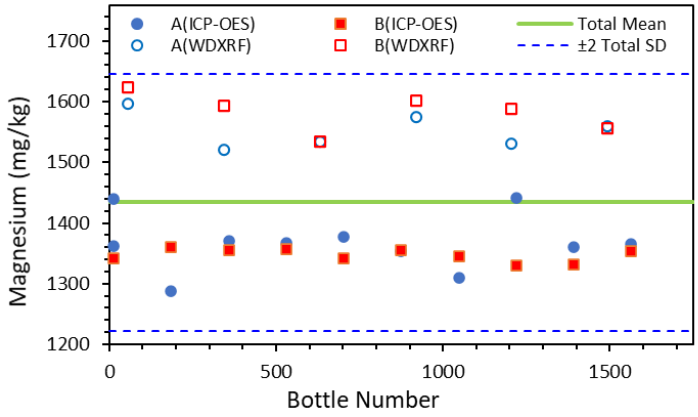


Fig. 24. Magnesium (Mg) Mass Fraction as a Function of Bottle Number.

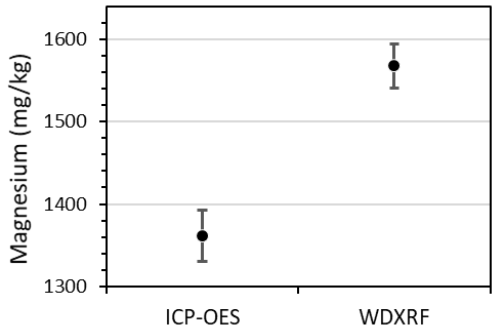


Fig. 25. Comparison of Magnesium (Mg) Mass Fraction Values by Method.

Each dot represents a mean magnesium mass fraction estimate for SRM 1568c by method. The error bars represent measurement repeatability standard deviations.

5.2.11. Manganese Results

The NIST ICP-OES and NIST WDXRF results for manganese (Mn) on a dry-mass basis are summarized in Table 37. Columns A and B are used in the table below to distinguish between the first and second aliquot taken from each bottle. The results are displayed in Fig. 26 as a function of the sample bottle number. The summary results for these methods are compared in Fig. 27. The uncertainty budgets for determination of Mn using these methods are presented in Sections 4.1.3 and 4.1.8.

Table 37. Summary of Results for Manganese (Mn), mg/kg.

NIST ICP-OES

Bottle #	A	B	Mean	SD
13	31.1	30.4	30.8	0.5
13-1	30.7		30.7	
185	31.1	31.0	31.0	0.0
358	31.3	30.4	30.8	0.6
530	31.2	30.7	31.0	0.4
702	32.0	30.9	31.4	0.7
875	31.0	31.0	31.0	0.0
1048	31.3	31.1	31.2	0.1
1219	32.0	30.3	31.2	1.2
1392	31.1	30.8	30.9	0.2
1564	31.4	30.7	31.1	0.5
		N:	11	
		Mean, Pooled SD:	31.00	0.56
		SD:	0.21	

NIST WDXRF

Bottle #	A	B	Mean	SD
57	31.92	30.14	31.03	1.27
344	29.93	31.16	30.55	0.87
631	30.64	30.85	30.75	0.14
919	30.97	30.99	30.98	0.01
1206	31.01	30.51	30.76	0.35
1493	31.51	30.07	30.79	1.01
		N:	6	
		Mean, Pooled SD:	30.81	0.77
		SD:	0.18	

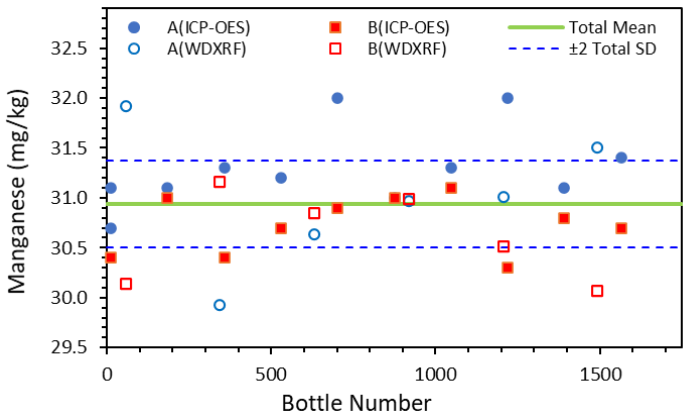


Fig. 26. Manganese (Mn) Mass Fraction as a Function of Bottle Number.

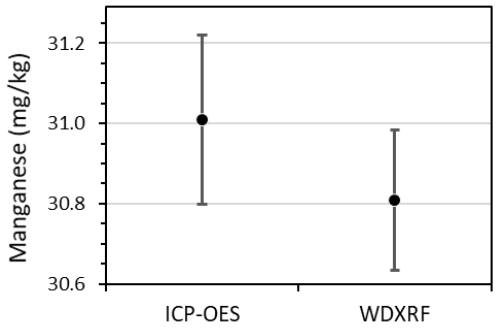


Fig. 27. Comparison of Manganese (Mn) Mass Fraction Values by Method.

Each dot represents a mean manganese mass fraction estimate for SRM 1568c by method. The error bars represent measurement repeatability standard deviations.

5.2.12. Mercury Results

The NIST ID-CV-ICP-MS and the HAMQAP Exercise 6 results for mercury (Hg) are summarized in Table 38. HAMQAP Exercise 6 results for Hg were used for confirmation of NIST data. Columns A, B, and C are used in the table below to distinguish between the different aliquots taken from each bottle or by each participating laboratory from a single bottle. The NIST results are reported on a dry-mass basis; the HAMQAP results are reported on an as-received basis. The NIST results are displayed in Fig. 28 as a function of the sample bottle number. The summary results for the two datasets are compared in Fig. 29, with the HAMQAP results corrected to a dry-mass basis assuming a moisture content of 9.62 %. The uncertainty budget for the NIST ID-CV-ICP-MS method is presented in Section 4.1.4.

Table 38. Summary of Results for Mercury (Hg), mg/kg.

NIST ID-CV-ICP-MS

Bottle #	A
53	0.00174
340	0.00182
627	0.00186
915	0.00179
1202	0.00175
1489	0.00175
N:	6
Mean:	0.00179
SD:	0.00005

HAMQAP Exercise 6 [a]

Lab	A	B	C	Mean	SD	Method
1	0.000	0.000	0.001	0.0003	0.0002	Microwave digestion
2	0.002	0.003	0.002	0.0023	0.0006	Microwave digestion
5	0.003	0.005	0.004	0.0039	0.0006	Hot block digestion
11	0.001	0.001	0.001	0.0013	0.0001	Microwave digestion
27	0.007	0.015	0.009	0.0102	0.0043	Microwave digestion
42	0.002	0.001	0.002	0.0015	0.0001	Microwave digestion
52	0.010	0.010	0.011	0.0102	0.0003	Microwave digestion
69	0.010	0.010	0.010	0.0100	0.0000	Microwave digestion
74	0.003			0.0035		Microwave digestion
79	0.001	0.001	0.001	0.0011	0.0003	Microwave digestion
			N:	11		
			Mean, Pooled SD:	0.0042	0.0014	
			SD:	0.0040		

[a] Seventeen results excluded based on being below the participant's detection limit or outside the dataset's consensus tolerance limits.

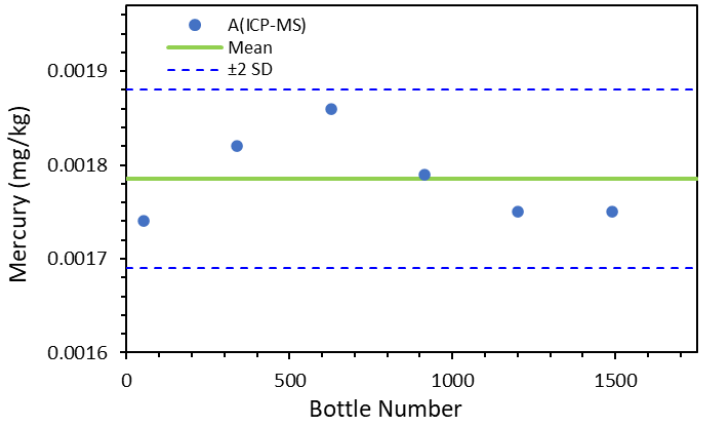


Fig. 28. Mercury (Hg) Mass Fraction as a Function of Bottle Number.

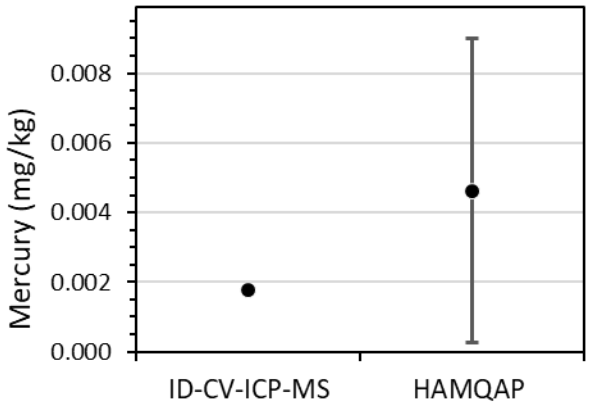


Fig. 29. Comparison of Mercury (Hg) Mass Fraction Values by Method.

Each dot represents a mean mercury mass fraction estimate for SRM 1568c by method. The error bars represent measurement repeatability standard deviations.

Error bars are present for the NIST ID-CV-ICP-MS data, but the magnitude is small enough not to be seen, as indicated by the data in Table 38.

5.2.13. Molybdenum Results

The NIST ICP-MS and INAA results for molybdenum (Mo) on a dry-mass basis summarized in Table 39. Columns A and B are used in the table below to distinguish between the first and second aliquot taken from each bottle. These results are displayed in Fig. 30 as a function of the sample bottle number. The summary results for these methods are compared in Fig. 31. The uncertainty budgets for determination of Mo using these methods are presented in Sections 4.1.5 and 4.1.6.

Table 39. Summary of Results for Molybdenum (Mo), mg/kg.

	NIST ICP-MS					NIST INAA				
Bottle #	A	B	Mean	SD		Bottle #	A	B	Mean	SD
15	0.636	0.644	0.640	0.006		20	0.68	0.793	0.737	0.080
187	0.679	0.634	0.657	0.032		154	0.52	0.637	0.579	0.083
360	0.654	0.620	0.637	0.025		441	0.738	0.73	0.734	0.006
532	0.626	0.580	0.603	0.032		728	0.623	0.732	0.678	0.077
704	0.608	0.628	0.618	0.014		872	0.488	0.462	0.475	0.018
877	0.672	0.634	0.653	0.027		882	0.682	0.613	0.648	0.049
1049	0.647	0.643	0.645	0.003		1159	0.675	0.696	0.686	0.015
1221	0.666	0.662	0.664	0.003		1302	0.605	0.635	0.620	0.021
1393	0.677	0.642	0.659	0.025		1456	0.532	0.72	0.626	0.133
1651	0.601	0.656	0.629	0.039		1589	0.622	0.529	0.576	0.066
		N:	10					*N*:	10	
		Mean, Pooled SD:	0.640	0.024				Mean, Pooled SD:	0.636	0.067
		SD:	0.019					SD:	0.080	

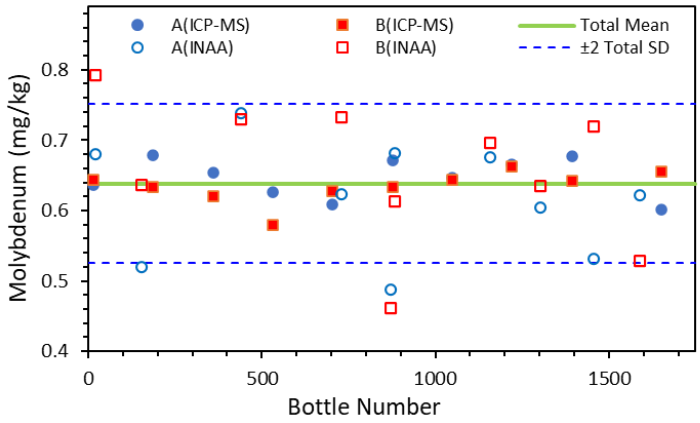


Fig. 30. Molybdenum (Mo) Mass Fraction as a Function of Bottle Number.

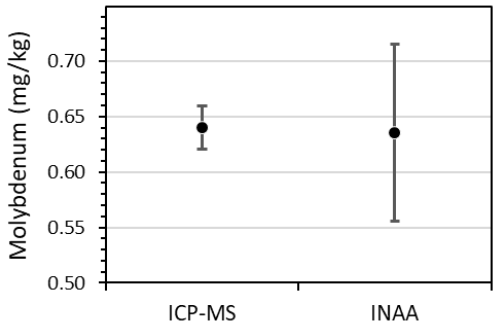


Fig. 31. Comparison of Molybdenum (Mo) Mass Fraction Values by Method.

Each dot represents a mean molybdenum mass fraction estimate for SRM 1568c by method. The error bars represent measurement repeatability standard deviations.

5.2.14. Phosphorus Results

The NIST ICP-OES and WDXRF results for phosphorus (P) on a dry-mass basis are summarized in Table 40. Columns A and B are used in the table below to distinguish between the first and second aliquot taken from each bottle. The results are displayed in Fig. 32 as a function of the sample bottle number. The summary results for these methods are compared in Fig. 33. The uncertainty budgets for determination of P using these methods are presented in Sections 4.1.3 and 4.1.8.

Table 40. Summary of Results for Phosphorus (P), mg/kg.

NIST ICP-OES

Bottle #	A	B	Mean	SD
13	3813	3569	3691	173
13	3587		3587	
185	3348	3818	3583	332
358	3696	3663	3680	23
530	3404	3400	3402	2
702	3789	3577	3683	150
875	3727	3628	3677	70
1048	3699	3431	3565	190
1219	4064	3858	3961	146
1392	3749	3786	3768	26
1564	3496	3654	3575	112
		N:	11	
		Mean, Pooled SD:	3650	150
		SD:	140	

NIST WDXRF

Bottle #	A	B	Mean	SD
57	4966	4937	4951	20
344	4848	4916	4882	48
631	4890	4842	4866	34
919	4955	4916	4935	28
1206	4873	4954	4914	57
1493	4907	4873	4890	24
		N:	6	
		Mean, Pooled SD:	4906	38
		SD:	33	

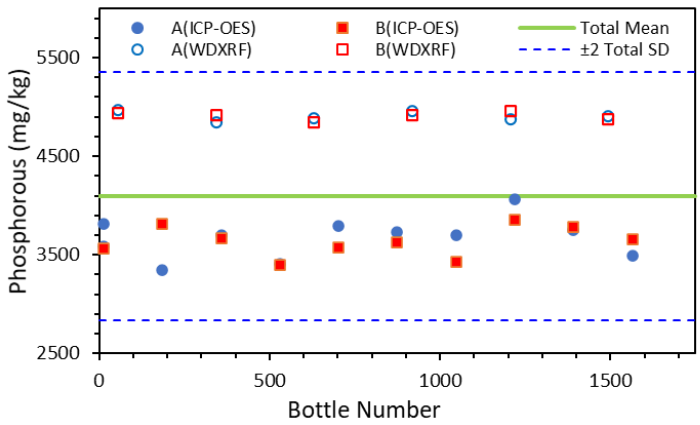


Fig. 32. Phosphorous (P) Mass Fraction as a Function of Bottle Number.

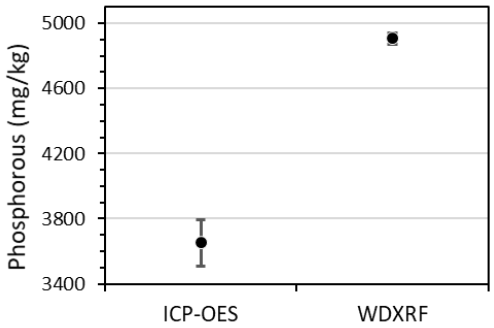


Fig. 33. Comparison of Phosphorus (P) Mass Fraction Values by Method.

Each dot represents a mean phosphorus mass fraction estimate for SRM 1568c by method. The error bars represent measurement repeatability standard deviations.

5.2.15. Potassium Results

The NIST ICP-OES and WDXRF results for potassium (K) on a dry-mass basis are summarized in Table 41. Columns A and B are used in the table below to distinguish between the first and second aliquot taken from each bottle. The results are displayed in Fig. 34 as a function of the sample bottle number. The uncertainty budgets for determination of K using these methods are presented in Sections 4.1.3 and 4.1.8.

Table 41. Summary of NIST Results for Potassium (K), mg/kg.

NIST ICP-OES

Bottle #	A	B	Mean	SD
15	2862	2871	2867	6
187	2861	2958	2910	69
360	3034	2890	2962	102
532	2936	2950	2943	10
704	2928	2908	2918	14
877	3061	2940	3001	86
1049	2904	2910	2907	4
1221	3025	2910	2968	81
1393	2960	2995	2978	25
1651	2837	3047	2942	148
		N:	10	
		Mean, Pooled SD:	2939	72
		SD:	40	

NIST WDXRF

Bottle #	A	B	Mean	SD
57	3425	3383	3404	29
344	3370	3375	3372	4
631	3353	3383	3368	21
919	3376	3390	3383	10
1206	3340	3369	3354	20
1493	3400	3333	3367	47
		N:	6	
		Mean, Pooled SD:	3375	26
		SD:	17	

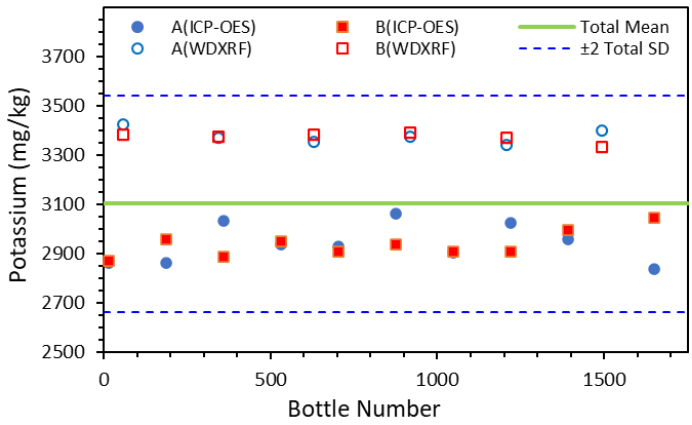


Fig. 34. Potassium (K) Mass Fraction as a Function of Bottle Number.

The as-received results for K from HAMQAP Exercise 5 are summarized in Table 42. Columns A, B, and C are used in the table below to distinguish between the different aliquots taken by each participating laboratory from a single bottle.

Table 42. Summary of HAMQAP Results for Potassium (K), mg/kg.

			HAMQAP Exercise 5 [a]			
Lab	A	B	C	Mean	SD	Method
1	2770	2760	2780	2770	10	ID ICP-MS
2	3176	3215	3211	3201	21	ICP-OES
3	2465	2320	2393	2393	73	ICP-MS
5	2887	2774	2697	2786	96	ICP-OES
7	2580	2550	2620	2583	35	ICP-OES
15	2439	2360	2398	2399	40	ICP-OES
25	2467	2588	2470	2508	69	ICP-OES
29	2922	2854	2954	2910	51	ICP-OES
30	2720	2750	2632	2701	61	ID ICP-MS
33	2765	2803	2776	2781	20	ICP-MS
35	2480	2620	2530	2543	71	ICP-OES
41	2253	2566	2726	2515	241	ICP-MS
45	2941	2948		2945	5	ICP-OES
47	2630	2730	2820	2727	95	ICP-OES
51	2726	2766	2726	2739	23	ICP-MS
			N:	15		
			Mean, Pooled SD:	2700	61	
			SD:	226		

[a] Two results excluded based on being outside the dataset's consensus tolerance limits and one result for no analytical method reported.

The summary results for the three datasets are compared in Fig. 35, with the HAMQAP results corrected to a dry-mass basis assuming a moisture content of 9.62 %.

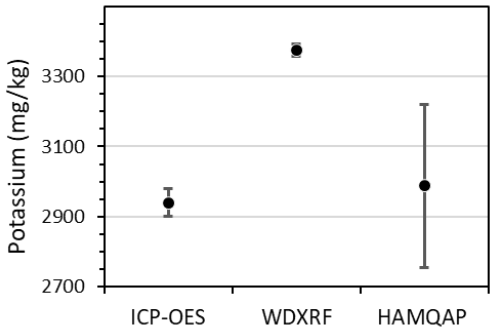


Fig. 35. Comparison of Potassium (K) Mass Fraction Values by Method.

Each dot represents a mean potassium mass fraction estimate for SRM 1568c by method. The error bars represent measurement repeatability standard deviations.

5.2.16. Rubidium Results

The NIST ICP-MS results for rubidium (Rb) on a dry-mass basis are summarized in Table 43. Columns A and B are used in the table below to distinguish between the first and second aliquot taken from each bottle. These results are displayed in Fig. 36 as a function of the sample bottle number. The uncertainty budget for determination of Rb using this method is presented in Section 4.1.5.

Table 43. Summary of Results for Rubidium (Rb), mg/kg.

	NIST ICP-MS			
Bottle #	A	B	Mean	SD
15	9.63	8.54	9.09	0.77
187	8.64	9.37	9.00	0.52
360	9.21	8.52	8.86	0.49
532	9.07	9.17	9.12	0.07
704	8.34	9.61	8.98	0.90
877	10.06	8.73	9.39	0.94
1049	8.88		8.88	
1221	8.82	8.76	8.79	0.04
1393	8.93	8.36	8.64	0.40
1651	8.11	8.24	8.17	0.09
		N:	10	
		Mean, Pooled SD:	8.89	0.58
		SD:	0.32	

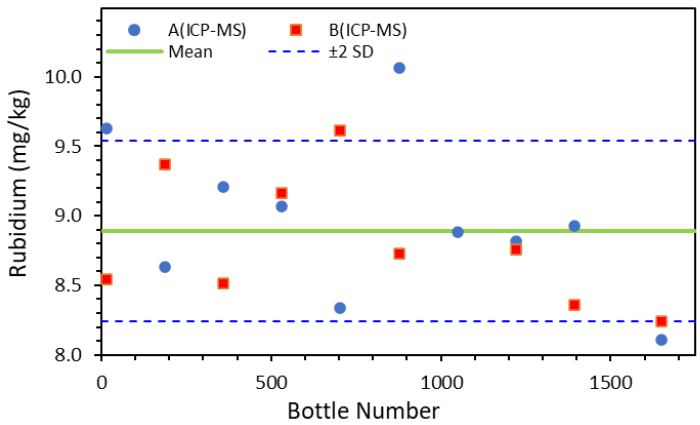


Fig. 36. Rubidium (Rb) Mass Fraction as a Function of Bottle Number.

5.2.17. Selenium Results

The NIST ICP-MS and INAA results for selenium (Se) on a dry-mass basis are summarized in Table 44. Columns A and B are used in the table below to distinguish between the first and second aliquot taken from each bottle. These results are displayed in Fig. 37 as a function of the sample bottle number. The summary results for these methods are compared in Fig. 38. The uncertainty budgets for determination of Se using these methods are presented in Sections 4.1.5 and 4.1.6.

Table 44. Summary of Results for Selenium (Se), mg/kg.

NIST ICP-MS				
Bottle #	A	B	Mean	SD
15	0.0643	0.0676	0.0659	0.0024
187	0.0633	0.0663	0.0648	0.0021
360	0.0528	0.0680	0.0604	0.0108
532	0.0665	0.0598	0.0632	0.0047
704	0.0680	0.0693	0.0687	0.0009
877	0.0674	0.0677	0.0675	0.0002
1049	0.0677	0.0656	0.0667	0.0015
1221	0.0644	0.0678	0.0661	0.0024
1393	0.0705	0.0672	0.0689	0.0023
1651		0.0656	0.0656	
		N:	10	
		Mean, Pooled SD:	0.0658	0.0042
		SD:	0.0026	

NIST INAA				
Bottle #	A	B	Mean	SD
20	0.0684	0.0628	0.0656	0.0040
154	0.0600	0.0641	0.0621	0.0029
441	0.0703	0.0658	0.0681	0.0032
728	0.0671	0.0638	0.0655	0.0023
872	0.0625	0.0728	0.0677	0.0073
882	0.0658		0.0658	
1159	0.0599	0.0647	0.0623	0.0034
1302	0.0542	0.0635	0.0589	0.0066
1456	0.0634	0.0588	0.0611	0.0033
1589	0.0606	0.0593	0.0600	0.0009
		N:	10	
		Mean, Pooled SD:	0.0637	0.040
		SD:	0.0032	

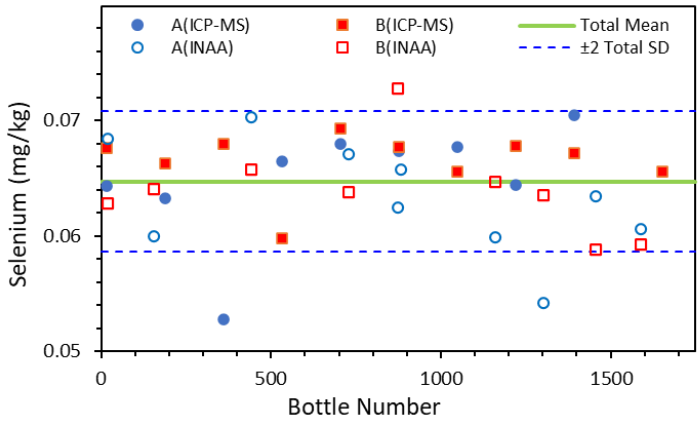


Fig. 37. Selenium (Se) Mass Fraction as a Function of Bottle Number.

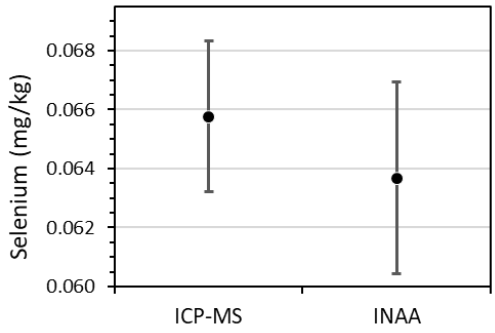


Fig. 38. Comparison of Selenium (Se) Mass Fraction Values by Method.

Each dot represents a mean selenium mass fraction estimate for SRM 1568c by method. The error bars represent measurement repeatability standard deviations.

5.2.18. Sodium Results

The NIST ICP-OES and HAMQAP Exercise 5 results for sodium (Na) are summarized in Table 45. Columns A, B, and C are used in the table below to distinguish between the different aliquots taken from each bottle or by each participating laboratory from a single bottle. The NIST results are reported on a dry-mass basis; the HAMQAP results are reported on an as-received basis. The NIST results are displayed in Fig. 39 as a function of the sample bottle number. The summary results for these two datasets are compared in Fig. 40. The uncertainty budget for determination of Na using the NIST ICP-OES method is presented in Section 4.1.3.

Table 45. Summary of Results for Sodium (Na), mg/kg.

0					HAMQAP Exercise 5 [a]						
Bottle #	A	B	Mean	SD	Lab	A	B	C	Mean	SD	Method
15	15.0	15.1	15.0	0.1	2	25.0	23.5	21.6	23.4	1.7	ICP-OES
187	15.3	15.5	15.4	0.2	3	19.0	16.0	18.0	17.7	1.5	ICP-MS
360	15.3	17.1	16.2	1.3	7	12.3	12.9	12.4	12.5	0.3	ICP-OES
532	14.8	16.1	15.4	0.9	16	6.0	8.3	7.5	7.3	1.1	ICP-OES
704	15.2	15.4	15.3	0.1	25	14.3	14.9	14.5	14.6	0.3	ICP-OES
877	16.6	15.7	16.2	0.6	29	17.8	17.2	17.7	17.5	0.3	ICP-OES
1049	15.0	17.5	16.3	1.7	30	14.8	13.8	13.5	14	0.7	ICP-OES
1221		17.0	17.0		33	26.3	15.3	23.8	21.8	5.8	ICP-OES
1393	16.4	16.8	16.6	0.3	35	19.4	18.4	18.8	18.9	0.5	ICP-OES
1651	15.1	15.5	15.3	0.3	41	11.7	13.2	15.0	13.3	1.7	ICP-MS
		N:	10		47	14.1	10.8	12.2	12.4	1.7	ICP-OES
		Mean, Pooled SD:	15.87	0.83	51	14.8	14.3	14.3	14.5	0.3	ICP-MS
		SD:	0.65					*N*:	12		
								Mean, Pooled SD:	15.7	1.3	
								SD:	3.9		

[a] Two results excluded based on being below the participant's detection limit or outside the dataset's consensus tolerance limits and two results for incorrect analytical method reported.

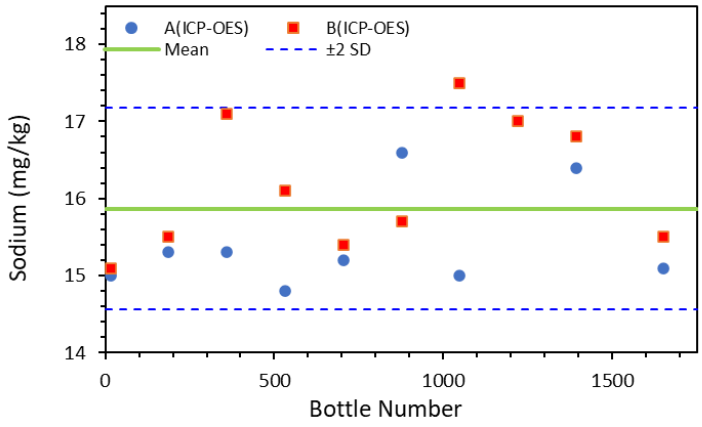


Fig. 39. Sodium (Na) Mass Fraction as a Function of Bottle Number.

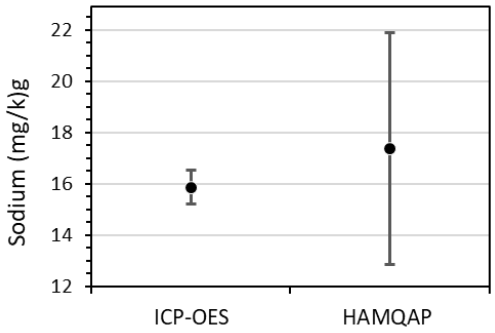


Fig. 40. Comparison of Sodium (Na) Mass Fraction Values by Method.

Each dot represents a mean sodium mass fraction estimate for SRM 1568c by method. The error bars represent measurement repeatability standard deviations.

5.2.19. Strontium Results

The NIST ICP-MS and ICP-OES results for strontium (Sr) on a dry-mass basis are summarized in Table 46. Columns A and B are used in the table below to distinguish between the first and second aliquot taken from each bottle. These results are displayed in Fig. 41 as a function of the sample bottle number. The summary results for these methods are compared in Fig. 42. The uncertainty budgets for determination of Sr using these methods are presented in Sections 4.1.5 and 4.1.3.

Table 46. Summary of Results for Strontium (Sr), mg/kg.

NIST ICP-MS				
Bottle #	A	B	Mean	SD
15	0.4931	0.4768	0.4850	0.0115
187	0.4884	0.4868	0.4876	0.0012
360	0.4821	0.4868	0.4844	0.0033
532	0.4913	0.4920	0.4917	0.0005
704	0.4795	0.4738	0.4767	0.0040
877	0.4860	0.4846	0.4853	0.0009
1049	0.4802	0.4995	0.4899	0.0137
1221	0.4710	0.4898	0.4804	0.0133
1393	0.4746	0.4784	0.4765	0.0026
1651	.	0.4806	0.4806	
		N:	10	
		Mean, Pooled SD:	0.4838	0.0077
		SD:	0.0052	

NIST ICP-OES				
Bottle #	A	B	Mean	SD
13	0.490	0.640	0.565	0.106
185	0.450	0.470	0.460	0.014
358	0.470	0.460	0.465	0.007
530	0.450	0.490	0.470	0.028
702	0.510	0.450	0.480	0.042
875	0.550	0.500	0.525	0.035
1048	0.460	0.470	0.465	0.007
1219	0.450	0.470	0.460	0.014
1392	0.440	0.450	0.445	0.007
1564	0.450	0.510	0.480	
		N:	10	
		Mean, Pooled SD:	0.482	0.042
		SD:	0.036	

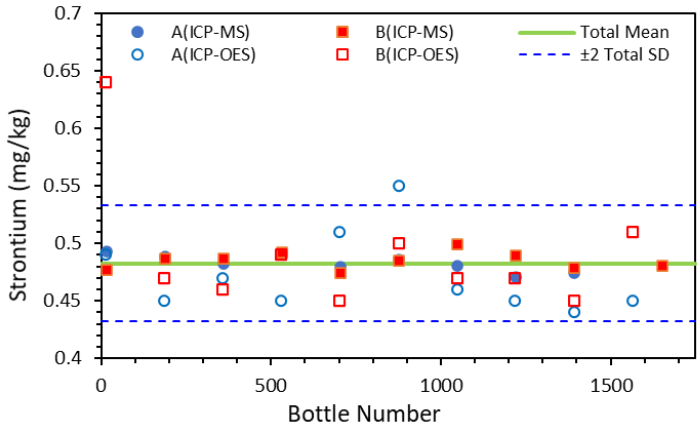


Fig. 41. Strontium (Sr) Mass Fraction as a Function of Bottle Number.

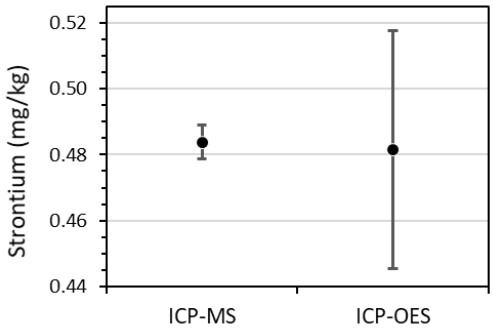


Fig. 42. Comparison of Strontium (Sr) Mass Fraction Values by Method.

Each dot represents a mean strontium mass fraction estimate for SRM 1568c by method. The error bars represent measurement repeatability standard deviations.

5.2.20. Sulfur Results

The NIST TNPGAA and WDXRF results for sulfur (S) on a dry-mass basis are summarized in Table 47. Columns A and B are used in the table below to distinguish between the first and second aliquot taken from each bottle. These results are displayed in Fig. 43 as a function of the sample bottle number. The summary results for these methods are compared in Fig. 44. The uncertainty budgets for these methods are presented in Sections 4.1.7 and 4.1.8.

Table 47. Summary of Results for Sulfur (S), mg/kg.

NIST TNPGAA	
Bottle #	A
20	1159
154	1149
441	1170
728	1147
1456	1126
1589	1158
N:	6
Mean:	1152
SD:	15

NIST WDXRF				
Bottle #	A	B	Mean	SD
57	1156.5	1166.8	1161.7	7.3
344	1144.2	1147.9	1146.1	2.6
631	1153.2	1159.4	1156.3	4.4
919	1169.4	1156.9	1163.2	8.8
1206	1178.7	1163.0	1170.9	11.1
1493	1148.0	1169.8	1158.9	15.4
N:			6	
Mean, Pooled SD:			1159.5	9.3
SD:			8.2	

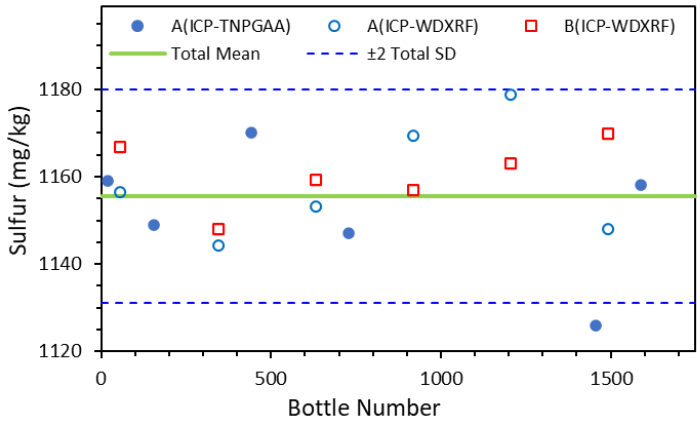


Fig. 43. Sulfur (S) Mass Fraction as a Function of Bottle Number.

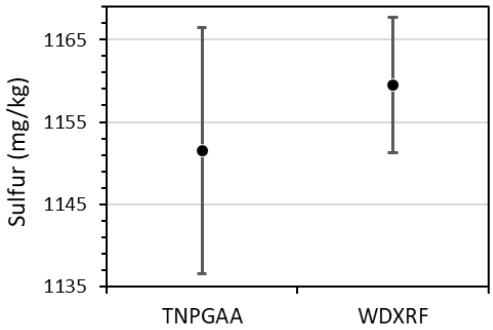


Fig. 44. Comparison of Sulfur (S) Mass Fraction Values by Method.

Each dot represents a mean sulfur mass fraction estimate for SRM 1568c by method. The error bars represent measurement repeatability standard deviations.

5.2.21. Zinc Results

The NIST ICP-OES and WDXRF results for zinc (Zn) on a dry-mass basis are summarized in Table 48. Columns A and B are used in the table below to distinguish between the first and second aliquot taken from each bottle. The results are displayed in Fig. 45 as a function of the sample bottle number. The summary results for these methods are compared in Fig. 46. The uncertainty budgets for determination of Zn using these methods are presented in Sections 4.1.3 and 4.1.8.

Table 48. Summary of Results for Zinc (Zn), mg/kg.

NIST ICP-OES

Bottle #	A	B	Mean	SD
13	23.10	23.00	23.05	0.07
13	23.60		23.60	
185	23.60	23.40	23.50	0.14
358	23.40	22.80	23.10	0.42
530	24.10	23.40	23.75	0.49
702	24.20	23.20	23.70	0.71
875	23.80	23.80	23.80	0.00
1048	23.00	23.40	23.20	0.28
1219	24.20	22.60	23.40	1.13
1392	23.20	23.30	23.25	0.07
1564	23.50	23.20	23.35	0.21
		N:	11	
		Mean, Pooled SD:	23.43	0.49
		SD:	0.26	

NIST WDXRF

Bottle #	A	B	Mean	SD
57	24.11	23.31	23.71	0.57
344	23.92	24.04	23.98	0.08
631	23.34	23.33	23.34	0.01
919	23.12	24.02	23.57	0.64
1206	23.08	23.15	23.12	0.05
1493	23.23	23.05	23.14	0.13
		Mean:	6	
		Mean, Pooled SD:	23.48	0.35
		SD:	0.34	

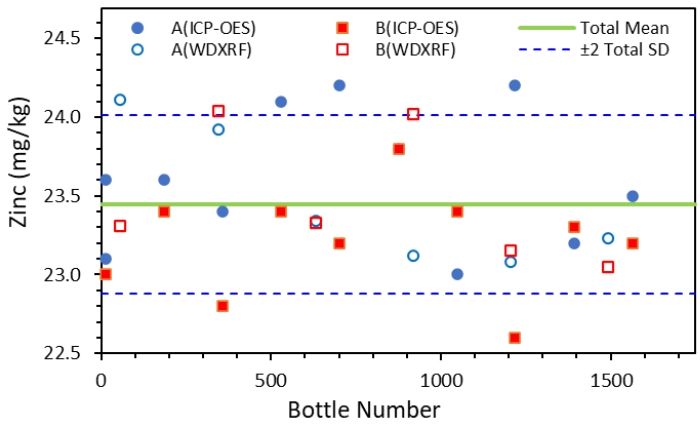


Fig. 45. Zinc (Zn) Mass Fraction as a Function of Bottle Number.

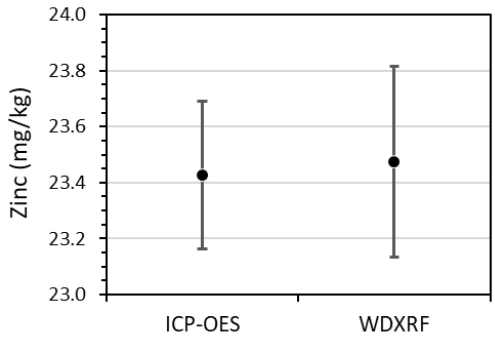


Fig. 46. Comparison of Zinc (Zn) Mass Fraction Values by Method.

Each dot represents a mean zinc mass fraction estimate for SRM 1568c by method. The error bars represent measurement repeatability standard deviations.

5.2.22. Silicon Results

The NIST WDXRF results for silicon (Si) on a dry-mass basis are summarized in Table 49. Columns A and B are used in the table below to distinguish between the first and second aliquot taken from each bottle. The results are displayed in Fig. 47 as a function of the sample bottle number. The uncertainty budget for determination of Si using this method is presented in Section 4.1.8.

Table 49. Summary of Results for Silicon (Si), mg/kg.

	NIST WDXRF			
Bottle #	A	B	Mean	SD
57	205.3	222.1	213.7	11.9
344	196.6	188.6	192.6	5.7
631	186.5	195.8	191.2	6.6
919	196.9	206.7	201.8	6.9
1206		205.5	205.5	
1493	196.6	199.3	198.0	1.9
		N:	6	
		Mean, Pooled SD:	200.5	6.7
		SD:	8.5	

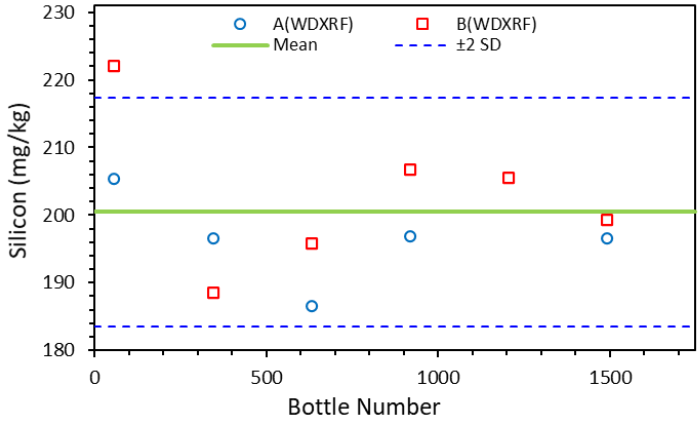


Fig. 47. Silicon (Si) Mass Fraction as a Function of Bottle Number.

5.3. Arsenic Species

All NIST and NMIJ organic and inorganic arsenic species were determined using LC-ICP-MS methods on a dry-mass basis. In all cases, the quality assurance measurement results were concordant with the values delivered by the control material, SRM 1568b Rice Flour. The LC-ICP-MS methods and their uncertainty budgets are presented in Sections 4.1.9 and 4.2.

5.3.1. Organic Arsenical Results

Table 50 summarizes the NIST LC-ICP-MS results for monomethylarsonic acid (MMA) and dimethylarsinic acid (DMA). Columns A and B are used in the table below to distinguish between the first and second aliquot taken from each bottle. The results are displayed in Fig. 48 as functions of the sample bottle number.

Table 50. Summary of NIST Results for Organic Arsenicals: MMA and DMA; mg/kg.

	Monomethylarsonic acid (MMA)				Dimethylarsinic acid (DMA)			
Bottle	A	B	Mean	SD	Mean	SD	Mean	SD
63	0.0108	0.0112	0.0110	0.0003	0.1825	0.1784	0.1805	0.0029
350	0.0105	0.0109	0.0107	0.0002	0.1800	0.1818	0.1809	0.0013
637	0.0111	0.0113	0.0112	0.0002	0.1803	0.1925	0.1864	0.0086
1214	0.0104	0.0098	0.0101	0.0004	0.1769	0.1822	0.1796	0.0037
1499	0.0109	0.0111	0.0110	0.0001	0.1868	0.1873	0.1871	0.0004
1569	0.0110	0.0108	0.0109	0.0002	0.1863	0.1813	0.1838	0.0035
		N:	6				6	
		Mean, Pooled SD:	0.0108	0.003			0.1830	0.0043
		SD:	0.0004				0.0032	

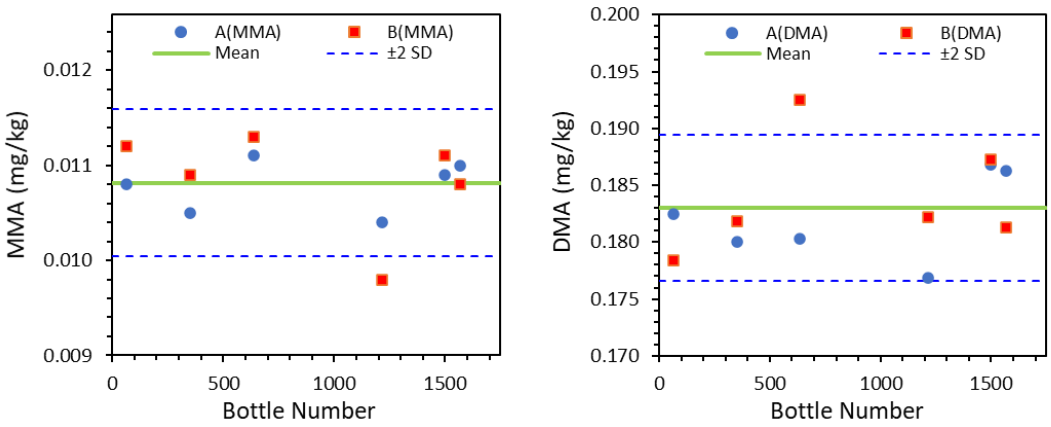


Fig. 48. NIST's Organic Arsenic Acids Mass Fractions as Functions of Bottle Number.

Table 51 summarizes the NMIJ HPLC-ICP-MS results for MMA and DMA. Columns A and B are used in the table below to distinguish between the first and second aliquot taken from each bottle. Table 51 also lists NMIJ's estimated standard and expanded uncertainty values. The results are displayed in Fig. 49. The NIST and NMIJ summary results (mean ± SD) are compared in Fig. 50.

Table 51. Summary of NIST Results for Organic Arsenic Acids: MMA and DMA; mg/kg.

	Monomethylarsonic acid (MMA)				Dimethylarsinic acid (DMA)			
Index	A	B	Mean	SD	Mean	SD	Mean	SD
1	0.0112	0.0110	0.0111	0.0002	0.1821	0.1812	0.1817	0.0007
2	0.0110	0.0113	0.0111	0.0003	0.1819	0.1834	0.1826	0.0011
3	0.0114	0.0111	0.0112	0.0002	0.1824	0.1833	0.1829	0.0006
4	0.0113	0.0109	0.0111	0.0003	0.1822	0.1832	0.1827	0.0007
5	0.0114	0.0112	0.0113	0.0001	0.1837	0.1833	0.1835	0.0003
6	0.0109	0.0111	0.0110	0.0001	0.1825	0.1839	0.1832	0.0010
N:			6				6	
Mean, Pooled SD:			0.0112	0.0002			0.1828	0.0008
SD:			0.0001				0.0006	
u(NMIJ):			0.0002				0.0016	
U_{95}(NMIJ):			0.0004				0.0031	

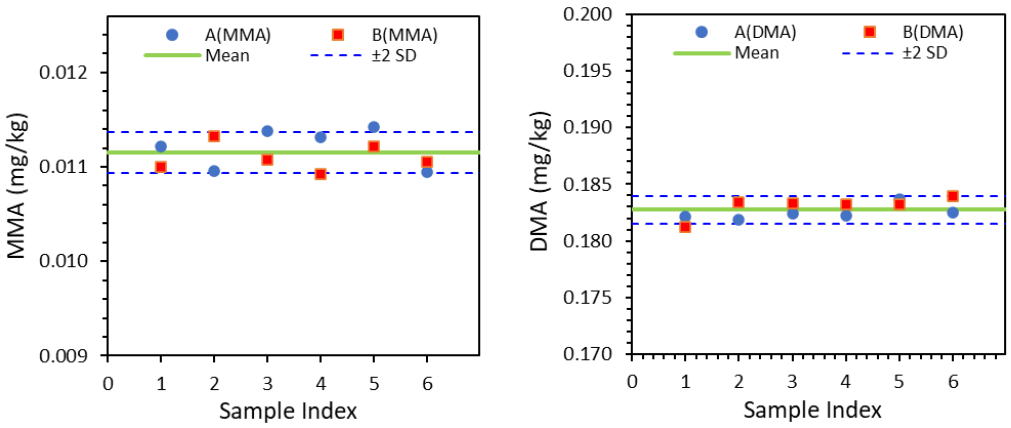


Fig. 49. NMIJ's Organic Arsenical Mass Fractions as Functions of Sample Index.

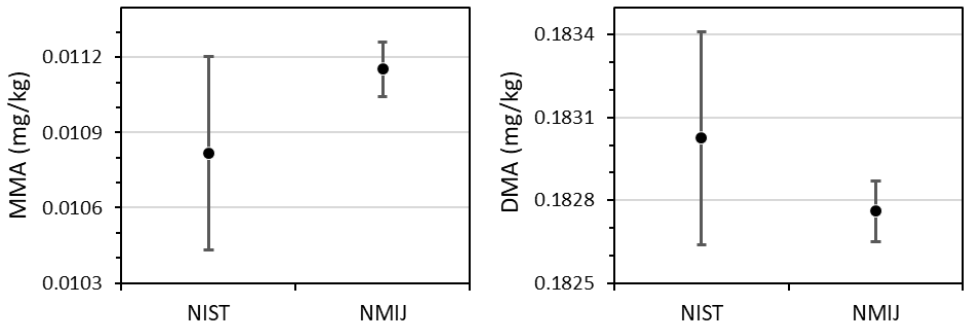


Fig. 50. Comparison of MMA and DMA Mass Fraction Values by Method.

5.3.2. Inorganic Arsenical Results

Table 52 summarizes the NIST LC-ICP-MS results for arsenous acid (AsIII), arsenic acid (AsV), and total inorganic arsenic (iAs). Columns A and B are used in the table below to distinguish between the first and second aliquot taken from each bottle. The results are displayed in Fig. 51 as functions of the sample bottle number.

Table 52. Summary of NIST Results for Inorganic Arsenic Species: AsIII, AsV, and iAs; mg/kg.

	Arsenous Acid (AsIII)				Arsenic Acid (AsV)				Inorganic Arsenic (iAs)			
Bottle	A	B	Mean	SD	A	B	Mean	SD	A	B	Mean	SD
63	0.0206	0.0207	0.0207	0.0001	0.1421	0.1479	0.1450	0.0041	0.1628	0.1686	0.1657	0.0041
350	0.0205	0.0191	0.0198	0.0010	0.1463	0.1441	0.1452	0.0016	0.1668	0.1631	0.1650	0.0026
637	0.0207	0.0205	0.0206	0.0001	0.1446	0.1452	0.1449	0.0004	0.1653	0.1657	0.1655	0.0003
1214	0.0213	0.0205	0.0209	0.0005	0.1450	0.1493	0.1472	0.0030	0.1663	0.1698	0.1681	0.0025
1499	0.0208	0.0166	0.0187	0.0030	0.1403	0.1495	0.1449	0.0065	0.1611	0.1661	0.1636	0.0035
1569	0.0214	0.0220	0.0217	0.0005	0.1520	0.1442	0.1481	0.0055	0.1733	0.1663	0.1698	0.0049
N:			6				6				6	
Mean, Pooled SD:			0.0204	0.0013			0.1459	0.0041			0.1663	0.0033
SD:			0.0010				0.0014				0.0023	

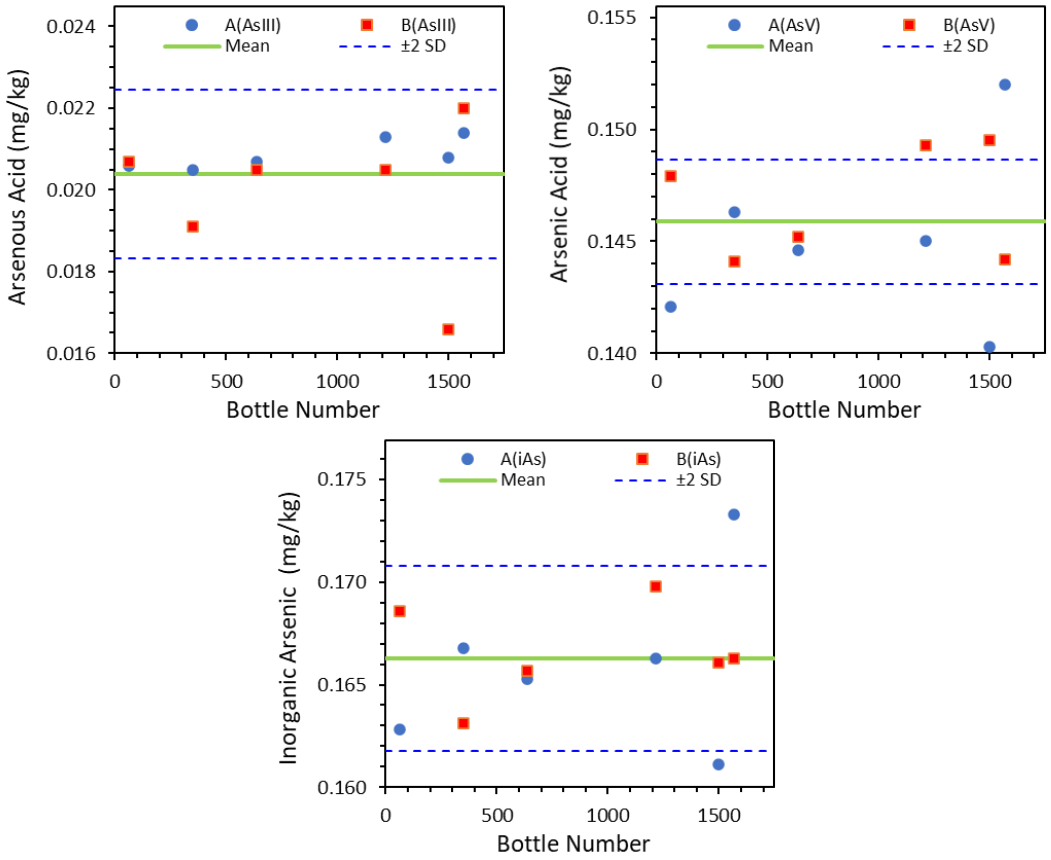


Fig. 51. Inorganic Arsenic Species Mass Fractions as Functions of Bottle Number.

Table 52 summarizes the NMIJ HPLC-ICP-MS results for total inorganic arsenic (iAs). Columns A and B are used in the table below to distinguish between the first and second aliquot taken from each bottle. Table 52 also lists NMIJ's estimated standard and expanded uncertainty values. The results are displayed in Fig. 52 as functions of the sample index. The NIST and NMIJ summary results (mean ± SD) are compared in Fig. 53.

Table 53. Summary of NIST Results for Total Inorganic Arsenic (iAs); mg/kg.

	Inorganic Arsenic (iAs)			
Bottle	A	B	Mean	SD
1	0.1674	0.1678	0.1676	0.0002
2	0.1652	0.1679	0.1666	0.0019
3	0.1669	0.1680	0.1675	0.0008
4	0.1648	0.1668	0.1658	0.0014
5	0.1668	0.1666	0.1667	0.0001
6	0.1646	0.1690	0.1668	0.0031
		N:	6	
		Mean, Pooled SD:	0.1668	0.0016
		SD:	0.0006	
		u(NMIJ):	0.0015	
		U_{95}(NMIJ):	0.0031	

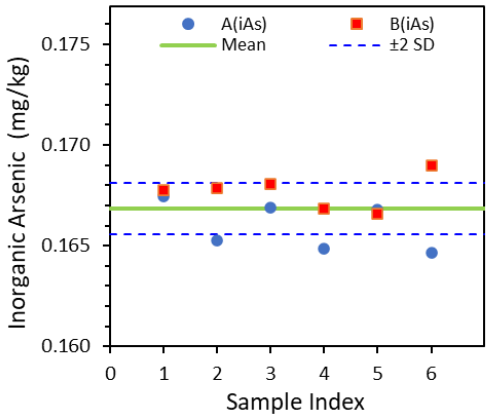


Fig. 52. NMIJ's Total Inorganic Arsenic (iAs) Mass Fractions as a Function of Sample Index.

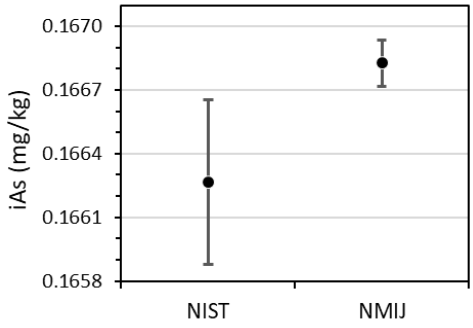


Fig. 53. Comparison of Total Inorganic Arsenic (iAs) Mass Fraction Values by Method.

5.4. Proximates

HAMQAP Exercise 6 participants provided results for proximates on an as-received basis. In addition to the individual measurement results from each participating HAMQAP laboratory, the summary table for each of the proximates also lists the number of accepted results (*N*), the arithmetic mean of the accepted results (Mean), the standard deviation of the accepted results (SD), and the square root of the sum of the squares of the measurement SDs (Pooled SD).

The results in provided in Sections 5.4.1 through 5.4.6 are provided on an as-received basis; tabulated results provided in the COA for SRM 1568c Rice Flour (Section 7) for fat, protein, carbohydrates, and calories have been converted to a dry-mass basis.

5.4.1. Fat Results

The HAMQAP Exercise 6 results for total fat are summarized in Table 54. Columns A, B, and C are used in the table below to distinguish between the aliquots taken by each participating laboratory from a single bottle.

Table 54. Summary of Results for Total Fat, %.

Lab [a]	A	B	C	Mean	SD	Method
5	3.16	3.22	3.17	3.18	0.03	Not specified or Other
9	3.2	3.1	3.4	3.23	0.15	RG/M acid digestion
20	3	3.1	2.9	3.00	0.10	Not specified or Other
30	2.7	2.67	2.77	2.71	0.05	RG/M acid digestion
31	3.11	3.04	3	3.05	0.06	Gravimetry
39	2.64	2.66	2.63	2.64	0.02	Not specified or Other
59	3.05	3.04	3.18	3.09	0.08	Oven drying
61	2.84	3.08	3.12	3.01	0.15	Gravimetry
62	2.83	2.7	2.67	2.73	0.09	Not specified or Other
79	3.49	3.4	3.4	3.43	0.05	Not specified or Other
80	2.6	2.74	2.64	2.66	0.07	Not specified or Other
			N:	11		
			Mean, Pooled SD:	2.98	0.09	
			SD:	0.26		

[a] One result excluded based on being outside the dataset's consensus tolerance limits.

5.4.2. Protein Results

The HAMQAP Exercise 6 results for total protein are summarized in Table 55. Columns A, B, and C are used in the table below to distinguish between the aliquots taken by each participating laboratory from a single bottle.

Table 55. Summary of Results for Protein, %.

Lab [a]	A	B	C	Mean	SD	Method
9	8.2	8	8	8.07	0.12	Kjeldahl
17	7.8	8.06	8.05	7.97	0.15	Combustion
20	8	7.9	7.93	7.94	0.05	Combustion
30	8.22	8.27	8.25	8.25	0.03	Kjeldahl
31	8.06	8.16	7.98	8.07	0.09	Kjeldahl
39	7.97	7.97	7.79	7.91	0.10	Kjeldahl
59	7.87	7.87	7.99	7.91	0.07	Not specified or Other
61	8.36	8.39	8.39	8.38	0.02	Kjeldahl
62	8.3	8.27	8.28	8.28	0.02	Kjeldahl
79	7.65	7.64	7.58	7.62	0.04	Not specified or Other
80	8.03	8	8.03	8.02	0.02	Combustion
			N:	11		
			Mean, Pooled SD:	8.04	0.08	
			SD:	0.21		

[a] Two results excluded based on being outside the dataset's consensus tolerance limits.

5.4.3. Carbohydrates Results

The HAMQAP Exercise 6 results for total carbohydrates are summarized in Table 56. Columns A, B, and C are used in the table below to distinguish between the aliquots taken by each participating laboratory from a single bottle.

Table 56. Summary of Results for Carbohydrates, %.

Lab [a]	A	B	C	Mean	SD	Method
9	76.4	76.9	76.6	76.63	0.25	100-Solids-Protein-Fat-Ash
20	74.8	75.1	75.4	75.10	0.30	100-Solids-Protein-Fat-Ash
31	76	75.9	75.9	75.93	0.06	100-Solids-Protein-Fat-Ash
39	76.63	76.42	76.82	76.62	0.20	100-Solids-Protein-Fat-Ash
79	75.85	76.05	76.08	75.99	0.13	Not specified
80	76.23	76.39	76.38	76.33	0.09	100-Solids-Protein-Fat-Ash
			N:	6		
			Mean, Pooled SD:	76.10	0.19	
			SD:	0.57		

[a] Three results excluded based on being outside the dataset's consensus tolerance limits.

5.4.4. Solids Results

The HAMQAP Exercise 6 results for solids are summarized in Table 57. Columns A, B, and C are used in the table below to distinguish between the aliquots taken by each participating laboratory from a single bottle.

Table 57. Summary of HAMQAP 6 Results for Solids, %.

Lab [a]	A	B	C	Mean	SD	Method
5	89.6	90.4	90.5	90.17	0.49	Vacuum oven
9	89.5	89.6	89.7	89.60	0.10	Forced-air oven
19	89.35	89.48	89.49	89.44	0.08	Not specified or Other
30	88.66	88.59	88.66	88.64	0.04	Thermogravimetric
31	88.53	88.49	88.28	88.43	0.13	Forced-air oven
39	88.63	88.45	88.63	88.57	0.10	Forced-air oven
59	88.81	89.08	89.14	89.01	0.18	Vacuum oven
61	89.4	89.4	89.4	89.40	0.00	Gravimetry
79	88.36	88.42	88.45	88.41	0.05	Not specified or Other
80	88.15	88.4	88.33	88.29	0.13	Forced-air oven
			N:	10		
			Mean, Pooled SD:	89.00	0.18	
			SD:	0.63		

[a] One result excluded based on being outside the dataset's consensus tolerance limits.

5.4.5. Ash Results

The HAMQAP Exercise 6 results for ash are summarized in Table 58. Columns A, B, and C are used in the table below to distinguish between the aliquots taken by each participating laboratory from a single bottle.

Table 58. Summary of Results for Ash, %.

Lab [a]	A	B	C	Mean	SD	Method
5	1.5	1.46	1.44	1.467	0.031	Weight loss after ignition
11	1.14	1.35	1.3	1.263	0.110	Weight loss after ignition
17	1.45	1.47	1.57	1.497	0.064	Weight loss after ignition
19	1.52	1.45	1.51	1.493	0.038	Not specified or Other
20	1.5	1.5	1.5	1.500	0.000	Weight loss after ignition
30	1.36	1.36	1.32	1.347	0.023	Thermogravimetric
31	1.41	1.39	1.37	1.390	0.020	Gravimetry
39	1.39	1.4	1.39	1.393	0.006	Weight loss after ignition
59	1.31	1.28	1.28	1.290	0.017	Weight loss after ignition
61	1.35	1.37	1.39	1.370	0.020	Gravimetry
62	1.38	1.33	1.38	1.363	0.029	Not specified or Other
79	1.37	1.36	1.36	1.363	0.006	Weight loss after ignition
80	1.29	1.27	1.28	1.280	0.010	Weight loss after ignition
88	1.334	1.326	1.304	1.321	0.016	Not specified or Other
			N:	14		
			Mean, Pooled SD:	1.381	0.039	
			SD:	0.081		

[a] Two results excluded based on being outside the dataset's consensus tolerance limits.

5.4.6. Calories Results

The HAMQAP Exercise 6 results for calories are summarized in Table 59. Columns A, B, and C are used in the table below to distinguish between the aliquots taken by each participating laboratory from a single bottle.

Table 59. Summary of Results for Calories, kcal/100 g.

Lab [a]	A	B	C	Mean	SD	Method
	367	368	369	368.0	1.0	9(Fat)+4(Protein)+4(Carbohydrate)
31	373	372	371	372.0	1.0	9(Fat)+4(Protein)+4(Carbohydrate)
39	392	392	392	392.0	0.0	Not specified or Other
79	365	365	365	365.0	0.0	Not specified or Other
80	360.44	362.22	361.4	361.4	0.9	9(Fat)+4(Protein)+4(Carbohydrate)
			N:	5		
			Mean, Pooled SD:	371.7	0.7	
			SD:	12.0		

[a] One result excluded based on being outside the dataset's consensus tolerance limits.

6. Statistical Approaches for Value Assignment

Statistical analysis was provided by the NIST Statistical Engineering Division. Where more than one method was available or when interlaboratory study data was available in addition to a NIST method for a measured analyte, the estimated value is the mean of the method and the interlaboratory study data estimates available for this analyte. The uncertainty was estimated using a bootstrap procedure based on a Gaussian random effects model for the between-method effects [32–35]. If only one method was available for an analyte, then that method estimate is the analyte estimate.

The uncertainties of all values except ash and solids incorporate a relative uncertainty of 0.1 % due to moisture correction.

To identify possible inhomogeneity of the SRM, both ANOVA with 5 % significance level and graphical analyses were run on NIST data where bottle information was available. The uncertainties for Cd, Mg, Mn, and Na values incorporate an additional component for possible heterogeneity based on results from different NIST methods or from interlaboratory studies.

Very marked differences are often observed between the results from the laboratories participating in an interlaboratory study. For each interlaboratory study, the method estimate for that study for each analyte is the weighted median of the individual laboratory means for that analyte, where the weights are based on a Laplace random effects model [35]. For this SRM, the weighted median is equal to or very close to the unweighted median of laboratory means for most analytes. The uncertainty of the weighted median is estimated using a bootstrap procedure based on a Laplace random effects model for the between-laboratory and within-laboratory effects [32–36]. The weights and uncertainty of the weighted median are based in part on the uncertainties of the individual laboratory means. Here, the uncertainty assigned to each laboratory mean is the standard deviation of that mean. If a laboratory reported only one measurement for an analyte, then for the purposes of the computation that value is assigned an uncertainty equal to the maximum of the uncertainties reported by the other laboratories for that analyte.

Several extreme outlier measurements from the interlaboratory studies were flagged by the analysts and omitted from the calculations. The deviance of these measurements from the others exceeded the usual variation, often differing by an order of magnitude or more. Other measurements may be questionable but could not be determined to be unrepresentative extreme outliers because of the sparseness and variation of the rest of the data.

7. Certificate of Analysis

The results of the statistical analysis for all analytes are presented in the COA for SRM 1568c Rice Flour. A NIST COA is defined below.

“In accordance with ISO Guide 31: 2000, a NIST SRM certificate is a document containing the name, description, and intended purpose of the material, the logo of the U.S. Department of Commerce, the name of NIST as a certifying body, instructions for proper use and storage of the material, certified property value(s) with associated uncertainty(ies), method(s) used to obtain property values, the period of validity, if appropriate, and any other technical information deemed necessary for its proper use. A Certificate is issued for an SRM certified for one or more specific physical or engineering performance properties and may contain NIST reference, information, or both values in addition to certified values. A Certificate of Analysis is issued for an SRM certified for one or more specific chemical properties. Note: ISO Guide 31 is updated periodically; check with ISO for the latest version.” [37]

For the most current version of the COA for NIST SRM 1568c Rice Flour, please visit: https://www-s.nist.gov/srmors/view_detail.cfm?srm=1568c.

References

[1] U.S. FDA. Arsenic in Food and Dietary Supplements. https://www.fda.gov/food/metals-and-your-food/arsenic-food-and-dietary-supplements. Accessed on 6/24/2025.

[2] National Institute of Standards, Certificate of Analysis, Standard Reference Material 1568 Rice Flour. 1978. https://tsapps.nist.gov/srmext/certificates/archives/1568.pdf.

[3] National Institute of Standards, Certificate of Analysis, Standard Reference Material 1568a Rice Flour. 1995. https://tsapps.nist.gov/srmext/certificates/archives/1568a.pdf

[4] National Institute of Standards and Technology, Certificate of Analysis, Standard Reference Material SRM 1568b Rice Flour. 2021. https://tsapps.nist.gov/srmext/certificates/archives/1568b.pdf.

[5] National Institute of Standards and Technology, Certificate of Analysis, Standard Reference Material SRM 1568c Rice Flour. 2022. https://tsapps.nist.gov/srmext/certificates/1568c.pdf.

[6] Wolf WR. Reference materials; In “Methods of Analysis for Nutrition Labeling”; Sullivan DM. Carpenter DE, Eds; AOAC INTERNATIONAL: Arlington, VA, 1993; pp 111−122.

[7] Sharpless KE, Greenberg RR, Schantz MM, Welch MJ, Wise SA, Ihnat M. Filling the AOAC triangle with food-matrix standard reference materials. Anal Bioanal Chem 2004;378(5):1161-1167. https://doi.org/10.1007/s00216-003-2384-1

[8] Christopher SJ, Long SE, Rearick MS, Fassett JD. Development of High Accuracy Vapor Generation Inductively Coupled Plasma Mass Spectrometry and its Application to the Certification of Mercury in Standard Reference Materials. Anal Chem;2001:73(10):2190-2199. https://doi.org/10.1021/AC0013002

[9] Ragland, J. M. (2022). Isotope Dilution Assistant (IDA) (Version 1.0) [Computer software]. https://github.com/jmr-nist-gov/IDA. Accessed on 6/24/2025.

[10] Sahin D, Radulović V, Lindstrom RM, Trkov A., Reevaluation of neutron flux characterization parameters for NIST RT-2 facility. J Radioanal Nucl Chem 2014;300:499-506. https://doi.org/10.1007/s10967-014-3076-3

[11] Greenberg RR, Fleming RF, Zeisler R. High sensitivity neutron activation analysis of environmental and biological standard reference materials. Environm Intern 1984;10(2):129-136. https://doi.org/10.1016/0160-4120(84)90088-6

[12] Lindstrom RM. Sum and mean. Standard programs for activation analysis. Biol Trace Elem Res 1994;43-45:597-603. https://doi.org/10.1007/978-1-4757-6025-5_69

[13] National Institute of Standards and Technology, Certificate of Analysis, Standard Reference Material SRM 2684c Bituminous Coal (Nominal Mass Fraction 3 % Sulfur). 2014. https://tsapps.nist.gov/srmext/certificates/2684c.pdf.

[14] National Institute of Standards and Technology, Certificate of Analysis, Standard Reference Material 2718a Green Petroleum Coke. 2017. https://tsapps.nist.gov/srmext/certificates/2718a.pdf.

[15] Paul RL, Mackey EA. Neutron scattering by hydrogen in cold neutron prompt gamma-ray activation analysis. J Radioanal Nucl Chem. 1994;181(2):321-333. https://doi.org/10.1007/bf02037638

[16] Mackey EA, Gordon GE, Lindstrom RM, Anderson DL. Effects of target shape and neutron scattering on element sensitivities for neutron capture prompt gamma-ray activation analysis. Anal Chem 1991;63(3):288-292. https://doi.org/10.1021/ac00003a019

[17] Mackey EA, Gordon GE, Lindstrom RM, Anderson DL. Use of spherical targets to minimize effects of neutron scattering by hydrogen in neutron capture prompt gamma-ray activation analysis. Anal Chem 1992;64(20):2366-2371. https://doi.org/10.1021/ac00044a012

[18] Paul RL. The use of element ratios to eliminate analytical bias in cold neutron prompt gamma-ray activation analysis. J Radioanal Nucl Chem 1995;191:245-256. https://doi.org/10.1007/BF02038220

[19] Paul RL. Prompt gamma-ray activation analysis for certification of sulfur in fuel oil SRMs. J Radioanal Nucl Chem 2017;311:1149-1154. https://doi.org/10.1007/s10967-016-4935-x

[20] Paul RL, Sahin D, Cook JC, Brocker C, Lindstrom RM, O'Kelly DJ. NGD cold-neutron prompt gamma-ray activation analysis spectrometer at NIST. J Radioanal Nucl Chem 2015;304:189-193. https://doi.org/10.1007/s10967-014-3635-7

[21] Narukawa T, Inogoki K, Kuroiwa T, Chiba K (2008) The extraction and speciation of arsenic in rice flour by HPLC–ICP-MS. Talanta 77(1):427–432. https://doi.org/10.1016/j.talanta.2008.07.005.

[22] Narukawa T, Hioki A, Chiba K (2012) Speciation and Monitoring Test for Inorganic Arsenic in White Rice Flour. J Agric Food Chem 60(4):1122−1127. https://doi.org/10.1021/jf204240p.

[23] Narukawa T, Suzuki T, Inogoki K, Hioki A (2014) Extraction techniques for arsenic species in rice flour and their speciation by HPLC–ICP-MS. Talanta 130:213–220. https://doi.org/10.1016/j.talanta.2014.07.001.

[24] Narukawa T, Chiba , Sinaviwat S, Fewldmann J (2017) A rapid monitoring method for inorganic arsenic in rice flour using reversed phase-high performance liquid chromatography-inductively coupled plasma mass spectrometry. J Chromatog A 1479:129–136. https://doi.org/10.1016/j.chroma.2016.12.001.

[25] National Institute of Standards and Technology, Certificate of Analysis, Standard Reference Material SRM 3030 Monomethylarsonic Acid Standard Solution. 2018. https://tsapps.nist.gov/srmext/certificates/3030.pdf.

[26] National Institute of Standards and Technology, Certificate of Analysis, Standard Reference Material SRM 3031 Dimethylarsinic Acid Standard Solution. 2018. https://tsapps.nist.gov/srmext/certificates/3031.pdf.

[27] National Institute of Standards and Technology, Certificate of Analysis, Standard Reference Material SRM 3036 Arsenic Acid (AsV) Standard Solution. 2018. https://tsapps.nist.gov/srmext/certificates/3036.pdf.

[28] National Institute of Standards and Technology, Certificate of Analysis, Standard Reference Material SRM 3037 Arsenous Acid (AsIII) Standard Solution. 2018. https://tsapps.nist.gov/srmext/certificates/3037.pdf.

[29] National Institute of Advanced Industrial Science and Technology, National Metrology Institute of Japan, Reference Material Certificate, NMIJ CRM 7901-a Arsenobetaine Solution. Date of shipment. https://unit.aist.go.jp/nmij/english/refmate/crm/cert/7901a_en.pdf.

[30] Barber CA, Burdette CQ, Hayes HV, Luvonga C, Phillips MM, Rimmer CA, Wood LJ, Yu LL (2021) Health Assessment Measurements Quality Assurance Program: Exercise 5 Final Report. NIST Interagency Report (NIST IR) 8343. https://doi.org/10.6028/NIST.IR.8343

[31] Barber CA, Burdette CQ, Hayes HV, Johnson ME, Kotoski SP, Murray JA, Phillips MM, Rimmer CA, Wood LJ, Yarberry AJ (2021) Health Assessment Measurements Quality Assurance Program: Exercise 6 Final Report. NIST Interagency Report (NIST IR) 8343. https://doi.org/10.6028/NIST.IR.8394

[32] JCGM 101:2008, Evaluation of measurement data—Supplement 1 to the "Guide to the expression of uncertainty in measurement'"—Propagation of distributions using a Monte Carlo method; Joint Committee for Guides in Metrology (2008), https://www.bipm.org/en/publications/guides

[33] Efron B, Tibshirani RJ. (1993) An Introduction to the Bootstrap, Chapman & Hall, UK.

[34] Searle S, Casella G, McCulloch C. (1992) Variance Components; John Wiley, Hoboken, NJ.

[35] Rukhin AL, Possolo A. Laplace random effects models for interlaboratory studies, Computational Statistics and Data Analysis 2011;55:1815-1827. https://doi.org/10.1016/j.csda.2010.11.016

[36] JCGM 100:2008, Evaluation of Measurement Data — Guide to the Expression of Uncertainty in Measurement (ISO GUM 1995 with Minor Corrections); Joint Committee for Guides in Metrology (2008); https://www.bipm.org/en/publications/guides
See also Taylor, B.N.; Kuyatt, C.E.; Guidelines for Evaluating and Expressing the Uncertainty of NIST Measurement Results; NIST Technical Note 1297; https://doi.org/10.6028/NIST.TN.1297

[37] NIST. SRM Definitions. https://www.nist.gov/srm/srm-definitions.
Accessed on 6/24/2025.

Appendix A. List of Acronyms

AAS	atomic absorption spectrometry
ANOVA	analysis of variance
CNPGAA	cold neutron prompt gamma-ray neutron activation analysis
COA	Certificate of Analysis
cps	counts per second
DMA	dimethylarsinic acid
FEP	fluorinated ethylene propylene
HAMQAP	Health Assessment Measurements Quality Assurance Program
HPLC-ICP-MS	high-performance liquid chromatography inductively coupled plasma mass spectrometry
ICP-MS	inductively coupled plasma mass spectrometry
ICP-OES	inductively coupled plasma optical emission spectrometry
ID-CV-ICP-MS	isotope dilution cold vapor inductively coupled plasma mass spectrometry
INAA	instrumental neutron activation analysis
LC-ICP-MS	liquid chromatography inductively coupled plasma mass spectrometry
MMA	monomethylarsonic acid
NCNR	NIST Center for Neutron Research
NIST	National Institute of Standards and Technology
NMIJ	National Metrology Institute of Japan
PTFE	polytetrafluoroethylene
SI	International System of Units
SRM	Standard Reference Material
TMAO	trimethylarsine oxide
TNPGAA	thermal neutron prompt gamma-ray activation analysis
WDXRF	wavelength dispersive X-ray fluorescence spectrometry

Appendix B. Change Log from NIST.SP.260-229 (July 2022)

The following changes were made to this report to supersede NIST.SP.260-229 (July 2022):

- Entire document — Format extensively modified to conform with current NIST template; alternative text added to all figure to comply with Section 508 of the Rehabilitation Act of 1973; many figure captions have been expanded to provide more figure information.
- Cover and title pages— NMIJ author added, employment status of NIST authors updated.
- Section 1 Introduction — modified to describe reason for the update. Figures 2 and 3 updated to include 2023 through 2025 SRM 1568c sales history.
- Added new Section 4.2 “NMIJ Method for Arsenic Species Introduction.”
- Added new Section 5.1.3 “NMIJ Moisture Results.”
- Sections 5.3, 5.3.1, and 5.3.2 — Modified to include NMIJ results.
- References — DOI status confirmed and updated when needed
- Added Appendix B.